The University of Maine

DigitalCommons@UMaine

Summer 8-20-2021

Illuminating Corneal Nerve Injury: Analysis of Neuronal Phenotypes Following Acute and Chronic Corneal Nerve Injury

Cara Sullivan
University of Maine, cara.sullivan@maine.edu

Recommended Citation

ILLUMINATING CORNEAL NERVE INJURY: ANALYSIS OF NEURONAL PHENOTYPES

FOLLOWING ACUTE AND CHRONIC CORNEAL NERVE INJURY

By

Cara E. Sullivan

B.A., College of the Holy Cross, 2007

M.S. Neuroscience, University of Hartford, 2015

A DISSERTATION

Submitted in Partial Fulfillment of the

Requirements for the Degree of

Doctor of Philosophy

(in Biomedical Sciences)

The Graduate School

The University of Maine

August 2021

Advisory Committee:

    Ian. D. Meng, The University of New England, Advisor

    Christine Lary, Maine Medical Center Research Institute

    Calvin Vary, Maine Medical Center Research Institute

    Derek Molliver, The University of New England

    Benjamin Harrison, The University of New England

ILLUMINATING CORNEAL NERVE INJURY: ANALYSIS OF NEURON PHENOTYPE

FOLLOWING ACUTE AND CHRONIC CORNEAL NERVE INJURY

By Cara E. Sullivan

Dissertation Advisor: Dr. Ian Meng, PhD

An Abstract of the Dissertation Presented

In Partial Fulfillment of the Requirements for the

Degree of Doctor of Philosophy

(in Biomedical Sciences)

August 2021

The cornea is uniquely avascular, transparent, and densely innervated with a highly complex and rapidly adapting sensory system. Combined with the tear film coating its surface, it is the first line of protection for the visual system. Clear vision provides tremendous survival advantage and thus uses long evolved and highly conserved mechanisms within the corneal protective barrier to preserve its function. Corneal nerves have a critical role in maintaining corneal homeostasis, initiating blinking, and tearing circuits to block potentially damaging environmental insults, and for engaging rapid-response regeneration programs. Many of these critical molecular mechanisms have been broadly characterized over the past century. However, with new advances in transgenic models and precision medicine, current studies focus on specific molecular factors that can be targeted in translational research and treatments. Sry-Box Transcription Factor 11 (SOX11) is a known upstream regulator of the injury response regeneration associated gene network and is highly expressed in primary afferent neurons following injury. Currently, little is known about the role of SOX11 in nerve regeneration

following corneal injury.   The aim of this study was to examine corneal injury-induced pathology in direct and indirect corneal injury models, which include trephine-only (TO), corneal abrasion (CA), and lacrimal gland excision (LGE). Both wild-type C57B6/J, *Nav1.8*Cre-tdTomato and *Nav1.8*Cre-*Sox11*-tdTomato mice were used to characterize corneal pathology following these injuries. LGE-induced dry eye reduces the aqueous component of tears, resulting in persistent corneal epithelial cell damage and retraction of corneal afferent nerve terminals. TO ligates axon terminals to the subbasal plexus in the corneal epithelium. CA first uses TO injury directly followed by mechanically removing the corneal epithelium and axon terminals from the central cornea. Before and after injury, assays were performed to evaluate tearing, mechanical sensitivity, ocular discomfort, and the corneal epithelium. Tissue was collected at terminal timepoints, and whole-mount corneas were imaged, and afferent terminals were analyzed. Before injury, corneal cell bodies were labeled using retrograde tracer, and somal phenotype was evaluated using immunohistochemistry and in situ hybridization. Additionally, rt-qPCR was performed on both corneas and trigeminal ganglia in some experiments. The results show that while corneal innervation density decreased between 1-2 weeks following LGE in control animals, nerves regenerated to near normal levels by four weeks, albeit in a disorganized manner. In *Nav1.8*Cre-tdTomato-*Sox11*$^{f/f}$ (*Sox11*$^{fl/fl}$) animals, innervation density was significantly reduced at the 4-week time point compared to control animals. As determined with fluorescein staining, corneal epithelial cell damage was similar between *Sox11*$^{fl/fl}$ and control animals over the 4 -weeks after LGE. Directly following CA-induced injury, both control and *Sox11*$^{fl/fl}$ animals showed significant decreases in innervation density at 24 hours. By 48 hours after injury, *Sox11*$^{fl/fl}$ animals showed a small yet significant increase in nerve growth. Both control and *Sox11*$^{fl/fl}$ animals demonstrated comparable reductions in corneal epithelial cell

damage 48 hours after injury. Taken together, these results provide support for the critical role

of SOX11 in nerve regeneration and healing following corneal injury.

DEDICATION

To the surprising number of family, friends and acquaintances who have related their own

painful and irritating experiences dealing with corneal injury and dry eye disease.

And to all the creatures sacrificed to further our knowledge of the nervous system to help

alleviate human pain and disease and whose sacrifice has elevated the scientific body of

knowledge in ways that would be impossible without them.

ACKNOWLEDGMENTS

I acknowledge and thank the past and present members of the Meng Lab who trained me, challenged me, and collaborated with me to complete this work. I would like to thank the advisory members of my thesis committee, Dr. Christine Lary, Dr. Derek Molliver, Dr. Cal Vary, Dr. Benjamin Harrison and Dr. Ian Meng. It was through our discussions and debates that I have been able to grow as a scientist and think in a more meaningful way. Through the good and bad of the past 6 years, their support was ever present and their insights into the complexities of neuroscience, research techniques and data science forever inspiring. I would like to specifically thank my advisor and PhD mentor, Dr. Ian Meng who took a huge chance on a complete novice and provided unrelenting patience and guidance through a critical period of growth.

TABLE OF CONTENTS

x

LIST OF TABLES

LIST OF FIGURES

CHAPTER 2:

CHAPTER 3:

CHAPTER 4:

LIST OF ABBREVIATIONS

Aδ: A-delta

ATF3: Activating transcription factor 3

BDNF: Brain-Derived Neurotropic Factor

β4: Beta-4 integrin

CA: Corneal Abrasion

CGRP: Calcitonin Gene-Related Peptide

CNS: Central Nervous System

DED: Dry eye disease

DHA: Decosahexanoic acid

DiI: 1,1'-Dioctadecyl-3,3,3',3'-Tetramethylindocarbocyanine Perchlorate

DPC: days post coitum

DRG: Dorsal root ganglia

Ex.: excitation

Em.: emission

FB: Fast Blue

FG: FluoroGold

FM: FM-143x

GAPs: Growth-associated proteins

Gap43: Growth associated protein 43

GDNF: Glial-cell Derived Neurotropic Factor

IB4: Isolectin B4

IL-1: Interleukin-1

IL-1beta: Interleukin-1beta

LASIK: Laser in situ keratomileusis

LGE: Lacrimal Gland Excision

MMP-9: Metalloprotease-9

MRGprd: MAS Related GPR Family Member D

NGF: Nerve Growth Factor

NT-3: Neurotrophin 3

NT-4: Neurotrophin 4

p75NTR: p75 neurotrophin receptor

PBS: Phosphate buffered saline

PBST: Phosphate buffered saline and triton-X

PDGF-B: Platelet-derived growth factor-B

PGP9.5: Protein gene product 9.5

PIEZO2: Piezo Type Mechanosensitive Ion Channel Component 2

PKC: protein kinase C phosphorylation

PNS: Peripheral nervous system

PRK: Photorefractive keratectomy

RAGs: Regeneration associated genes

SOX11: Sry-Box Transcription Factor 11

Sox11^{fl/fl}: *Nav1.8*Cre-tdTomato- *Sox11^{fl/fl}*

SPRRP1A: Small proline-rich repeat protein 1A 13

SP: Substance P

Td: tdTomato

TG: Trigeminal ganglion

TO: Trephine-only

trkA: Tropomyosin receptor kinase A

TRPV1: Transient receptor potential cation channel subfamily V member 1

TRPM8: Transient Receptor Potential Cation Channel Subfamily M Member 8

TTX-R: Tetrodotoxin-resistant channels

TTX-S: Tetrodotoxin-sensitive channels

TGF-a: Transforming growth factor-alpha

Tubb3: B-tubulin III

VEGF: Vascular endothelial growth factor

Vi/Vc: Interpolaris/caudalis

CHAPTER 1

A REVIEW OF CORNEAL NERVE INJURY

Sight is the ultimate superpower. Evolutionarily, vision improves survival and reproduction, and at least for humans, increases perceived quality of life (Stelmack, 2001; Vu et al., 2005). The visual system is a highly conserved, redundant sensory process with specialized protection mechanisms to prevent damage and promote quick healing after injury. Immune privileged, the cornea is the transparent epithelial barrier, its avascular and innervated predominantly by nociceptive c-fibers with the highest density of terminals per $micron^2$ (Rozsa et al.,1982; Muller et al., 1997; Streilein, 2003; Hos et al., 2017). Specialized neurons comprise sensory subpopulations which help to regulate homeostatic functions and the response to a variety of potentially noxious stimuli. When visual impairments cannot be easily corrected, such as in cases of chronic neuropathic pain caused by corneal nerve injury, affected patients' quality of life is significantly reduced (Li et al., 2011; Hayman et al., 2007; Rosenthal and Borsook, 2016; Kalteniece et al., 2020). Not surprisingly, dry eye, which is marked by persistent eye irritation and visual ability (Goto et al., 2002), is often the reason for non-routine ophthalmologist visits (Uchino and Schaumberg, 2013), is seen in over 50% of contact lens wearers (Nichols et al., 2013) and associated with decreased quality of life.

1.1 Introduction

The cornea, a uniquely transparent and densely innervated structure, is essential for preserving the visual system and has been critical to survival across species. Light reflected off every element in our environment must pass through the cornea to the rods and cones of the retina. As the physical front line to one of the most important sensory systems, the cornea is a complex, uniquely specialized sensory structure. The ability for light to pass with minimal

refraction allows for a cleaner signal for visual processing in these primary neurons. Uniformity and precise organization of epithelial cells and axon terminals within the cornea are essential in maintaining visual homeostasis. Redundant neuroprotective systems, with the ability to detect and respond to a broad spectrum of stimuli and disease processes, are required to ensure that light can reach retinal cells with precision and minimal refraction (Dartt, 2004; Lamb et al., 2007; Yazdanpanah et al., 2017; Schwab, 2018; Marfurt et al., 2019). This thesis characterizes corneal neurons in acute and chronic injury states and identifies critical molecular regulators, at least in part, responsible for incurable corneal irritation in a growing clinical population.

1.1.1 Corneal Anatomy

The cornea comprises the central superficial surface of the eye and acts as the transparent protective barrier. The cornea is convex and becomes thicker in its periphery. The cornea with tear film act as the first refractive filter of light entering the eye. The cornea is responsible for the largest proportion of total light refraction at about 70%, with a refractive index of approximately 1.376 and 1.436 in the human cornea and cornea-tear film, respectively (Yazdanpanah et al., 2017; Sridhar, 2018; Patel and Tutchenko, 2019). Pathology, injury, or even hydration level changes to the cornea can greatly alter the refractive index and cause visual deficits (Patel et al., 2004; Kim et al., 2004; Meek and Knupp, 2015; Patel and Tutchenko, 2019). Corneal tissue comprises collagen, glycosaminoglycans, axon terminals, keratocytes, Langerhans, epithelial and endothelial cells (Sridhar, 2018). The cornea is organized into discrete cellular layers (epithelium, Bowman's layer, stroma, Descemet's membrane, endothelium) throughout which axon terminals concentrically project through (Sridhar, 2018). Within these layers, specialized cells work together to evenly spread tear film, maintain

transparency, and block or destroy pathological infiltrators (Sridhar, 2018). Across these layers, both cells and axon terminals are precisely organized.

1.1.2 Tears

In health, the cornea is avascular, which maintains the transparency of the structure. Without a vascular system to bring nutrients or remove waste products, tears help to in part replace these functions. Tears are crucial for maintaining homeostasis for corneal epithelium and neurons and act as the most superficial protective barrier (Mishima and Hedbys, 1968). The tear film, much like the cornea, is layered with endothelial mucus, an aqueous middle layer and a lipid layer which is most superficial, acting to prevent tear evaporation. Goblet cells in the conjunctiva produce the mucins and electrolytes of the mucus layer, which is spread through the glycocalyx network on the superficial surface of the corneal epithelial cells (Hodges and Dartt, 2013; Sridhar, 2018). Ipsilateral lacrimal glands produce the aqueous component of the tear film, while the meibomian glands supply the lipid for the outer most layer (Dartt, 2004, Hodges and Dartt, 2013). Afferent sensory nerve terminals embedded within the cornea comprise one distal end of pseudounipolar neurons whose cell bodies reside in the trigeminal ganglion (TG). Their other distal axons project to trigeminal brain stem nuclei, synapse to second-order neurons which project to the thalamus, and in turn synapse to third-order neurons projecting to the somatosensory cortex in the central nervous system (CNS). The cornea responds locally with tearing and blink reflexes and sends signals to central nuclei for more complex processing in the face of potential mechanical or noxious chemical injury. Sympathetic and parasympathetic nerves work together to respond to afferent sensory information and maintain tear homeostasis by innervating lacrimal gland cells to induce secretion of the water, proteins and electrolytes that make up the aqueous layer of tear film (Dartt, 2013; Meng and Kurose, 2013). Spontaneous

3

blinking is also required to help maintain tear film and ocular surface moisture. Just as afferents provide sensory inputs to modify tear film secretions, they contribute in part to the regulation of spontaneous blinking through transmission in the interpolaris/caudalis (Vi/Vc) brainstem regions (Kaminer et al., 2011; Meng and Kurose, 2013). These neural circuits stimulate the lacrimal reflex arc to produce fluid delivered through tubular ducts to coat the corneal surface and maintain that moisture (Dartt, 2009).

1.1.3 Corneal Nerve Morphology

The cornea maintains its unique transparent and avascular structure, despite being highly innervated by densely branching axons stemming from approximately 50-450 neuronal somas, which reside in the TG (Shaheen et al., 2004; Muller et al., 2003; Marfurt et al., 2010). Corneal axons project from the ophthalmic branch of the trigeminal nerve (Cranial Nerve V). through the superior orbital fissure on the border of the anterior and middle cranial fossae (Netter, 2010). To a lesser extent, innervation to the inferior cornea from the maxillary branch has been found in several neuronal tracing studies and projects through the foramen rotundum in the middle cranial fossae (Netter, 2010). Axonal bundles enter the anterior stroma adjacent to the corneal limbus and radiate in a spiral pattern in the stromal layer of the cornea (Dua et al., 2018). The afferent terminals separate in the subbasal layer and begin to branch and move anteriorly, resulting in dense uniform innervation across the corneal epithelial surface. Most corneal neurons are sensory inputs projecting from the TG, while a small percentage (5-10%) originate from the autonomic ciliary and superior cervical ganglia (Marfurt et al., 1993; Belmonte et al., 2017; Bouheraoua et al., 2019).

1.1.4 Corneal Nerve Subtypes

Many different subtypes of neurons play a role in sensory signaling, using their diverse characteristics to communicate different information about the internal or external environment. Corneal neurons are made up of a combination of A-delta (Aδ) and C-fibers. Aδ fibers make up approximately 20% of corneal neurons, are lightly myelinated, larger in diameter, and have higher conduction velocities (Muller et al.,2003; Meng and Kurose, 2013; Guerrero-Moreno et al., 2020). While C-fibers comprise 80% of corneal neurons, are unmyelinated, have small diameters, and have notably slower conduction velocities (Muller et al.,2003; Meng and Kurose, 2013; Guerrero-Moreno et al., 2020). Further divided, roughly 70% of corneal neurons can be classified as polymodal nociceptors, which detect noxious thermal, chemical and mechanical stimuli and of which can be either Aδ or C-fiber in disposition (Meng and Kurose, 2013; Wooten et al., 2014; Guerrero-Moreno et al., 2020). The second-largest subclassification of corneal neurons is defined as mechanoreceptors which make up about 20% of the afferent sensory abilities and are exclusively Aδ in nature and detect mechanical stimuli (Meng and Kurose, 2013; Gonzalez-Gonzalez et al., 2017; Guerrero-Moreno et al., 2020). Although a minority proportion to corneal sensory afferents, cold receptors can be Aδ or C-fibers and make up an estimated 10% of corneal neurons and have critical roles in detecting innocuous cooling and maintaining moisture on the ocular surface (Meng and Kurose, 2013). Electrophysiological studies provide evidence to support the characterization that high-threshold mechanoreceptors are exclusively Aδ fibers, while polymodal and cool sensing neurons are made up of a combination of Aδ and C fibers (De Armentia et al., 2000; Gallar et al., 1993). The smaller proportion of Aδ fibers seen within the cornea may be explained due to the need to maintain transparency, uniform thickness, and generally unimpaired transmission of light to the retina. Aδ afferents lose their myelination upon entry into the corneal epithelium to accommodate these

homeostatic needs while maintaining increased conduction velocities to central regions to effectively communicate mechanical insults that could cause significant injury to the cornea (Meng and Kurose, 2013; Marfurt, 1981).

1.1.5 Pain sensing Corneal Afferents

Nav1.8 and Nav1.9 are tetrodotoxin-resistant (TTX-R) voltage-gated sodium channels, expressed primarily in afferent nociceptors in TG and dorsal root ganglia (DRG) (Black et al., 2002; Strickland et al., 2008; Gautron et al., 2011; Lin et al., 2016). Nav1.8 is present on neurons that have significant roles in signaling different types of pain. Ion channels and their transduction properties ultimately define corneal neuron subclasses. Transient receptor potential cation channel subfamily V member 1 (TRPV1) is expressed in a majority of polymodal nociceptors (Alami et al., 2015), Piezo Type Mechanosensitive Ion Channel Component 2 (PIEZO2) is characteristic of mechanoreceptors (Bron et al., 2014) and Transient Receptor Potential Cation Channel Subfamily M Member 8 (TRPM8) is an accepted molecular marker of cold receptors (Madrid et al., 2006; Parra et al.,2010). Likewise, TTX-R channels define a large corneal afferent subclass that spans across unmyelinated corneal neurons, are heavily expressed, and offer the opportunity for the use of a transgenic reporter to label the majority of corneal neurons across multiple subclasses. The recent gain in popularity of corneal neuron transgenic reporters enables consistent labeling across samples which can be used for reliable morphological and functional analyses. The cornea requires more extended incubation periods and often multiple full-thickness cuts for standard immunolabeling experiments to be effective. The use of transgenic reporters helps to reduce confounding experimental elements associated with these methods, provides consistent labeling across samples, and allows for subclassification of neurons based on the promoter used by the transgenic reporter.

1.1.6 Electrophysiological Properties

Diverse receptive properties are critical for polymodal corneal nociceptors to provide comprehensive protective responses. Electrophysiological studies have classified 50-70% of corneal neurons as polymodal neurons which respond to a combination of mechanical, thermal, and noxious stimuli (Gonzalez-Gonzalez et al., 2017; Kurose and Meng, 2013). Additionally, between 10-50% of corneal neurons have been determined to be cool cells which respond to cool thermal conditions (Gonzalez-Gonzalez et al., 2017; Kurose and Meng, 2013). Approximately 10-50% of corneal neurons respond as cold thermoreceptors (Gonzalez-Gonzalez et al., 2017; Kurose and Meng, 2013). Low-threshold cool cells, with decreased TRPM8 density and increased Kv1.1-1.2, potassium channels that limit inward TRPM8 generated current, have been observed to represent the majority of this population in healthy corneas and are critical for maintaining homeostatic tearing and surface moisture. High-threshold cool cells with higher TRPM8 density and lower Kv1.1-K1.2 expression are responsible for the sensory response to extreme cooling (Gonzalez-Gonzalez et al., 2017). While these classes of neurons have unique sensitivities, diverse noxious stimuli can evoke responses at high levels (Gonzalez-Gonzalez et al., 2017; Shaheen et al.,2014).

The electrical principles of corneal neurons have been carefully examined, and functional abilities have been evaluated in health and disease. In many studies, corneal neurons have been identified using a retrograde tracer applied to the corneal surface. Myelinated and unmyelinated neurons can be determined based on conduction velocities, and their electrical properties can be classified in active versus passive states. Studies have found that polymodal corneal neurons, including both Aδ and C fibers, have broad action potentials with slow depolarization and delayed repolarization (i.e., Slow-type or S-neurons), as indicated by a prominent convex ridge in the repolarization phase (De Armentia et al., 2000; Moreira et al.,

2007). Aδ fibers that are pure mechanoreceptors have been categorized as fast neurons (i.e.,

F-neurons) with narrow action potentials, a convex ridge during the repolarization phase, and

more significant hyperpolarization (De Armentia et al., 2000; Moreira et al., 2007). The quick-

firing nature of F-neurons has been associated with tetrodotoxin-sensitive channels (TTX-S), as

firing ultimately ceases in a TTX bath (Moreira et al., 2007). S-neurons, which are slow to

activate and inactivate, do not appear to exhibit altered firing behavior in the presence of TTX

(Moreira et al., 2007).

Similarly, polymodal and cool cells appear to exhibit characteristic slow activating and

inactivating properties as seen in S-neurons and, in turn, TTX-R neurons (De Armentia et al.,

2000; Moreira et al., 2007). The functions of the different subclasses fit the physiological need

for quick response to physical insult and prolonged signaling of nuanced noxious stimuli.

Understanding these corneal subclass-specific electrophysiological principles is critical for using

transgenic reporter lines, such as a *Nav1.8*-tdTomato mouse used in experiments presented in

this body of work.

Studies have found that corneal nerve injury causes changes to the electrophysiological

properties of these neurons (Shaheen et al., 2014; Hatta et al., 2019). Pathological changes to

the receptive properties of corneal neurons contribute to neuropathic pain conditions by

sensitizing cool neurons to other sensory insults following corneal nerve injury. TRPV1, as

previously described to be associated with polymodal nociceptors, TRPV1 agonists (i.e.,

capsaicin) are seen to evoke responses to TRPM8 neurons after LGE-induced dry eye (Hatta et

al., 2019). Additionally, Hatta et al., (2019) reported that the number of TRPM8 and co-

expressing TRPV1 neurons increased following LGE. The results from this study indicates that

the cold receptor subclass undergoes a functional change following corneal injury that

sensitizes that subpopulation to TRPV1 and its agonists.

1.1.7 Dry Eye Clinical Populations

Dry eye disease (DED) affects approximately 6.8% of American adults over 18 years old or 16.4 million American individuals each year (Hikichi et al., 1995; Schein et al., 1997; Schaumberg et al., 2003; Schaumberg et al., 2009; Jie et al., 2009; Chao et al., 2014; Galor et al., 2016; Kovács et al., 2016; Farrand et al., 2017; Kalangara et al.,2018). DED impacts adults over 75 years old at around 18.6% of Americans, with a higher prevalence in women at 8.8% or 11.1 million individuals and men representing 4.5% or 5.3 million individuals (Farrand et al., 2017). DED can be broadly defined as either aqueous deficient or evaporative, with these diagnostic divisions having distinct etiologies, symptoms, diagnostic criteria, and treatments (Lin and Yiu, 2014). Patients often report the experience of 'dry,' 'itchy,' 'burning' sensations. Typical environmental conditions, such as room temperature air (i.e., 20°C), can be perceived as a painful or irritating stimulus, similar to as if it were a more extreme temperature (i.e., 50°C) (Feng and Simpson, 2004). Of available treatments, artificial tears, oral omega-3 supplements, mucin replacements, ductal plugs, steroids, and immunosuppressants are of the most popular and effective treatments that many DED patients use with reported success (Pflugfelder et al., 2007; Lin and Yiu, 2014; Nichols et al., 2016; Findlay et al., 2018). DED is a significant contributor to decreased quality of life for those affected and inadequate treatment (Cook et al., 2019).

DED clinical populations are often divided into those who respond to available treatments and those who do not. DED subpopulations that cannot resolve symptoms develop chronic conditions and experience DED-neuropathic ocular pain resistant to available treatments. Without typical tear composition, chronic DED corneas are left unprotected and typically present with inflammation, sclerosis, and altered sensitivity to everyday stimuli (Baudouin, 2001; Wilson and Perry, 2007; Gayton, 2009). Patients experiencing DED often

9

complain of 'burning,' 'grittiness,' 'blurriness,' and 'pain' (Cook et al.,2019). Symptoms are

usually persistent, with many patients reporting minimal improvements after treatment (Bron et

al., 2014; Craig et al., 2017; Li et al., 2019; Kojima et al., 2020; Goyal et al., 2016; Rosenthal

and Borsook, 2016). Even what is clinically considered mild cases of chronic DED impact the

quality of life for patients. Most often reported symptoms include difficulties in the 'workplace,'

'electronic device usage,' 'reading,' and 'driving' (Cook et al., 2019). Reports of DED are

growing with the increase in digital eye strain with dry eye symptomology (Miura et al., 2013;

Coles-Brennan et al., 2018; Chawla et al., 2019). As more people will spend more time viewing

electronic devices in the future, the mechanisms that cause dry eye must be better understood.

1.1.8 Corneal neuroprotective factors

Corneal health and function requires precise regulation and maintenance of its cellular

components. The cornea needs to maintain its transparency and cellular organization to reduce

refractive errors, which cause blurred vision and ocular pain (Sheridan and Douthwaite, 1989;

Chen et al., 2009; Dhungel and Shrestha, 2017; Carpentras et al., 2018). The cornea is

composed of three cellular layers. These layers include the endothelial cell layer, the stroma

made up of keratocytes and collagen fibrils, and the superficial epithelium comprised of

squamous, wing, and basal cells (Rowsey and Karamichos, 2017). Trophic factors that help

maintain the corneal microenvironment's health and function are supplied by tears, epithelial

cells, microglia, and neurons (Esquenazi et al., 2005; Li, 2011; Sacchetti and Lambiase, 2017;

Kowtharapu and Stachs, 2020). Tear film supplies growth factors that support cellular

proliferation, survival, and healing following injury (Klenkler, 2007; Sacchetti and Lambiase,

2017; Pan et al., 2018). Corneal nerve fibers and epithelial cells provide each other with

additional trophic factors, which are essential in maintaining homeostasis and healing after

injury (Li and Tseng, 1995; You et al., 2000; Sacchetti and Lambiase, 2017; Bikbova et al., 2016).

Nerve growth factor (NGF), a well-characterized neurotrophin essential for neuronal survival (De Castro et al., 2009), is synthesized and expressed in epithelial and stromal corneal cells and supports epithelial healing through induction of keratocyte migration and neural regeneration via neurite growth (Lee et al., 2005; Pan et al., 2018). NGF acts on tropomyosin receptor kinase A (trkA) and p75 neurotrophin receptor (p75NTR) receptors which are expressed in epithelial cells and sensory afferents (You et al., 2000; Qi et al., 2008; De Castro et al., 2009). A study by Pan et al. (2018) reported that the proportion of NGF increases in tear film with increased density of regenerating nerve buds and generally found that NGF aids in nerve regeneration following corneal surgery. Another clinical study reported similar findings and observed that the proportion of NGF in tear film increased following laser eye surgeries (Lee et al., 2004). Lee et al. (2004) hypothesized that the observed increase in NGF following photorefractive keratectomy (PRK) directly relates to relative normal corneal sensation exhibited by patients, as compared to reduced sensation and lower post-operative NGF tear film levels identified in patients following laser in situ keratomileusis (LASIK) surgery. Per these findings, De Castro et al. (1998) found that nerve density, epithelium, and responses to mechanical, chemical, and thermal stimuli were all significantly reduced in corneas of trkA downregulated mice. Increased NGF following injury is likely mediated by the release of inflammatory markers in this period, including interleukin-1 (IL-1) (Shaheen et al., 2014). Additionally, proinflammatory mediators, including metalloprotease-9 (MMP-9) and beta-4 integrin (β4), are produced by epithelial cells following injury and can increase NGF and TrkA expression to aid in healing processes (Blanco-Mezquita et al., 2013; Pan et al., 2018). While NGF is attributed to enhancing corneal healing, sustained upregulation may contribute to pathology associated with

chronic corneal diseases such as DED (Shaheen et al., 2014). Conversely, NGF has been established as an effective treatment in healing corneal epithelium, improving corneal sensitivity and, when combined with docosahexaenoic acid (DHA), provides a combination of epithelial healing, nerve regeneration, and neuroprotection (Bonini et al., 2000; Esquenazi et al., 2004; Tan et al., 2006; Shaheen et al., 2014).

Other neurotrophins, including neurotrophin-3 (NT-3) and neurotrophin-4 (NT-4), are produced by epithelial and stromal cells and contribute to maintaining epithelial cell health and homeostasis (Shaheen et al., 2014). The roles of NT-3 and NT-4 are not well characterized concerning their involvement in corneal nerve regeneration, but findings generally suggest that they likely do not play a prominent role (Chaudhary et al., 2012; Shaheen et al., 2014).

Glial-cell derived neurotrophic factor (GDNF), produced by the stromal keratocytes, has been observed to work with NGF to induce transcriptomic changes which promote epithelial healing after injury, even when applied topically (You et al., 2000; You et al., 2001; Maddurri et al., 2009; Shaheen et al., 2014; Bikbova et al., 2016). Brain-derived neurotrophic factor (BDNF) is produced within epithelial, stromal, and neuronal cells (You et al., 2000; Muller et al., 2003; Shaheen et al., 2014). BDNF promotes the expression of neurotrophic factors and induces nerve regeneration and growth in both the CNS and PNS (Shaheen et al., 2014; Bikbova et al., 2016). It also stimulates the production of known nerve regeneration-associated genes (RAGs), including growth-associated protein 43 (GAP-43) (Kobayashi et al., 1997; Shaheen et al., 2014). GAP-43 is a neuronal protein expressed after nerve injury, usually induced by BDNF, but when suppressed by high doses of NGF, is associated with decreased nerve regeneration (Skene and Willard, 1981; Kobayashi et al., 1997; Hirata et al., 2002; Madduri et al., 2009; Shaheen et al., 2014; Bikbova et al., 2016). Small proline-rich protein 1-A (SPRR1A) increases correlate with BDNF and GAP-43 in post-injury corneas (Chaudhary et al., 2012; Starkey et al., 2009;

Shaheen et al., 2014). SPRR1A is present in the corneal epithelium and is only expressed after injury and is regarded as a regeneration-specific RAG (Bonilla et al., 2002; Starkey et al., 2009; Chaudhary et al., 2012; Shaheen et al., 2014). Comparably increased with BDNF and SPRR1A, and induced by NGF following corneal injury, B-tubulin III (Tubb3) is a neuronal protein that structurally enables neurite outgrowth following injury (Mitchison and Kirschner, 1988; Fernyhough et al., 1989; Xu et al., 2002; Chaudhary et al., 2012; Shaheen et al., 2014).

Corneal neurons express other classes of trophic factors which support development, guidance, and regeneration after injury. Corneal neurons express factors including calcitonin gene-related peptide (CGRP), substance P (SP), neuropeptide Y (NPY), vasointestinal peptide (VIP, among others (Shaheen et al., 20014; Sacchetti and Lambiase, 2017). Neuronal release of these factors, such as SP and CGRP, increases corneal epithelial healing after injury (Nishida et al., 2007; Mastropasqua et al., 2017; Sacchetti and Lambiase, 2017). These neuromediators work in complementary ways to promote epithelial healing, as trophic factors released by the epithelial and stromal cells provide support for corneal nerve health (Muller et al., 2003; Mastropasqua et al., 2017; Sacchetti and Lambiase, 2017). Vascular endothelial growth factor (VEGF) is an interesting example connecting the complementary mechanisms of these corneal trophic factors and is associated with both protective and pathological roles following corneal nerve injury (Chang et al., 2012; Shaheen et al., 2014). Expression of VEGF and its receptors have been identified within the TG following corneal injury (Yu et al., 2008). VEGF is also widely expressed by epithelial, endothelial, and inflammatory cells after corneal injury (Philipp et al., 2000; Cattin et al., 2015; Hillenbrand et al., 2015; Caillaud et al., 2019). VEGF upregulation is promoted by infiltrating macrophages induced by CGRP release after injury (Cattin et al., 2015; Hillenbrand et al., 2015; Caillaud et al., 2019). While VEGF contributes to corneal healing after injury, its expression promotes neoangiogenesis in injured

corneas, contributing to the cornea's pathological vascularization (Sharif and Sharif, 2019). The tightly regulated interplay of trophic support provided by neighboring but divergent cell types within the cornea can promote quick healing and regeneration or perpetuate chronic pathological conditions that exhibit severe nerve and epithelial damage.

1.1.9 Nerve injury and regeneration

Corneal nerve injury, pathological or surgical in origin, alter neurophysiological functioning in ways that often lead to DED and neuropathic pain (Meng and Kurose, 2013; Shaheen et al.,2014; Galor et al., 2015; Kovacs et al., 2016; Belmonte et al., 2017). Typically, nerve injury and repair cascades initiate rapidly and restore corneal homeostasis in the acute period following injury. Infiltration of inflammatory molecules decreases firing thresholds, increases activation of corneal nociceptors, and causes hypersensitization that may or may not resolve, exhibited by divergent patient outcomes (Galor et al., 2015; Iyengar et al., 2017; Labetoulle et al., 2019).

Peptidergic fibers are critical drivers of neuroprotection, regeneration programs, and altered sensitization following injury (Ueda et al., 1989; Jones et al., 1998; Marfort et al., 2010; Cavanaugh et al., 2011; Russell et al., 2014; Schou et al., 2017). Corneal neurons typically present with distinctly peptidergic neurons and non-peptidergic neuronal populations with only around 10% overlap across these populations in naïve conditions (Marfurt and Dvorscak, 2006; Alamri et al., 2015). Peptidergic populations (~31% corneal neurons) are characterized by the expression of neuropeptides such as CGRP and SP, while non-peptidergic populations (~46% corneal neurons) bind isolectin B4 (IB4) or express MAS Related GPR Family Member D (MRGprd) (Marfurt and Dvorscak, 2006; Alamri et al., 2015). After corneal injury, these once distinct populations show phenotypic plasticity where IB4-positive (+) neurons exhibit increases

in expression of peptidergic markers in the experiments presented here. Increased expression and release of neuropeptides, which generally increases sensitivity and lowers firing thresholds in the cornea, at least in part, can explain clinical symptoms including altered corneal sensitivity and neovascularization of the cornea.

In other tissues, such as the DRG, CGRP has a known role as a proinflammatory neuropeptide and vasodilator (Croom et al., 1997; Bucelli et al., 2008; Kawarai et al., 2018; Key et al., 2018). In the cornea, CGRP has a dual role acting as both a proinflammatory mediator by promoting macrophage infiltration (Cattin et al., 2015; Hillenbrand et al., 2015; Caillaud et al., 2019) and as an anti-inflammatory mediator through its targeted inhibition of dendritic cell cytokine production through the cAMP/PKA pathway (Mikami et al., 2014). Likewise, CGRP also has a dual role of promoting corneal healing through reepithelization and neoangiogenesis but in sustained injury models with perpetual upregulation, can significantly contribute to a vascularized pathological corneal microenvironment (Mikulec et al., 1996; Toda et al., 2008; Mikami et al., 2014; Zhang et al., 2020).

TRPV1 has also been demonstrated to increase expression and activation following corneal nerve injury (Kim et al., 2008; Beggs et al., 2010; Zakir et al., 2012; Bereiter, 2018; Hatta et al., 2019 Huang et al., 2020; Fakih et al., 2021). Studies have correlated increased corneal hypersensitivity with increased TRPV1 expression observed in trigeminal neurons in acute periods following injury (Kim et al., 2008). Specifically, Kim et al. (2008) identified increased TRPV1 in both injured and uninjured trigeminal neurons, further substantiating the idea that TRPV1 may contribute to secondary hyperalgesia following injury. Additionally, TRPV1 evokes CGRP release and, with increased expression, likely perpetuates injury-induced sensitization (Meng et al., 2009; Alamri et al., 2015; Iyengar et al., 2017; Li et al., 2019). Prior studies report that approximately 37% of corneal neurons are TRPV1 positive, with a third of

those also positive for CGRP and SP (Tominaga et al., 1998; Piper, 1999; Murata and Masuko, 2006; Murata et al., 2006; Rosenbaum and Simon, 2007; Cao et al.,2013; Alamri et al., 2015; Li et al., 2019). Furthermore, TRPV1 activates pronociceptive genes, leading to sustained corneal sensitization changes (Fakih et al., 2021). Fakih et al. (2021) found that applying a TRPV1 antagonist, capsazepine, inhibited the expression of those same pronociceptive genes (i.e., cannabinoid receptor1-CB1, mu-opioid receptor-MOR, proenkephalin-PENK) and additionally eliminated clinical signs of ocular pain. This study provides further support for the hypothesis that TRPV1, and likely CGRP, are critical regulators of the neuroprotective and, at times, neuropathological phenotype that corneal neurons display after corneal injury.

Activating Transcription Factor 3 (ATF3) has also been identified with increased expression following nerve injury, specifically in the TG following injury (Averill et al., 2004; Kim et al., 2008). Upregulated expression of nerve regeneration-associated transcription factors, such as ATF3, correlate with successful axon repair and elongation following peripheral nerve injury (Seijffers et al., 2006; Hegarty et al., 2018; Guerrero-Moreno et al., 2020). Unlike in acute injury models (Hegarty et al., 2018), increases in ATF3 upregulation are sustained at least three weeks after dry eye conditions begin (Fakih et al., 2019).

CGRP contributes to multiple aspects of regeneration mechanisms (Mikulec et al., 1996; Chung et al., 2018) and likely acts in conjunction with ATF3 to support regenerative processes. LGE initiates nerve injury markers and nerve regeneration mechanisms to repair damaged axon terminals, resulting from reduced aqueous tearing. Upregulated RAGs promote robust axon regeneration, even within the context of severe chronic corneal injury. Recently studies have characterized ATF3 expression in Mrgprd neurons following spared nerve injury, suggesting a potential link between ATF3 and post-injury increases of CGRP and TRPV1 (Wang et al., 2021; Warwick et al., 2021). The results of these studies identify correlations between post-injury

modulators, CGRP, TRPV1 and ATF3, following peripheral injury. With need for further investigation, these connections suggest that nerve regeneration-associated signaling may play an integral role in disordered morphological reinnervation and neuropathic pain observed in severe and chronic dry eye.

1.1.10 Regeneration Associated Genes

RAGs are well known for their response to injury in peripheral neurons (McPhail et al., 2004; MacGillavry et al., 2011; Van Kesteren et al., 2011; Jing et al., 2012). Transcription factors, including SOX11 and ATF3, are known to initiate known RAGs, including GAP43 and SPRR1a (Aigner et al., 1995; Van Kesteren et al., 2011; Jing et al. 2013). RAG regulation of nerve injury is unique to the PNS and could be the mechanism that makes PNS regeneration more effective than that seen in the CNS.

Downstream molecules in the RAG network include GAPs, which were identified in early studies to promote regeneration in peripheral nerves and even in peripheral nerves transplanted into spinal cord nerve bundles (Skene and Willard, 1981; Skene, 1989; Tetzlaff et al., 1991; David and Aguayo, 1981; Richardson et al., 1982; Van Kesteren et al., 2011). Both neurotrophic factors and changes in transcription factor expression have been identified to promote GAP expression and peripheral nerve regeneration. Transgenic models using GAP43 overexpression show increased nerve sprouting in neuromuscular junctions and mossy fibers of the hippocampus (Aiger et al., 1995). In the CNS, GAP43 requires presynaptic protein kinase C phosphorylation (PKC), and when that action is inhibited, subsequent nerve sprouting is inhibited (Aiger et al., 1995). GAP43 has been identified as critical axon growth and guidance molecule through downregulation experiments in retinal ganglion cells (Strittmatter et al., 1995;

Sretavan and Kruger, 1998). Sretavan and Kruger (1998) found that retinal ganglion cell axon trajectories became disorganized and functionally problematic in GAP43 deficient groups.

Other groups have identified downstream RAG targets, such as SPRRP1A, as critical influences on membrane F-actin elongation after injury (Bonilla et al., 2002). Although downstream actors, such as GAP43 and SPRRP1A, are essential for successful PNS regeneration, upstream transcription factors, such as SOX11 and ATF3, are required to initiate broader RAG-responses to injury. C-JUN was the first of these transcription factors identified as essential to activating the RAG-response to peripheral injury (Herdegen et al., 1991; Jenkins and Hunt, 1991). Subsequent studies identified other critical upstream transcription factors including SOX11 (Jankowski et al., 2006; Jankowski et al., 2009) and ATF3 (Tsujino et al., 2000, Seijjers et al., 2006).

The overexpression of SOX11 has been used to delineate the mechanisms of pro-regenerative transcription programs in the PNS (Salerno et al.,2013) and CNS (Wang et al., 2015). Regeneration after injury is more prevalent and successful in the PNS, as compared to the CNS. Wang et al. (2015) confirmed findings from prior studies and reported that the upregulation of SOX11 in the PNS promotes nerve regeneration and reduces neuronal damage. This study used C57B6, AAV-induced SOX11 overexpression, ventral midline incision, and behavioral assays, including pellet retrieval and horizontal ladder. Results from CNS experiments reported that overexpression of SOX11 in the cortex also promoted axonal regeneration after acute and chronic injury. However, unlike in PNS studies, SOX11 overexpression failed to recover forelimb function, as measured by footfall errors. These authors concluded that while SOX11 could contribute to axon elongation and branching dynamics, the physical regrowth of these neurons was unable to integrate into descending pathways and recover functional losses. They hypothesize that the failure of SOX11 overexpression to recover

CNS functional deficits may be resolved by targeting downstream RAGs with specifically targeted programs that could successfully create these connections. Interestingly, an earlier study by Guo et al. (2014) found that overexpression of SOX11 did improve locomotor recovery following spinal cord injury and identified SOX11 induced-BDNF as central to this success. This study used Kunming mice, lentiviral overexpression, spinal hemisection, and functional recovery assessment using the Basso mouse scale.

1.1.11 SRY-box containing gene 11

SOX11 is a transcription factor characterized within the high-mobility-group (HMG) C of chromosomal proteins (Jankowski, 2008). Protein mass quantification and sequence analysis first identified HMG proteins and classified them in DNA binding abilities (Soullier et al., 1999). Soullier et al. (1999) found that the SOX family of HMG-box (HMG) class proteins uniquely binds to specific duplex DNA sequences and can also non-specifically bind to oligonucleotide intersections and bind non-specifically to the minor groove DNA (King and Weiss, 1993; Reeves, 2010). These contrasting properties enhance the complexity of DNA modulation that this class of transcriptions can exert over diverse molecular cascades. In SOX11, this factor has a binding region termed the SRY-box as it was initially found to bind and regulate the genetic determinate in male development (King and Weiss, 1993; Soullier et al., 1999). HMG proteins have a wide variety of specialized roles, but they generally bind to nucleosomes and are classified by their divergent structures and binding properties (Goodwin et al., 1973; Bustin et al., 1996; Yang et al., 2010). Parallel ~80-amino acid sequences make up the box with a ~30-amino acid long tail which regulates binding sites on DNA nucleosomes and can exert influence over many different genes (Hargrave et al., 1997; Reeves, 2010). Parsimony analysis, which looks for the fewest changes between aligned sequences, identified the SOX class of genes as

a distinct group within HMG proteins (Soullier, 1999). SOX genes comprise a large class of genes that are further divided based on their diverse functions within different tissues, at developmental time points, and in response to varying pathological states.

SOX11 was one of several identified by Wright et al. in 1993 and was seen to be expressed between 8.5 and 15.5 days post coitum (DPC) in mouse embryos (Wright et al., 1993; Hargrave et al.,1997). Later studies found SOX11 widely expressed in the CNS and PNS and at epithelial-mesenchymal sites (Hargrave et al., 1997). Sequence analysis identified conserved carboxy-terminal motifs and serine-rich regions across mice and humans, suggesting the importance of considering SOX11 as a gene of interest in translational studies (Hargrave et al., 1997). Also identified by Hargrave et al. (1997) are sequences of rich, acidic residues linked closely to the transcriptional regulation of SOX11. SOX11 was expressed broadly at early timepoints, and around 9.5 DPC began to show tissue specification, mainly within the CNS and PNS. Specifically, SOX11 was observed in both DRG and TG between 11.5 and 15.5 DPC (Uwanogho, 1995; Hargrave et al., 1997). SOX11 is part of group C Sry-HMG transcription factors and has critical roles in neuronal development and pathology (Dy et al., 2008). Compared to the other two transcription factors, SOX4 and SOX12, that make up group C in vertebrates, SOX11 is substantially more influential on transcriptional modifications (Dy et al., 2008). Prior studies have found that the deletion of SOXC genes (4, 11, 12), which generally inhibit Notch signaling through Hes5 binding, impair axon growth and differentiation of contralateral retinal ganglion cells (Kuwajima, 2017; Mu et al., 2017). An additional study by Chang et al. (2017) identified the mechanism in which the SOXC genes 4 and 11 alter molecular pathways for retinal ganglion cell development. SOX4 binding to a ubiquitin modifier on SOX11 (SUMOylation) suppresses nuclear localization of SOX11 and inhibits its ability to promote retinal ganglion cell differentiation (Chang et al., 2017).

While many studies have examined the role of SOX11 in visual system development as it relates to retinal ganglion cells, glaucoma, and subsequent blindness, SOX11 has also been studied in peripheral nerve regeneration after other injury types, including nerve cut (Tanabe et al., 2003; Jankowski et al., 2006) and nerve crush (Jankowski et al., 2009). Studies have shown that SOX11 may be a critical upstream regulator of at least one regeneration cascade that aids in peripheral nerve regeneration following injury (Jankowski et al., 2006; Jankowski et al., 2009). Jankowski et al. (2006) examined SOX11 in Neuro2a neuroblastoma cells and cultured DRG cells to understand its role in neuron survival and neurite outgrowth. Their experiments showed that SOX11 is upregulated to aid in primary neuron differentiation and stages of neurite extension. When inhibited by siRNA, the absence of SOX11 decreased neurite growth and increased cell apoptosis through increased expression of pro-apoptosis genes BNIP3 and decreased expression of TANK, an anti-apoptosis gene in Neuro2a cells (Jankowski et al., 2006).

Additionally, SOX11 downregulation inhibited neurite growth and branching through a decrease in actin-related protein complex 3 (Arpc3), a gene involved in axon growth in DRG cells. SOX11 downregulation also increased apoptosis within DRG cultures, with evidence of decreased TANK expression (Jankowski et al., 2006). SOX11 has been recently studied in alveolar type 2 epithelial cells, Fang et al. (2021) found that reduced SOX11 can increase stretch-induced mechanical injury. This study examined the mechanism by which SOX11 signals FAK and Akt expression and apoptosis inhibition within epithelial cells. These results show that SOX11 likely influences the same molecular pathways in response to injury in different cell types, or at least in part.

A subsequent study by Jankowski et al. (2009) used an in vivo system to downregulate SOX11 in the saphenous nerve and found that regeneration was inhibited even after nerve

crush injury. This study also found that ATF3 was expressed in injured nerves, but its expression was significantly reduced with siRNA downregulation of SOX11 (Jankowski et al., 2009). ATF3 has been identified in prior studies to increase following nerve injury (Tsujino et al., 2000; Lindå, 2011) and influence the expression of other genes that support neuron survival and axon growth after injury. ATF3 has been associated with JNK-activated c-jun on the influence on axonal regeneration following nerve ligation (Lindwall et al., 2004), and binding sites for c-Jun on ATF3 further support this connection (Liang, 1996). A study by Lindwall et al. (2004) found that inhibition of JNK did not influence overall neuronal survival but did reduce axon regeneration and ATF3 expression. ATF3, specifically upregulated after PNS injury, has been found to promote the regeneration of thinly branching neurites, but its overexpression does not increase c-Jun expression (Seijffers et al., 2006). Seijffers et al. (2006) further identifies ATF3 as a necessary molecular factor in PNS regeneration and identifies it as a downstream factor of c-Jun. Results from Seijffers et al. (2006) and Jankowski et al. (2009), place ATF3, SOX11 and c-Jun in shared regeneration pathways with potential overlap and compensatory activation mechanisms that have not yet been explicitly reported. ATF3 downregulation only decreases ATF3 expression, and no change in SOX11 expression is observed (Jankowski et al., 2009). As in earlier studies showing ATF3 is under c-Jun regulatory control, ATF3 may be under SOX11 regulation. This places c-Jun and SOX11 as upstream transcription factors regulating other transcription factors that have influential contributions to nerve regeneration.

ATF3 has been established as an essential transcription factor in not only peripheral nerve injury response but also in other cellular stress responses (Wu et al., 2010; Hoetzenecker et al., 2012; Gold et al., 2012; Wolford et al., 2013; Yuan et al., 2013; Wang et al., 2015; Zhao et al., 2016). Changes to normal ATF3 responses in periods of biology stress and disease can

lead to severe chronic pathology. ChIP-seq and microarray analysis has identified that ATF3 likely regulates genes proximal to p300 and H3k27ac transcription promoters (Zhao et al., 2016). Additionally, the gene expression analysis done by Zhao et al. (2016) showed that ATF3 colocalized with p53 and likely influences other transcription factors that bind to p300 and H3k27ac regions that have multiple bindings sites for many other transcription factors. An earlier study describes ATF3 binding as a homodimer to repress transcription. When co-expressed as a heterodimer, it is found to activate transcription (Hai, 1999). Together, these results suggest that ATF3 can influence multiple response cascades during times of cellular stress and injury.

1.2. Experimental Overview

Many studies have characterized corneal neurons in health and after injury. A comprehensive understanding of corneal anatomy, neuronal subclasses, neurophysiology, and diverse sensory functioning has been achieved through these studies. In recent years, a controversial idea in corneal neuroscience is one where once distinctly defined corneal subclasses adopt neuroprotective, and at times pathological, post-injury phenotypes. Additionally, while insights into corneal healing and regenerative processes have been revealed in recent years, questions remain regarding essential molecular contributors to neuronal and epithelial healing and how they can be used in clinically effective treatment paradigms. The series of experiments subsequently presented will investigate questions surrounding the phenotypic shifts observed after corneal injury and explore critical regeneration factors and their specific contributions to post-injury phenotypes.

The first study will isolate corneal neurons using an optimized retrograde labeling method to isolate the corneal subpopulation within the TG. mRNA and protein expression will be evaluated within the tracer labeled subpopulation to identify phenotypes in health and injury

states. Extensive exploration of labeling properties of different fluorescent tracers ensures that any phenotypic changes identified are purely from pathophysiological processes and not due to tracer labeling bias. Embedded corneal neuron fibers are quantified using a combination of *Nav1.8*Cre-tdTomato mouse and innervation density analysis. Epithelial injury and nerve regeneration processes are evaluated in the context of a chronic DED-injury model, which is validated through tearing and ocular discomfort assays.

The second study uses downregulated SOX11 in *Nav1.8*Cre-tdTomato-*Sox11f/f* neurons to investigate the role of a known upstream RAG in the epithelial and nerve regeneration processes in the previously described chronic DED-injury model. This study identifies phenotypic changes occurring in the corneal TG subpopulation in the absence of SOX11. Epithelial healing and nerve regeneration are also explored in this chronic injury model.

The third study uses the same downregulation of SOX11 with *Sox11$^{fl/fl}$* animals but in an acute model of CA-induced injury. In contrast to the chronic injury model, corneas are able to restore homeostasis through normal regenerative and healing processes following the acute injury. The role of SOX11 can be further understood in how it impacts standard healing mechanisms that are impossible in the chronic DED model of corneal injury. Phenotypic changes within the corneal TG subpopulation are also investigated, as are epithelial healing and nerve regeneration.

CHAPTER TWO

LACRIMAL GLAND EXCISION INDUCES A PHENOTYPIC SWITCH IN CORNEAL NEURONS

2.1. Abstract

Dry eye is a common cause of ocular pain. The aim of this study was to investigate corneal sensitivity, innervation, and alterations in corneal afferent phenotypes in a mouse model of severe aqueous tear deficiency. Chronic dry eye was produced by ipsilateral excision of the extra- and intraorbital lacrimal glands in male and female mice. Tearing was measured using a phenol thread and corneal epithelial damage assessed using fluorescein. Changes in corneal ongoing ocular pain was evaluated by measuring palpebral opening ratio. Corneal axons were visualized using *Nav1.8*-tdTomato reporter mice. Immunohistochemistry was performed to characterize somal expression of CGRP, the capsaicin sensitive TRPV1, and ATF3 in tracer labeled corneal neurons following LGE. LGE decreased tearing, created severe epithelial damage, and decreased palpebral opening, indicative of chronic ocular irritation over the 14-day observation period. Corneal axon terminals exhibited an acute decrease in density after LGE, followed by a regenerative process over the course of 28 days that greater in male animals. Corneal neurons expressing CGRP, TRPV1, and ATF3 increased following injury, corresponding to axonal injury and regeneration processes observed during the same period. CGRP and TRPV1 expression was notably increased in IB4-positive cells following LGE. These results indicate that dry eye-induced damage to corneal afferents can result in a phenotypic switch in these neurons which may enhance neuroprotective mechanisms to create resiliency after chronic injury.

2.2. Introduction

DED is often accompanied by a pathological corneal microenvironment that injures axon terminals and promotes neuropathic pain (Meng and Kurose, 2013; Galor et al., 2016; Kovacs et al., 2016; Belmonte et al., 2017). Chronic ocular dysesthesias can be resistant to available treatments and interfere with the quality of life for an increasingly diverse and growing patient population (Gayton et al., 2009; Shah et al., 2015; Cook et al., 2019; Golebiowski et al., 2020). In preclinical studies, LGE-induced aqueous tear deficiency produces corneal epithelial damage and signs of ocular discomfort, as well as alterations in the properties of corneal primary afferent neurons (Kurose and Meng, 2013; Stevenson et al., 2014; Meng et al., 2015; Katagiri et al., 2015; Kovacs et al., 2016; Shinomiya et al., 2018; Hatta et al., 2019; Meng, 2019; Mecum et al., 2019; Skrzypecki et al., 2019; Mecum et al., 2020). Altered nerve morphology (Kovacs et al., 2016) and reduced axon density has also been reported following LGE (Kovacs et al., 2016; Fakih et al., 2019). While corneal injury and sensitivity changes have been well characterized after LGE, the mechanisms which lead to neuropathic-like ocular pain remain poorly defined.

Corneal nerves regulate tearing to maintain ocular homeostasis and protect from noxious insults (Dartt, 2009; Meng and Kurose, 2013). Tears typically provide the cornea with nutrients and oxygen and assist in the removal of cellular waste byproducts (Dartt, 2009). In their absence, angiogenic factors increase in order for corneal neovascularization to supplement these functions (Barabino et al., 2012). Following injury, compensatory neuroprotective mechanisms are initiated through increases in proangiogenic and proinflammatory neuropeptides, such as CGRP and SP, released from primary afferent neurons. Increased release of CGRP and SP after injury results in sensitization of corneal afferents and an increase in corneal sensitivity, which can provide protection from further injury (Jones and Marfurt, 1998;

26

Russell et al., 2014). In health, corneal C-fibers are made up of diverse peptidergic and non-peptidergic populations of mechanoreceptors (20%), cool cells (10%), and polymodal neurons (70%) (Belmonte et al., 2004; Moulton and Borsook, 2019). Peptidergic neurons are typically defined by their expression of neuropeptides such as CGRP and SP and in the mouse are primarily distinct from IB4 binding neurons (Marfurt and Dvoscak, 2006; LePichon and Chesler, 2014). Previous studies have shown increases in the capsaicin, heat, and acid sensitive TRPV1 and other pronociceptive genes after dry eye-induced corneal injury, yet whether these alterations occur selectively in peptidergic or non-peptidergic neurons remains unknown (Bereiter, 2018; Hatta et al., 2019; Fakih et al., 2021).

Other post-injury responses, including upregulation of ATF3, promote axonal regeneration directly following injury, guide successful axon elongation and corneal reinnervation (Seijffers, 2006; Hegarty, 2018; Fakih, 2019; Guerrero-Moreno, 2020). ATF3 is part of a complex regeneration signaling network that promotes neuroprotection and healing following injury of peripheral neurons (Seijffers et al., 2007; Gey et al., 2016; Wong et al., 2018). Increased activity in this network is sustained after corneal injury and may contribute to widespread shifts in corneal afferent sensitivity and molecular profiles (Chaudhary et al., 2012).

This study aimed to characterize corneal nerve injury and regeneration processes in an LGE mouse model of severe chronic DED. We report phenotypic changes in corneal afferent neurons, whereby IB4-positive neurons express CGRP after LGE, which may link the expression of critical molecular injury and regeneration regulators to ocular neuropathic pain.

2.3 Material and methods

2.3.1 Generation of *Nav1.8*-tdTomato mice

Nav1.8-Cre-C57B6/J mice obtained from Dr. Sulayman D. Dib-Hajj (Yale University, New Haven, CT, USA) were re-derived and bred with B6.Cg-Gt(ROSA)26Sortm14(CAG-tdTomato)Hze/J (Stock #007914, The Jackson Laboratory, Bar Harbor, ME, USA). The resulting F1 progeny that were heterozygous for *Nav1.8*-Cre and tdTomato were intercrossed to result in mice with specific expression of tdTomato fluorescent protein in *Nav1.8*-expressing neurons.

For genotyping, tissue was lysed by adding 50mM NaOH and then heated to at 95°C for 35 min, followed by the addition of 50mM HCl and 1M Tris HCl buffer. The sample was spun down and then stored at 4°C until processed. Polymerase chain reaction (PCR) was used to identify tdTomato using Econotaq Plus 2x Buffer (Lucigen, Middleton, WI, USA). Primers included: Td tomato Mutant Forward– CTGTTCCTGTACGGCATGG, Td Tomato Mutant Reverse – GGCATTAAAGCAGCGTATCC, Td Tomato Wild Type Forward – AAGGAGCTGCAGTGGAGTA, Td Tomato Wild Type Reverse – CCGAAAATCGTGGGAAGTC. *Nav1.8*-Cre reactions were prepared with Promega GoTag Flexi-buffer (Promega, Madison, WI, USA). Primers included: *Nav1.8*-Cre Common Forward – GGAATGGGATGGAGCTTCTTA, *Nav1.8*-Cre Mutant Reverse – CCAATGTTGCTGGATAGTTTTTACTGCC, *Nav1.8*-Cre Wild Type Reverse – TTACCCGGTGTGTGCTGTAGAAAG. Genotyping of all animals was conducted by the University of New England Behavior and Genotyping Core.

2.3.2. Animals

Adult male and female C57BL/6J (Jackson Laboratory, Bar Harbor, ME, USA) mice and *Nav1.8*-tdTomato mice (8-10 weeks old) were housed and given food ad libitum. All animal

study protocols were approved by the Committee on Animal Research at the University of New England. Animals were treated in accordance with policies and recommendations of the National Institutes of Health Guide for the Care and Use of Laboratory Animals.

2.3.3. Lacrimal gland excision

Unilateral dry eye was created by excising the left exorbital and infraorbital lacrimal glands under isoflurane anesthesia (Mecum et al.,2019). Sham surgery was performed on control animals by making incisions over the left exorbital and infraorbital gland sites. Animals were monitored daily for 5 days post-surgery (Figure 2.1.A).

2.3.4. Retrograde neuronal tracing

At 72 hrs prior to LGE or sham surgery tracers were applied to the cornea, including FluoroGold (FG, 3% in NaCl; Fluorochrome, Denver, CO, USA), Fast Blue (FB, 5% in NaCl; PolySciences, Warrington, PA), FM-143x (FM, 5% in NaCl, ThermoFisher Scientific, Waltham, MA, USA) and 1,1'-Dioctadecyl-3,3,3',3'-Tetramethylindocarbocyanine Perchlorate (DiI, 5% in 20% DMSO in H2O, ThermoFisher Scientific, Waltham, MA, USA). Under isoflurane anesthesia, a DC current (7 µA for 10 min) (Kumar et al., 2017) was passed between a copper wire in a capillary tube filled with either a single tracer or a combination of two (FG/FM143x, FB/FM143x, FG/DiI) and a copper cathode placed in the tail (Figure 2.1.A). An absorbent gelatin sponge (Gelfoam 12–7 mm; Pfizer Pharmaceuticals, New York, NY) was cut, inserted into the capillary tube, and placed in contact with both the cornea and the tracer solution within the capillary tube, thus allowing the current to pass through to the eye (Cassagne et al., 2016). In preliminary studies, iontophoresis did not produce signs of epithelial damage as evidenced by an absence of corneal fluorescein staining.

2.3.5. Palpebral opening

Eye closure, or squinting, as a sign of ocular discomfort, was evaluated by video recording the mice for 5 min after placing them on top of a glass dish (4 ¼" L x 3/8" W x 3"H). Five still shots were taken from the video and the height of the gap between the upper and lower eyelids and the distance separating the two canthi (Fakih et al., 2019) was measured using ImageJ/FIJI. The palpebral opening for each still shot was calculated as the height divided by the distance separating the two canthi, which were averaged together for an overall palpebral opening ratio.

2.3.6 Tear production

Tear volume was measured using phenol red thread (Zone-Quick, FCI Ophthalmic, Pembroke, MA, USA) inserted into the lateral canthus of the eye for 15 seconds in unanesthetized animals. The thread becomes red as it absorbs the tears and the length of the red portion of the thread was measured under a dissecting microscope (Figure 2.1.B).

2.3.7. Cornea fluorescein staining

Fluorescein staining was used to assess corneal epithelial damage. The staining was performed prior to and 2-weeks following LGE. A fluorescein solution (1%, 10µl; Sigma-Aldrich Corp., St. Louis, MO, USA) was applied to the cornea while animals were under isoflurane anesthesia. After 2 min, the eye was rinsed with artificial tears and visualized with a cobalt blue light (16 LED Blue Flashlight, 464 nm, LDP LLC, Carlstadt, NJ, USA). The area of staining was evaluated on a 0 to 4 scale. Total absence of staining was scored a 0, less than 1/8 of total area scored a 1, 1/8-1/4 was given a 2, 1/4-1/2 a 3, and any fluorescein staining greater than 50% of

the total corneal surface area was scored a 4 (Suwan-apichon et al., 2006; Kurose and Meng, 2013; Meng et al., 2015).

2.3.8. Cornea collection and processing

At 7,14, 28 days post-LGE or sham surgery, *Nav1.8*-tdTomato animals were deeply anesthetized with Euthasol (Henry Schein, Melville, NY, USA) and eyeballs were removed using curved blade fine scissors (Item # 14061-10, Fine Science Tools, Foster City, CA, USA). Eyeballs were briefly fixed with 10% formalin and transferred into phosphate buffered saline (PBS) before dissection. Corneas were dissected out and washed three times in PBS on a low-speed shaker at room temperature for 10 min. After making 3 pie cuts along the periphery to allow the corneas to lie flat, corneas were whole-mounted onto slides with DAPI infused mounting media (ProLong Gold Antifade with Dapi, ThermoFisher Scientific, Waltham, MA, USA). Corneas were imaged at 40x using a Keyence BZ-X series fluorescence microscope. Five images were taken, in a z-stack in 1 µm steps, with one in the central and four in the peripheral regions of the cornea. The center was selected based on the converged spiral of subbasal axons and the peripheral areas were chosen at a diagonal of the central image. Images were split into free nerve ending and sub basal layers and analyzed using FIJI/IMAGEJ. The maximum projection of each z-stack was converted to a mask and the Sholl Analysis plugin was used to quantify innervation density.

2.3.9. RT-qPCR analysis

RNA was isolated (Promega Total RNA Isolation System, Fitchburg, WI, USA) from whole corneas and TG dissected and stored in RNAlater solution (Sigma-Aldrich, St. Louis, MO, USA). The quantity and concentration of RNA was measured using a NanoDrop (Thermo

Scientific, Waltham, MA, USA). cDNA library was created using reverse transcription of RNA

samples (cDNA Reverse Transcription Kit, Thermo Scientific, Waltham, MA, USA). Quantitative

real-time PCR was performed with a solution of 8uL of cDNA, 10uL of PCR Master Mix

(TaqMan, Thermo Fisher, Waltham, MA, USA), 0.5 uL forward (5'-

GCGCGGATCCATGATGCTTCAACATCCA-3') and 0.5 uL reverse (5′-

GCGCAAGCTTTTAGCTCT GCAATGTTCCTTCTTTT-3') primers for ATF3 (Integrated DNA

Technologies, Coralville, Iowa, USA), with 1μL DEPC treated H_2O (UltraPure,Thermo Fisher,

Waltham, MA, USA) for 20 μL total volume. Each sample was amplified in triplicate. Expression

levels were normalized and data presented in fold-change in respect to control values.

2.3.10. Immunofluorescence staining

Two weeks after sham or LGE surgery, animals were deeply anesthetized with

pentobarbital (Euthasol, Henry Schein, Melville, NY, USA) and sacrificed by transcardial

perfusion with sodium chloride with 1% heparin (Sagent Pharmaceuticals, Schaumburg, IL),

followed by ice-cooled 10% neutral buffered formalin (Sigma Aldrich, St. Louis, MO, USA) or 4%

paraformaldehyde used for TRPV1 study. The TG were dissected, post-fixed in 10% formalin

overnight at 4°C, and transferred to 30% sucrose for a minimum of 72 hrs. Serial sections

(12μm) were cut using a cryostat (Leica CM1950, Leica Biosystems, Lincolnshire, IL, USA).

Slides were initially washed three times with PBS (0.1M PBS) for 5 min each. This was

followed by one 15 min wash in PBS with 0.1% triton-X (PBST). The slides were blocked in 5%

normal goat serum (Vector Laboratories, Burlingame, CA, USA) in PBST for 1 hour at room

temperature. Different serial sections were incubated overnight at 4°C with primary antibodies

for either CGRP (1:750, Bio-Rad Laboratories, Portland, ME, USA), IB4-488 (1:500, Bio-Rad

Laboratories, Portland, ME, USA), ATF3 (1:1250, Santa Cruz Biotechnology, Dallas, TX, USA)

or TRPV1 (1:1000, Santa Cruz Biotechnology, Dallas, TX, USA). Sections were washed three times with PBST to and then incubated with a secondary antibody (Alexa Fluor 488, 1:1000) for 1 hour at room temperature. A no primary antibody control was used to validate the observed fluorescence. After washing three times in PBS, slides were incubated with a nuclear stain (NucRed Live 647, ThermoFisher Scientific, Waltham, MA, USA), two drops diluted per ml of diH$_2$O for 20 min at room temperature. Slides were washed three more times with PBS, mounted using a fluorescence preserving mounting media (FluoroMount-G, ThermoFisher Scientific, Waltham, MA, USA) and sealed.

Immunohistochemistry for protein gene product 9.5 (PGP9.5) (ab108986, Abcam, Cambridge, MA, USA) was performed on whole mount corneas. After intraperitoneal injection (Euthasol, Henry Schein, Melville, NY, USA) and loss of corneal reflex, eyeballs were enucleated fixed for 30 minutes in 10% formalin, and corneas dissected in PBS. Corneas were fixed for 45 min in formalin, followed by three 5-minute PBS wash and incubated while shaking for 1 hour at room temperature in blocking solutions (0.5% triton x-100 in 10% normal donkey serum in 0.1 M PBS). Corneas were incubated overnight shaking at 4°C in anti-PGP9.5 (1:500 in 0.1M PBS in 0.3% triton x-100 + 5% normal donkey serum). Following this, corneas were washed in PBS three times for 5 min while shaking. The corneas were incubated overnight while shaking at 4°C with secondary antibody (donkey anti-rabbit Alexa Fluor 488, 1:200 in 0.1M PBS in 0.3% triton x-100 + 5% normal donkey serum). Corneas were washed in PBS three times for 5-minute before being whole mounted on slides with DAPI mounting media (ProLong Gold Antifade with Dapi, ThermoFisher Scientific, Waltham, MA, USA).

Sections were imaged at 20x with a Keyence BZ-X series fluorescent microscope (Keyence, Itasca, IL) using filter cubes for DAPI (excitation (ex.): 340–400 nm; emission (em.): 435–485 nm), GFP (ex.: 450–490 nm; em.: 500–550 nm), Cy3 (ex.: 530–560 nm; em.: 570–640

33

nm), and Cy5 (ex.: 590–650 nm; em.: 665–735 nm). Keyence Analyzer software was used to stitch images of each section in each channel. ImageJ software (National Institutes of Health, Bethesda, MD) was used to merge each fluorescent channel into a final composite. Images were randomized and blinded before counting. Cells positive for fluorescent markers were manually counted and marked using the Cell Counter plugin in ImageJ. Cells were counted as positive if the fluorescent marker was present in the channel specific image and if it corresponded to a cell containing nuclei when viewed as a merged composite. Co-labeled cells were counted as positive if they were determined to be within the same cell that contained a nucleus using individual and composite channel images. Percentages were calculated using the total number of tracer positive cells normalized for each animal total. Cell diameter was measured using the measurement tool in ImageJ/FIJI calibrated to the image scale. All images were blinded prior to analysis.

2.3.11. Data analysis

Statistical analyses for palpebral opening, tear production, cell counts, and cell diameters were performed with either t-tests, one-way, two-way or three-way ANOVAs with Tukey post-hoc tests. Fluorescein staining was evaluated using a Kruskal-Wallis one-way ANOVA with Dunn's post hoc test performed. All statistical analyses were performed using excel and R. Statistical significances were accepted as $p < 0.05$. Plots, tables and diagrams were created using R, Excel, and PowerPoint. Data are presented as the mean ± SEM.

2.4 Results

2.4.1. Lacrimal gland excision reduces tearing and damages corneal epithelium

Retrograde tracer was applied to the cornea 3-days before LGE (Figure 2.1.A). Tear levels and corneal epithelial damage were assessed 14-days after excision, prior to tissue collection. Consistent with previous studies (Mecum et al., 2019; Mecum et al., 2020), aqueous tearing in both male and female animals was reduced following LGE, as measured using a phenol thread test (Figure 2.1.B, $p<0.0001$, 3-way ANOVA, Table 2.1.). Examination of corneal fluorescein staining at this time found significant areas of corneal damage after LGE when compared to sham controls, with no apparent differences between male and female mice using the previously described 0-4 rating scale to quantify the fluorescein-stained corneal area (Figure 2.1.C, $p<0.0001$, Kruskal-Wallis ANOVA, Table 2.1.).

2.4.2. Lacrimal gland excision causes ongoing pain-like behavior

Squinting behavior has previously been established as a measure of ongoing corneal pain after LGE in the mouse by quantifying the size of the palpebral opening (Figure 2.2.A) (Fakih et al., 2019; Mecum et al., 2020). A reduction in palpebral opening is also accompanied by a unilateral grimace-like facial expression on the side of the ipsilateral eye to gland excision (Figure 2.2.B, left panel). Comparing the palpebral opening between LGE and sham treated animals demonstrated a significant reduction after LGE (Figure 2.2.B, $p<0.001$, 3-way ANOVA, Table 2.1.).

2.4.3. Corneal reinnervation after acute axonal retraction

Innervation of the cornea was visualized in whole-mounted corneas using a tdTomato fluorescent reporter expressed with the *Nav1.8*-cre promoter. *Nav1.8*-cre;tdTomato labeling of corneal innervation was validated using PGP9.5 as a pan-neuronal marker. A total of 87% of corneal axons labeled with PGP9.5 were co-labeled with tdTomato (Figure 2.3.A). As most corneal axons were labeled with tdTomato, subsequent studies quantified innervation density using the *Nav1.8*-cre;tdTomato reporter, conducting an overlayed Sholl analysis on the max projection z-stack images. Innervation density was evaluated in central and peripheral regions of the cornea, and in subbasal and intraepithelial layers (Figure 2.3.A, right panels). Sholl-determined intersections were combined from subbasal and intraepithelial layers and averaged across five area samples to get a mean innervation density for each eye (Mecum et al., 2020). At one-week following LGE, there was a dramatic decrease in corneal nerve innervation, with gradual reinnervation of the cornea occurring throughout 4-weeks. The reinnervation of the cornea remained disorganized when compared to the whirl pattern of the subbasal nerve plexus seen in the sham treated animals (Figure 2.3.B).

Quantification of the innervation density revealed a significant reduction in innervation in both female (Figure 2.3.C, $p<0.0001$, 2-way ANOVA, Table 2.1.) and male (Figure 2.3.D, $p<0.0001$, 2-way ANOVA, Table 2.1.) animals after LGE when compared to sham treated groups. Post-hoc analysis revealed that corneal innervation after LGE remained lower than sham levels in both female and male animals through day 28. However, only male animals showed an increase in innervation 28 days after LGE when compared the 7- and 14-day time points (Figure 2.3.D, $p < 0.001$).

2.4.4. Lacrimal gland excision increases the number of CGRP-positive corneal afferents

Corneal projecting somas were identified within the TG following the iontophoretic application of four different retrograde tracers. Corneal afferents have proven to be inefficient at taking up retrograde tracers without disrupting the epithelial barrier (Köbbert et al., 2000). While this is often accomplished by mechanical abrasion or chemical injury to the cornea, iontophoretic application resulted in tracer uptake without damage to the corneal epithelium as determined by the absence of corneal fluorescein staining after the procedure in preliminary studies. Since the preferential uptake of retrograde tracers by subpopulations of afferents can introduce selection bias, a direct comparison of labeled corneal neurons was performed after the dual application of tracers, each with separate emission spectra (FB-ex. 365nm/em. 420nm, FG-ex.414nm/em.541nm, FM-ex.475nm/em.580nm, DiI-ex.550nm-570nm). Tracer labeling preferences were evident from mean diameter measurements, which showed FG and FM labeled a wide range of different sized somas, while FB and DiI appear to have some bias toward labeling smaller diameter neurons (Figure 2.4.A). The total number of labeled neurons by each tracer also differed (Figure 2.1.B, 1-way ANOVA, Table 2.1.). Overall, the total number of DiI ($p<0.0001$) and FM143x ($p<0.01$) labeled neurons was significantly greater than both FB and FG. Surprisingly, when two tracers were co-applied, the two different tracers showed relatively little colocalization (<25%), with the majority of neurons labeled independently with only one tracer (Figure 2.4.B).

In sham treated animals, the percentage of corneal projecting neurons that were IB4-positive was similar across each of the four tracers (FG: 52.7 ± 5.0%, FB: 44.5 ± 5.4%, DiI: 40.1 ± 3.8%, FM: 35.5 ± 3.8%), with mean labeling of IB4 across all tracer positive cells at 43.2%. CGRP labeled an average of 37% of all tracer positive corneal neurons in sham treated animals (FG: 32.3 ± 6.0%, FB: 48.2 ± 5.1%, DiI: 33.8 ± 7.2%, FM: 33.7 ± 5.3%). While LGE had no

effect on the percentage of IB4-positive corneal cells (FG: 64.3 ± 6.6%, FB: 43.4 ± 3.3%, DiI: 42.4 ± 5.1%, FM: 37.1 ± 2.5%), a significant increase in CGRP co-labeled corneal neurons was found 14 days after LGE with FG (66.0 ± 4.0%), FB (66.8 ± 4.0%), and DiI (63.0 ± 5.0%) tracers, and approaching significance with FM (43.9 ± 2.7%) (Figure 2.4.D, FG p<0.0001, FB p<0.01, DiI p<0.001, t-test).

2.4.5. Lacrimal gland excision increases the percentage of IB4-positive cells co-labeled with CGRP and TRPV1

A single tracer was applied to the cornea to determine whether LGE altered the expression of CGRP and TRPV1 in IB4-positive corneal afferents. For these studies, FG was selected based on the relatively wide range of corneal cell soma sizes labeled with FG and the significant increase in CGRP-positive FG neurons observed when FG was co-applied with a second tracer (Figure 2.4.D). The ipsilateral TG were collected 14-days following unilateral LGE and co-labeled with CGRP and IB4 (Figure 2.5.), and in a separate set of animals with TRPV1 and IB4 (Figure 2.6.). The percentage of FG neurons co-labeled with both CGRP and IB4 was greater in LGE animals when compared to sham treatment (Figure 2.5.B, p<0.001, t-test). Consistent with this finding, LGE decreased the percentage of FG neurons that were IB4-positive and CGRP-negative (Figure 2.5.B, p<0.001, t-test). In addition, LGE increased the percentage of FG neurons that were CGRP-positive and IB4-negative (Figure 2.5.B, p<0.0001, t-test), indicating that CGRP increased in both the IB4-positive and IB4-negative cell populations.

Similarly, the percentage of FG-positive neurons labeled with TRPV1 increased in the IB4-positive population (Figure 2.6.B, p<0.01, t-test), with a parallel decrease found in the IB4-positive neurons that wereTRPV1-negative (Figure 2.6.B, p<0.001, t-test). Unlike CGRP, no

38

difference was found between LGE and sham treated animals in the IB4-negative population of neurons that were either TRPV1-positive neurons or TRPV1-negative (Figure 2.6.B, p>0.05).

2.4.6. Lacrimal gland excision increases the number of ATF3-positive corneal afferents

The nerve injury transcription factor ATF3 was quantified in the ipsilateral TG 14-days following LGE. Both immunohistochemistry and RT-qPCR were performed to determine overall changes in ATF3 expression. Immunolabeled ATF3 was quantified as a proportion of the total number of neurons using NeuN as a pan-neuronal marker (Figure 2.7.A). In naïve animals, less than 0.5% of TG neurons were ATF3-positive (Figure 2.7.B). LGE increased the number of ATF3-positive neurons by more than 2-fold, yet the overall percentage of ATF3-positive neurons remained under 1.5%. A comparison of ATF3-positive neurons in naïve, sham, and LGE animals showed a treatment effect, with greater numbers of ATF3-positive neurons after LGE when compared to naïve and sham treatment groups (Figure 2.7.B, $p<0.0001$, one-way ANOVA, Tukey post hoc). ATF3 expression evaluated using RT-qPCR more than doubled in both ipsilateral TG and in ipsilateral whole corneas over tissue from sham treated animals (Figure 2.7.C).

To further evaluate ATF3 within corneal neurons, ATF3 immunolabeling was quantified in LGE and sham treated animals following FG tracer application to the cornea. In FG labeled neurons, the percentage of ATF3-positive neurons increased after LGE compared to sham treatment (Figure 2.7.D left, $p<0.001$, t-test). In a subsequent cohort, ATF3 was quantified in IB4-positive and CGRP-positive corneal neurons. The percentage of FG neurons labeled with both IB4 and ATF3, or both CGRP and ATF3, was greater in LGE than sham treated animals (Figure 2.7.D right, $p<0.01$, t-test).

2.5. Discussion

Prior studies have excised the ipsilateral extraorbital and intraorbital lacrimal glands to produce severe aqueous tear deficient dry eye in both rats (Kurose and Meng, 2013; Meng et al., 2015; Mecum et al., 2019; Hatta et al., 2019; Skryzypecki et al., 2019) and mice (Shinomiya et al., 2018; Meng et al., 2019; Mecum et al., 2020). Corneal injury and pain-like behaviors have been well characterized in these studies. This study examined corneal innervation after LGE and investigated plasticity in corneal projecting neurons that may contribute to nerve regeneration, corneal wound healing, and nociceptor sensitization after injury. The results indicate that denervation and reinnervation of the cornea after LGE is accompanied by increased expression of the neuronal injury marker ATF3 and a phenotypic switch in corneal afferents, consisting of increased CGRP and TRPV1 expression in IB4-positive corneal neurons.

In agreement with prior findings (Meng et al., 2015; Shinomiya et al., 2018; Mecum et al., 2019), all LGE animals exhibited drastically reduced ipsilateral tearing and increased corneal fluorescein staining. Other primary dry eye symptoms included signs of persistent ocular irritation, evidenced by a decrease in palpebral opening (Gowrisankaran et al., 2007). Ocular pain is typically the chief complaint described in dry eye clinical populations (Galor et al., 2016; Kalangara et al., 2017; Elhusseiny et al., 2019; Donthineni et al., 2021). Dryness on the corneal surface sensitizes and activates corneal afferent nociceptors, which in turn evokes blinking, tearing, and squinting behaviors (Nakamori et al., 1997; Tsubota, 1998; Belmonte et al., 2017; Mecum et al., 2020). Studies in rats have reported increased blinking for 8-weeks following LGE that is reduced by topical application of a local anesthetic (Kurose and Meng, 2013; Meng et al., 2015). Unlike the rat, mice rarely exhibit spontaneous blinking after LGE, and as in prior studies

(Fakih et al., 2019; Mecum et al., 2020), we instead found a decrease in palpebral opening with an ipsilateral grimace following LGE.

Using *Nav1.8*-cre;tdTomato mice to examine corneal innervation, we observed an almost complete loss of axon terminals through superficial layers of the corneal epithelium to the subbasal nerve plexus at 7-days following LGE in both male and female mice. Innervation increased in intraepithelial and subbasal layers at 14-days and continued to increase when evaluated at 28-days, most prominently in male mice. A previous study, also using *Nav1.8*-cre;tdTomato mice, found no difference in innervation density at 14-days after excision of only the extraorbital lacrimal gland (Mecum et al., 2020), indicating that the severity of dry eye likely contributed to the amount of denervation observed in the present study. Other studies have examined corneal innervation in dry eye models using immunohistochemistry, typically, of beta-III tubulin, to visualized corneal nerve terminals (Aicher et al., 2015; Kovács et al., 2016; Yamazaki et al., 2017). Through these methods, one of these studies found that a semaphorin 3A inhibitor may provide a protective effect over nerve and epithelial integrity in DED (Yamazaki et al., 2017). Another study found that corneal cool cells may be responsible for ocular discomfort in DED (Kovács et al., 2016). Additionally, that denervation of the lacrimal gland may result in corneal hypoalgesia (Aicher et al. 2015). The use of the *Nav1.8*-cre;tdTomato reporter appeared to label the vast majority of corneal afferents, with the likely exception of autonomic neurons and up to 80% of cool sensing neurons that do not express Nav1.8, indicating that use of this mouse would be a valuable tool in longitudinal studies to track corneal sensory innervation (Bouheraoua et al., 2019; Luiz et al., 2019).

Clinical studies report DED can be accompanied by a decrease in corneal innervation, but no sex specific differences in innervation density or morphology have been reported (Erdelyi et al., 2007; Benítez-del-Castillo et al., 2007; Hamrah et al., 2017; Sullivan et al., 2017). In the

present study, there were no differences observed between male and female animals in basal innervation, yet corneal afferents in male animals regenerated more quickly when compared to females. Consistent with these results, male rats were observed to have increased axonal outgrowth when compared to female counterparts one week after sciatic nerve transection (Stenberg and Dahlin, 2014). However, in contrast to the present findings, in a corneal abrasion injury model female mice were observed to have increased nerve regeneration compared to male mice (Pham et al., 2019). Other studies of corneal injury have either reported no sex differences in corneal innervation (Kovács et al., 2016; He et al., 2019; Mecum et al., 2020) or have only used animals of a single sex (Aicher et al., 2015; Yamazaki et al., 2017; Hegarty et al., 2018).

After injury, corneal reinnervation benefits from the activation of RAGs. ATF3 is a nerve injury marker and upstream transcription factor, widely evaluated for its role in initiating nerve regeneration cascades (Takeda et al., 2000; Jankowski et al., 2009; Nascimento et al., 2011; Launay et al., 2016; Hegarty et al., 2018; Fakih et al., 2019). ATF3 expression increased in corneal neurons following LGE but no difference was found between male and female animals. The slower axonal regeneration in female mice after LGE may be due to a greater inflammatory response after injury (Mecum et al., 2019). In disease processes that also exhibit sustained inflammation, such as in chronic DED (Luo et al., 2004; Hessen and Akpek, 2014) and osteoarthritis (Ivanavicius et al., 2007; Nascimento et al., 2011), nerve damage is severe and regenerative processes are impaired.

To evaluate corneal neurons after dry eye-induced injury, iontophoretic retrograde tracer application was optimized to label corneal cell somas within the TG without injuring the cornea. Due to the inherent difficulty of labeling an immune-privileged structure, various corneal retrograde application methods have been studied. Most methods utilize some form of injury to

disturb terminal membranes, allowing fluorophores to enter the corneal axons and be transported up the terminal to the cell bodies in the TG. Injury methods have varied from a checkerboard scratch (Arvidson, 1977; Marfurt et al., 1989; Keller, 1999; Ivanusic et al., 2012; Bron et al., 2014; Alamri et al., 2015), to 70% ETOH deepithelization (Murata and Masuko, 2006; Launay et al., 2015) and microinjection (Nakamura et al., 2007). While not directly damaging, direct application requires animals to be anesthetized for extended periods (Moreira et al., 2007), which may lead to additional corneal damage (Turner et al., 2005; Koehn et al., 2015). Iontophoresis was used in the current study, as it requires only a short duration of anesthesia and we found no evidence of corneal epithelial damage after delivery (Chen and Hong-Sen, 1990, Schofield, 2008; Kumar et al., 2017; Hatta et al., 2019).

Potential bias in the cell populations labeled by the different tracers FG, FB, FM, and DiI was determined after co-application of different tracer combinations followed by staining for IB4 and CGRP. Both FG and FM labeled the largest range of neurons based on cell soma diameter measurements. In addition, FM labeled a larger proportion of neurons when simultaneously applied with FB or FG. As reported in other studies, it is possible that a portion of FM labeling could be a confound of tissue processing caused by adjacent cell leaking (Jockusch and Eberhard, 2007). Fast blue and FG labeled comparable numbers of corneal cells, yet FB appeared to preferentially label a higher number of small diameter neurons while FG labeled both small and small-medium diameter neurons. To our knowledge, this is the first study to report successful retrograde labeling of corneal neurons using DiI. The number of DiI labeled TG neurons was larger than any of the other tracers evaluated (FG, FB, FM). Differences in labeling efficiency may relate to the molecular weight (MW: FB 339.2, FG 472.54, FM 611.54, DiI 933.89 g/mol) and/or the uptake mechanisms of each tracer (Moreira et al., 2007).

With all tracers, a high proportion of neurons were not double labeled after dual application, with numbers of tracer-positive neurons for each tracer alone similar to previous reports (Marfurt et al., 1989; De Felipe et al., 1999; Nakamura et al., 2007; Alamri et al., 2015). This result suggests that previous studies relying on a single tracer may have significantly under-estimated the total number of corneal-projecting TG neurons. Despite these differences in cell size, total number of labeled neurons, and relatively low number of double-labeled neurons, similar proportions of peptidergic (CGRP-positive) and non-peptidergic (IB4-positive) neurons were observed across all four tracers in sham treated animals. Furthermore, LGE produced similar increases in the number of CGRP-positive cell bodies in FG, FB and DiI.

In health, corneal neurons have largely distinct peptidergic and non-peptidergic corneal cell populations (Marfurt et al., 2010). The increase in CGRP-labeled corneal neurons after LGE appears to be the result of de novo CGRP expression in IB4-positive neurons. This provides new evidence of an injury-induced phenotypic change in corneal neurons that may promote corneal wound healing (Mikulec and Tanelian, 1996; Zhang et al., 2020). An increase in the rate of corneal epithelial wound healing after application of CGRP has been reported (Mikulec and Tanelian, 1996). Furthermore, to aid in peripheral nerve regeneration, CGRP release recruits macrophages to clear debris and release VEGF to support regrowth of axon fibers (Cattin et al., 2015; Hillenbrand et al., 2015; Caillaud et la., 2019). This increase in CGRP may also contribute to corneal pathology by promoting neovascularization and angiogenesis, as well as nociceptor sensitization (Azar et al., 2006; Toda et al., 2008; McKay et al., 2019).

In addition to the observed increase in CGRP, TRPV1 was also increased in IB4-positive corneal neurons after LGE, consistent with previous studies reporting an increase in TRPV1 expression after corneal injury (Bereiter, 2018; Hatta et al., 2019; Fakih et al., 2021). The noxious heat and acid sensitive TRPV1 channel had previously been identified in 37% of

corneal neurons, consistent with the present findings in sham treated animals (Tominaga et al., 1998; Piper, 1999; Murata and Masuko, 2006; Rosenbaum and Simon, 2007; Cao et al.,2013). In LGE-induced dry eye, increased TRPV1 activation can cause peripheral sensitization of corneal afferents and lead to long-term alterations in pronociceptive gene expression (Meng and Kurose, 2013, Hatta et al., 2019; Fakih et al., 2021). A recent study found that the corneal application of the TRPV1 antagonist capsazepine inhibited overexpression of pronociceptive genes and clinical signs associated of ocular pain induced by lacrimal and harderian gland excision in mouse (Fakih et al., 2021). These findings reveal a primary role of CGRP and TRPV1 in facilitating phenotypic adaptation of corneal neurons occurring in chronic dry eye.

While evidence from this study suggests a phenotypic switch occurring in the corneal non-peptidergic IB4-positive population, additional experiments using lineage tracing to label individual neurons prior to corneal injury and follow expression and function of those same neurons after injury would be necessary to confirm these findings (Amitai-Lange et al., 2015; Hsu, 2015). Recent studies have identified specific functional changes in the non-peptidergic C-fiber population using the Mrgprd[cre] mouse and expression changes in ATF3/Mrgprd neurons following spared nerve injury (Wang et al., 2021; Warwick et al., 2021). In particular, the changes in expression patterns described in AFT3/Mrgprd neurons after nerve injury suggest the possibility of ATF3 regulatory control of CGRP and TRPV1 observed following corneal injury in this study (Wang et al., 2021).

In summary, LGE-induced corneal injury increased ATF3 expression in corneal neurons and produced de novo expression of CGRP and TRPV1 in IB4-positive neurons. This response may initially bolster axonal regeneration, yet the increase in CGRP and TRPV1 expression also likely contributes to ongoing corneal pain and hypersensitivity.
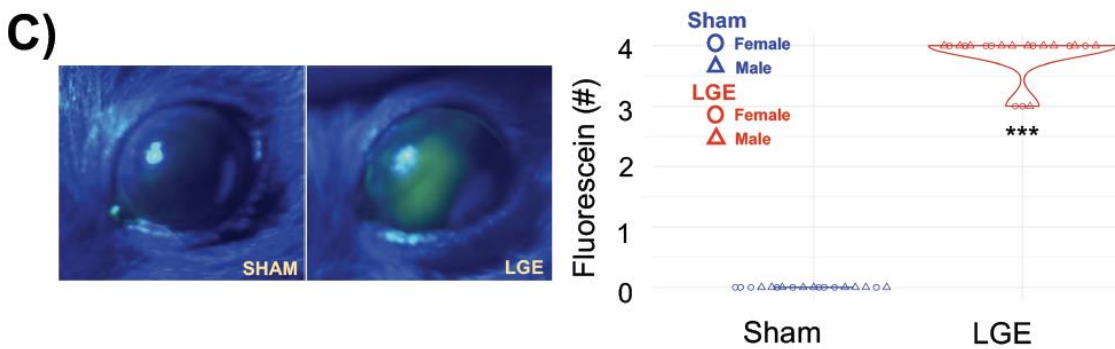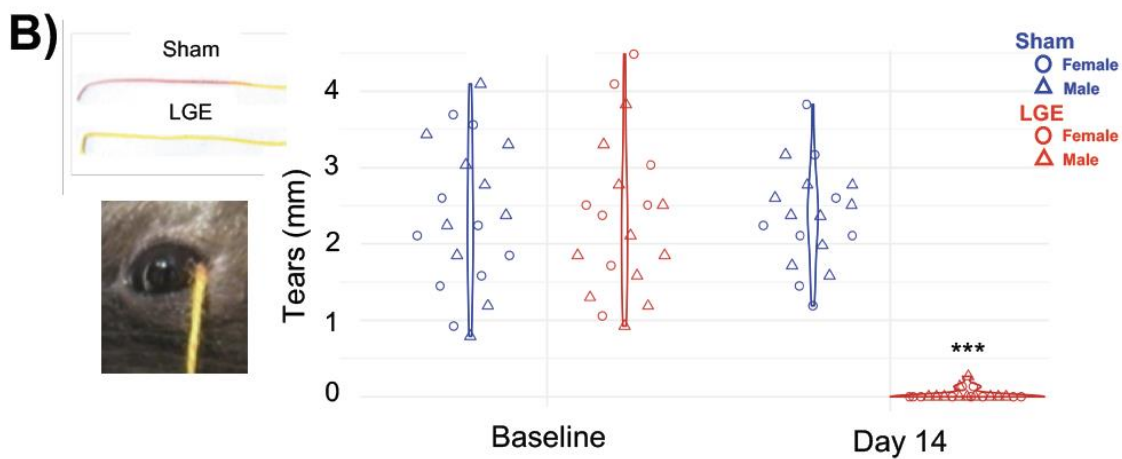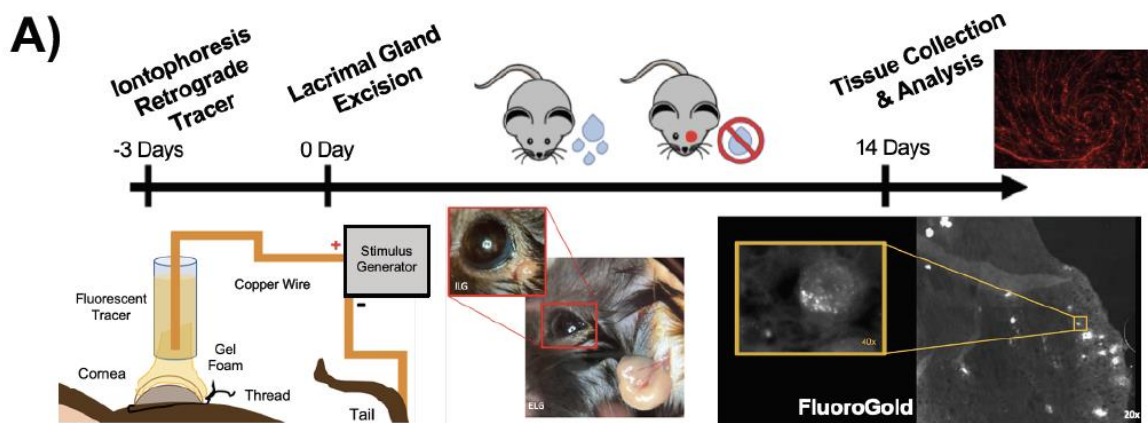
Figure 2.1. Experimental timeline and validation of dry eye following LGE. **A)** Fluorescent tracer was applied to the cornea using iontophoresis at least 72 hours prior to LGE and tissue

collected at 14-days following LGE. **B)** Tear volume was reduced after LGE when compared to baseline measurements and sham surgery treatment groups. **C)** Fluorescein luminescence was increased 14-days following LGE. *** p <0.001 compared to all other treatment groups. Sham n = 18; LGE n= 20.
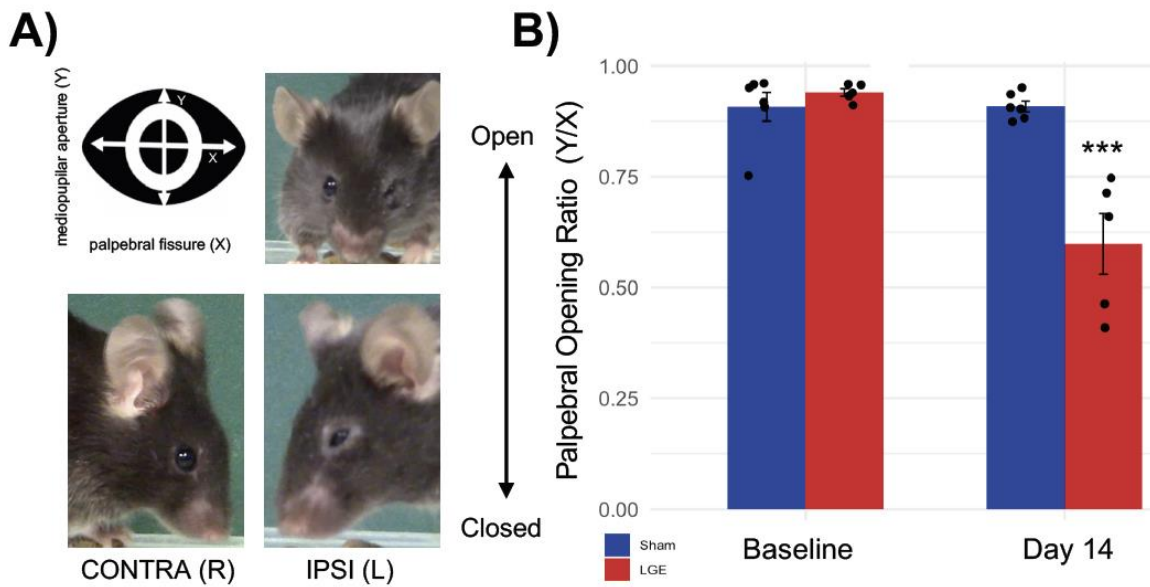
Figure 2.2. The effect of LGE on palpebral opening. **A)** Palpebral opening was calculated as the average vertical mediopupilar aperture (Y) divided by the horizontal palpebral fissure (X) (upper left panel). Images taken from the same mouse illustrate the unilateral nature of the change following LGE (lower left panels; CONTRA: contralateral to LGE; IPSI: ipsilateral to LGE). **B)** LGE produced a reduction in palpebral opening. *** $p < 0.0001$ compared to all other treatment groups. Sham n=6 (3M/3F); LGE n=5 (3M/2F).
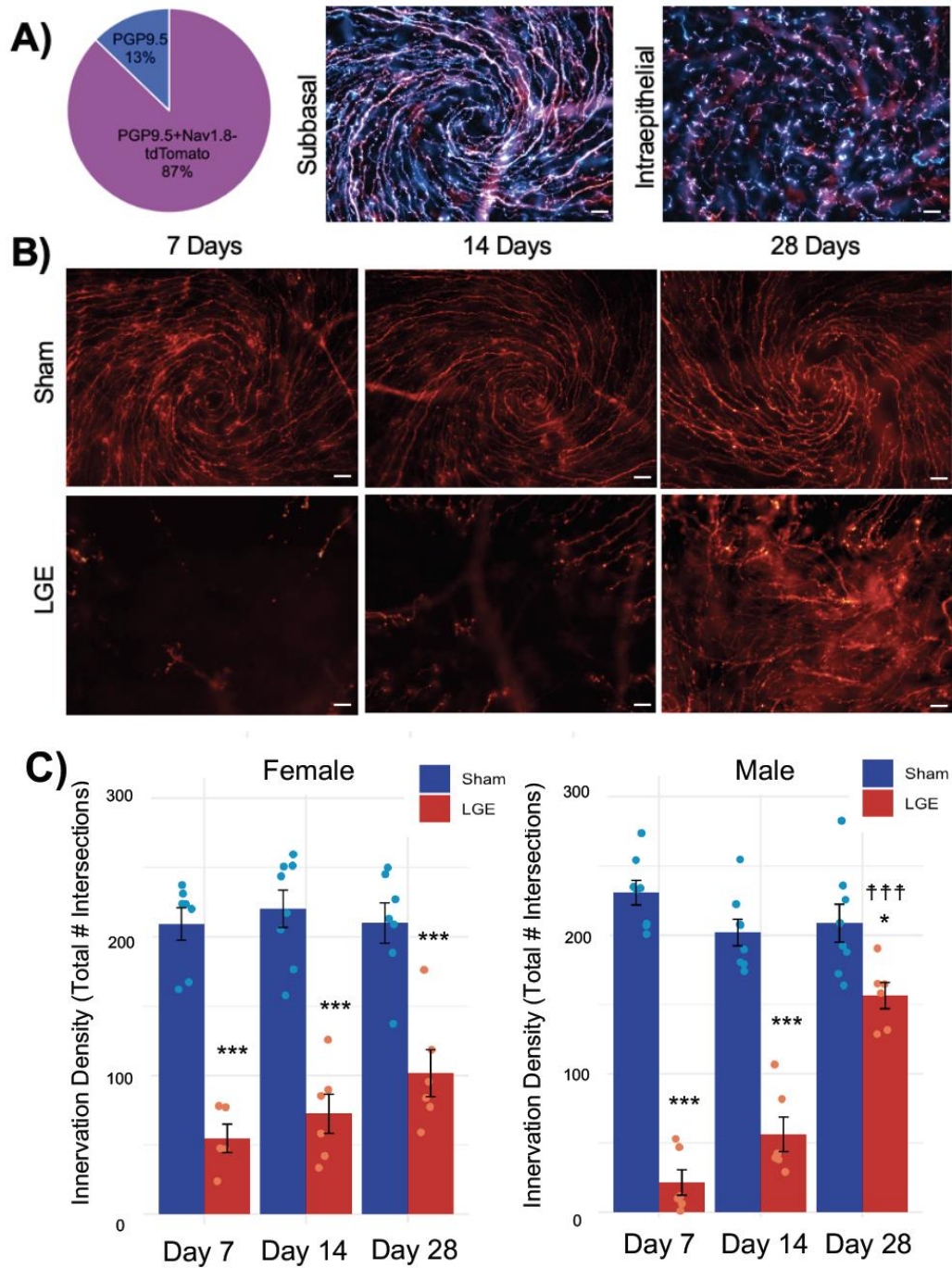
Figure 2.3. Corneal innervation after LGE. **A)** The majority of PGP9.5 labeled afferents were

also positive for tdTomato, which can be seen in the extensive overlap within both the subbasal

and intraepithelial nerve endings. Scale bar 20 µm. **B)** Representative images of corneal

innervation at 7-, 14- and 28-days following sham and LGE surgery. While significant

reinnervation occurred by day 28, the innervation pattern remained disorganized. Scale bar 20

µm. **C)** Innervation density as determined by Sholl analysis. Reinnervation of the cornea was

significantly lower 28 days after LGE in female compared to male animals. ††† p <0.001 LGE

day 28 vs 7 and 14 day timepoints; * p <0.01, *** p <0.0001 LGE vs sham at the same

timepoint. 7-day: Sham n=15 (8M/7F), LGE n=11 (6M/5F); 14-day: Sham n=16 (8M/8F); LGE

n=12 (6M/6F); 28-day: Sham n=15 (8M/7F); LGE n=12 (6M/6F).
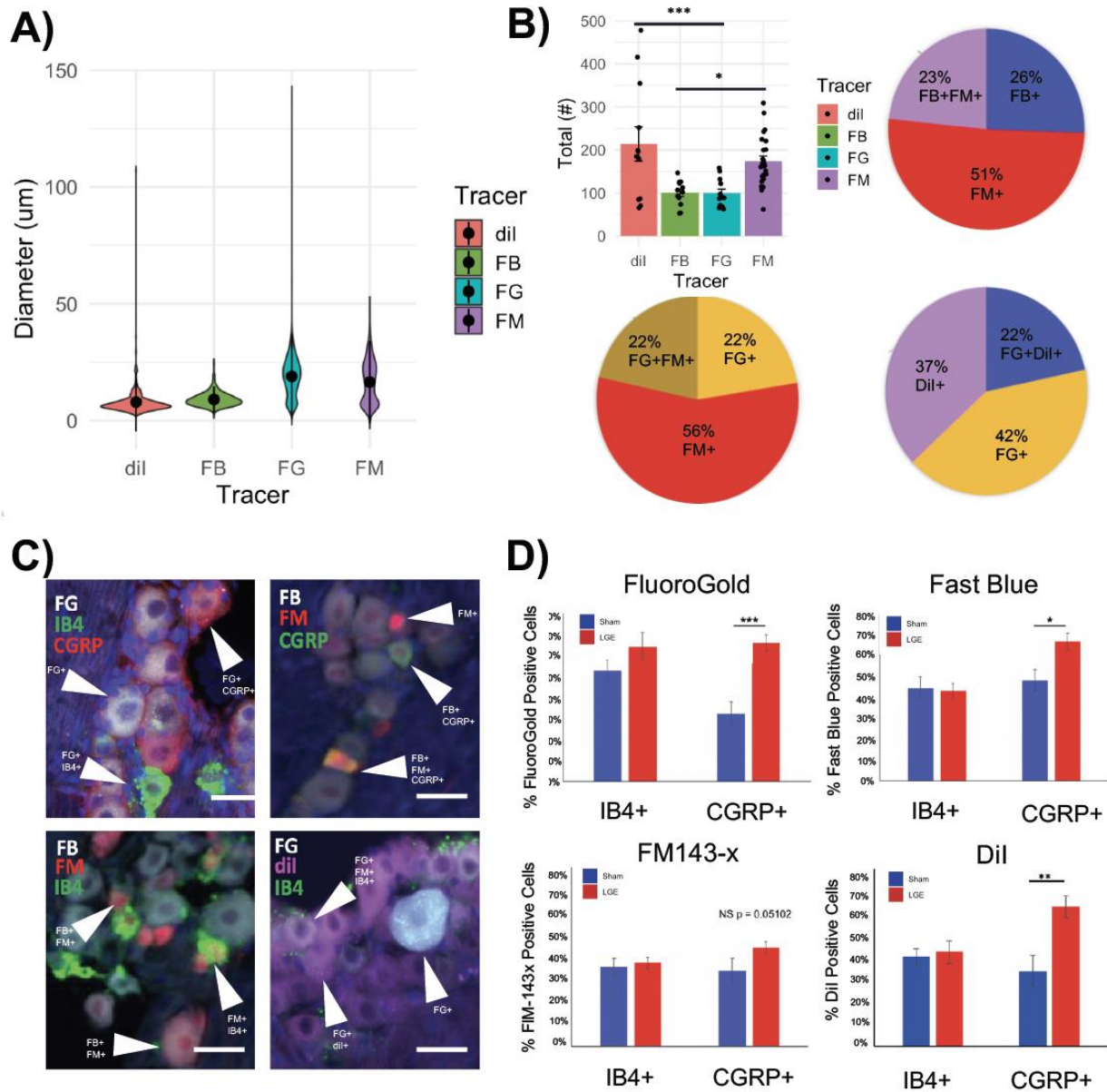
Figure 2.4. Somal characterization of corneal neurons after LGE. **A)** Diameters of corneal neurons using four different tracers: FB, FG, FM, and DiI. **B)** DiI and FM labeled more corneal cells per animal than FB and FG (upper left panel). Percent of total labelling of corneal neurons with each tracer using dual labeling of FB/FM (upper right), FG/FM (lower left), and FB/DiI (lower right). **C)** Representative images of FG, FB, FM and DiI labeled cells in the TG and co-

labelled with IB4 and/or CGRP. Scale bar 25 µm. **D)** IB4 and CGRP immunolabelling of FG, FB, FM and DiI 14 days following LGE. * p <0.01, ** p <0.001, *** p <0.0001 compared to all other groups. FB, FluoroGold; FB, Fast Blue; FM, FM143-x; DiI, DiIC18(3). FG/FM: Sham n=6 (3M/3F), LGE n=8 (5M/3F); FB/FM: Sham n=6 (3M/3F), LGE n=6 (3M/3F); diI/FG: Sham n=6 (3M/3F), LGE n=6 (3M/3F). Calibration bar 25 µm.
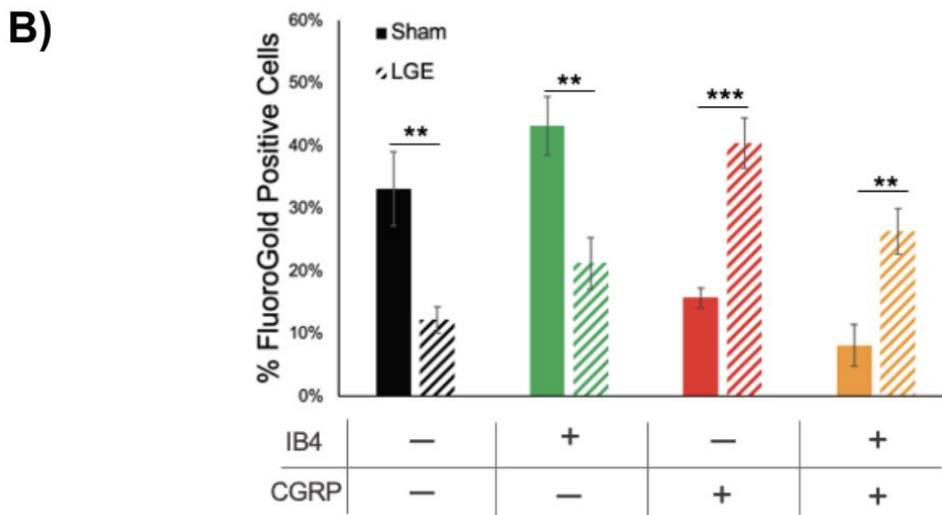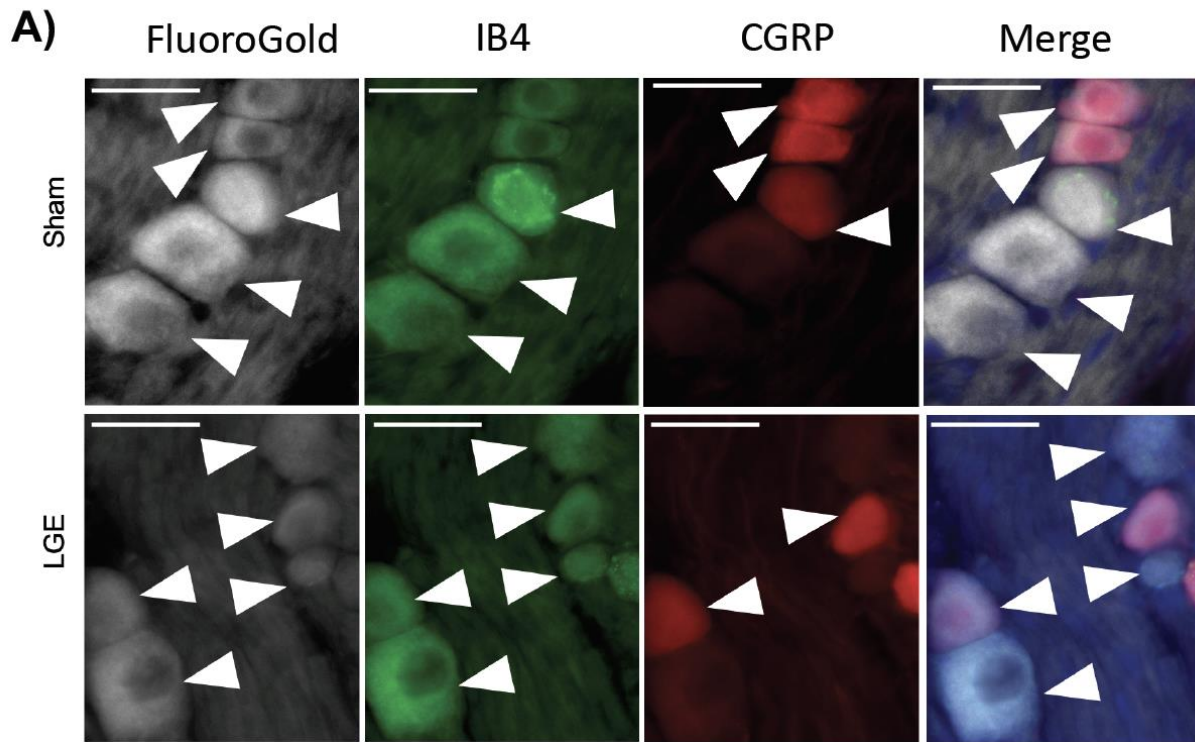
Figure 2.5. Co-labeling of CGRP with IB4 in cornea-projecting afferents. **A)** Representative images of IB4 and CGRP-positive neurons in the TG after FG application to the cornea. Calibration bar 25 µm. **B)** Percentage of FG labeled cells that were IB4 and/or CGRP-positive. * p <0.01, ** p <0.001, *** p <0.0001. N=12/treatment group (6M/6F).
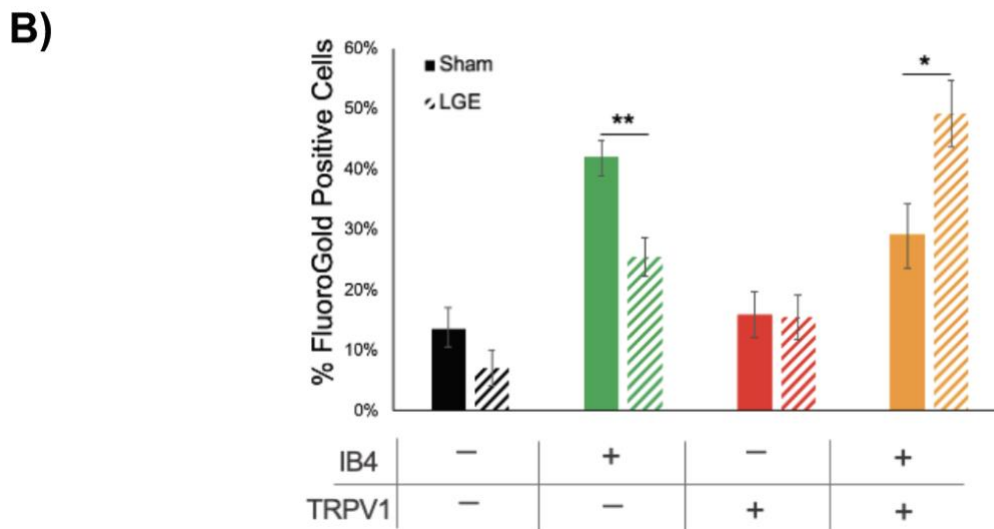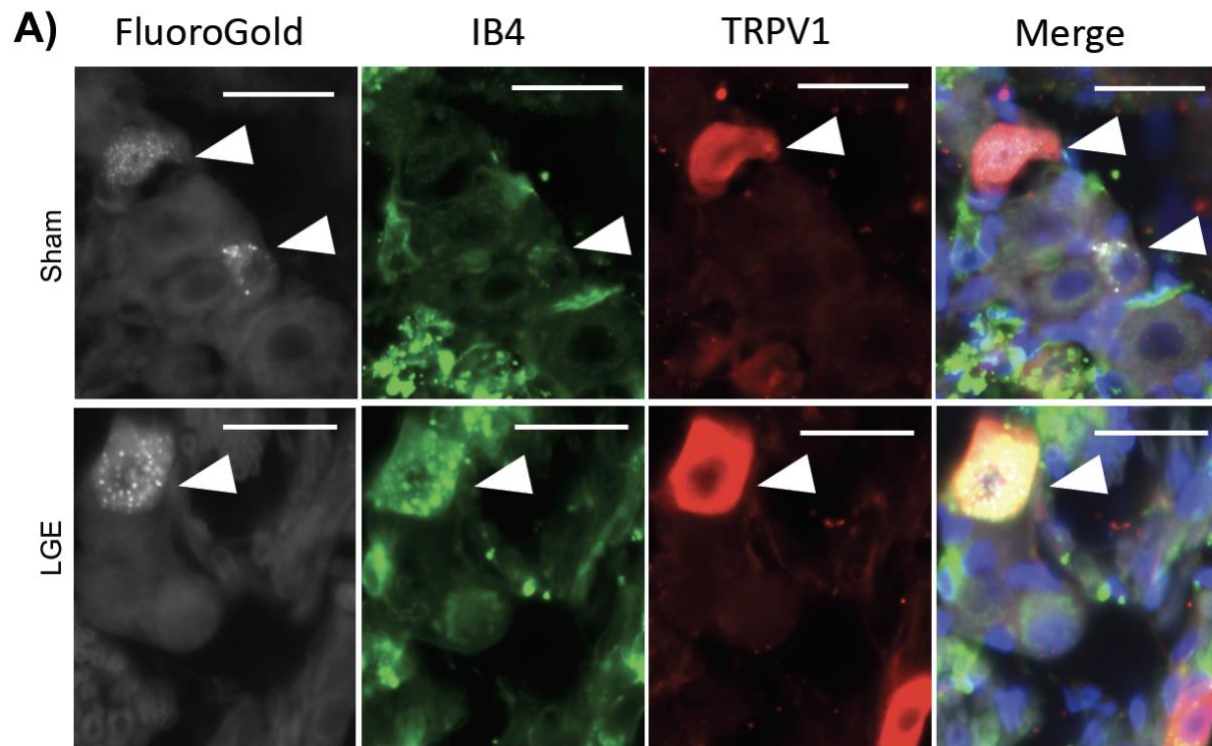
Figure 2.6. Co-labeling of TRPV1 with IB4 in cornea-projecting afferents. **A)** Representative images of IB4 and TRPV1-positive neurons in the TG after FG application to the cornea in sham and LGE treated animals. Calibration bar 25 μm. **B)** LGE increased the percentage of FG

labeled cells that co-labeled with TRPV1 and IB4. * p <0.05, ** p <0.01 compared to all other groups. N=12 per treatment group (6M/6F).
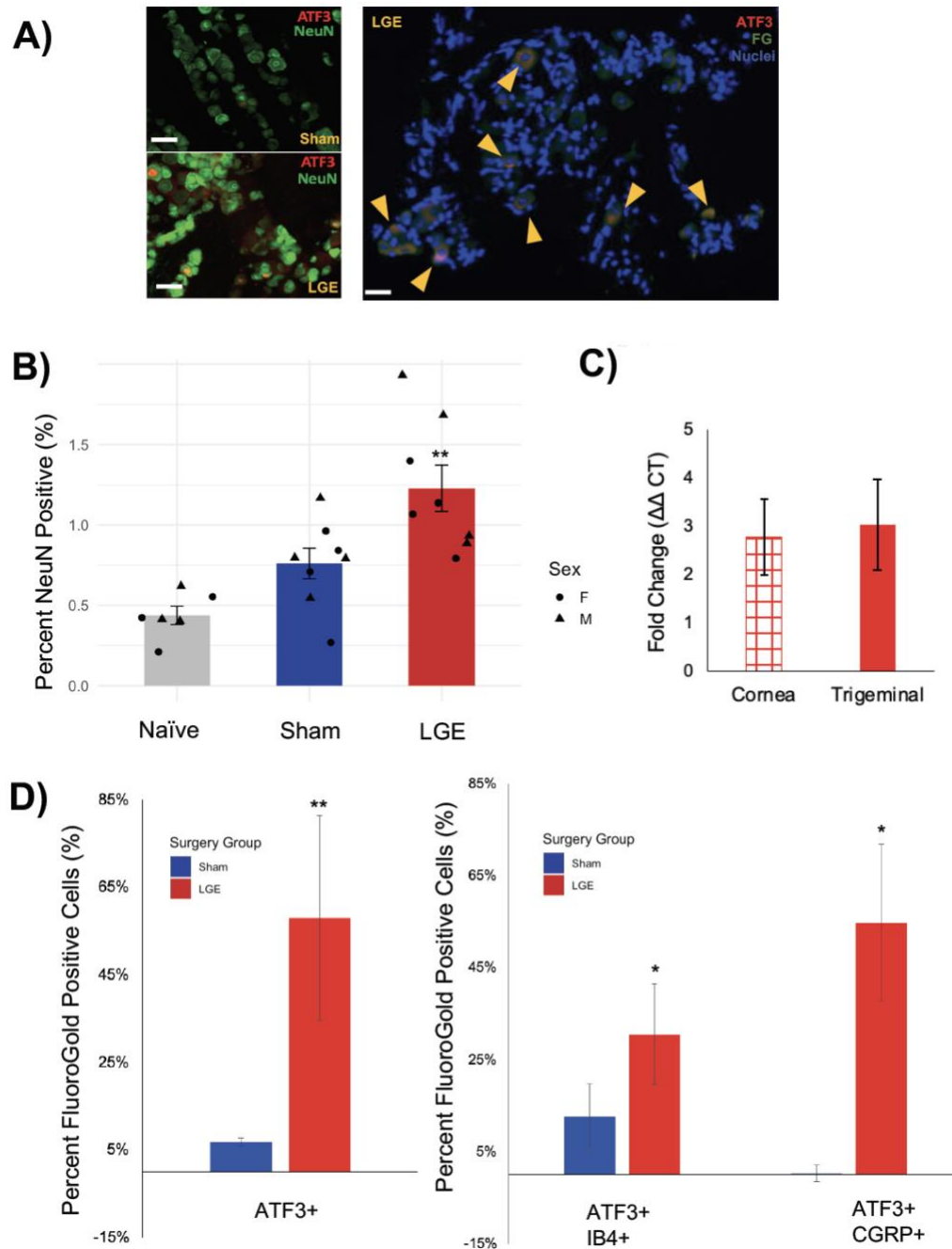
Figure 2.7. LGE increases ATF3. **A)** Representative images of ATF3 immunolabeling in TG sections (left panels) and in FG-labeled corneal neurons (right panels) following LGE.

Calibration bar 25 µm. **B)** Percent of ATF3 protein-positive TG neurons. **C)** ATF3 mRNA expression as compared to sham in the TG and cornea. **D)** Percent of FG labelled corneal neurons in the TG co-labeled with ATF3 protein. **E)** ATF3 protein co-localization with IB4 and CGRP in corneal neurons. * $p < 0.01$, ** $p < 0.001$ compared to sham and naïve treatment. N=12/treatment group (6M/6F).

Table 2.1. Results from multiple group comparisons for all data sets.

Figure	1B	1C	2B	3C	3C	4B	7B
Metric	ANOVA (3W)	Kruskal-Wallis	ANOVA (2W)	ANOVA (2W)	ANOVA (2W)	ANOVA (1W)	ANOVA (1W)
Measurement	Tears (mm)	Fluorescein (score)	Palpebral Opening (Y/X ratio)	Innervation Density (#) Females	Innervation Density (#) Males	Tracer Positive Cells (#)	NeuN Positive Cells (%)
Time							
DF-V	1		1	2	2		
DF-R	69		18	33	36		
F	51.171		18.12	0.632	11.83		
P	7.01E-10		4.75E-04	0.538	0.000112		
Surgery							
DF-V	1		1	1	1		
DF-R	69		18	33	36		
F	44.575		14.53	142.499	227.15		
P	5.11E-09		1.28E-03	1.61E-13	<2E-16		
Sex							
DF-V	1						
DF-R	69						
F	0.008	0.25532					
P	0.93	0.6134					
Tracer							
DF-V						3	3
DF-R						56	56
F						7.397	7.397
P						0.000293	0.000293
Time: Surgery							
DF-V	1		1	2	2		1
DF-R	69		18	33	36		79
F	43.383	37	21.99	1.588	25.64		205.9
P	7.41E-09	9.24E-09	1.83E-04	2.19E-01	1.19E-07		2.00E-16
Time: Sex							
DF-V	1						
DF-R	69						
F	0.274	0.25532					
P	0.602	0.6134					
Time: Surgery: Sex							
DF-V	1						
DF-R	69						
F	1.459						
P	0.231						

CHAPTER 3

DELAYED HEALING AND NAV1.8 NERVE REGENERATION FOLLOWING CORNEAL ABRASION INJURY WITH SOX11 DOWNREGULATION

3.1. Abstract

SOX11 expression is observed in primary afferent neurons early on after peripheral nerve injury and appears to play a critical role in regeneration. Currently, little is known about the role of SOX11 in nerve regeneration following corneal injury. The aim of this study was to examine corneal nerve regeneration in moderate and severe acute injury insults, trephine only (TO), and corneal abrasion (CA), using $Nav1.8$Cre-$Sox11^{f/f}$-tdTomato ($Sox11^{fl/fl}$) and $Nav1.8$Cre-$Sox11^{f/WT}$-tdTomato (littermate controls). TO makes a uniform circular cut through the epithelium and corneal axon terminals. CA uses first TO to demarcate a uniform area and depth, followed by the mechanical removal of the corneal epithelium and axon terminals using a rotating burr. Corneal fluorescein was used to examine the severity of epithelial damage. Mechanical sensitivity was evaluated using a corneal aesthesiometer, and nerve terminal density was imaged from whole mounts using a Keyence BZ-X700 fluorescent microscope and analyzed with FIJI. TO and CA cause graded severity of decreased innervation density and regeneration following injury. $Sox11^{fl/fl}$ increases the severity of denervation following both TO and CA injury. $Sox11^{fl/fl}$ also slows regeneration in timepoints following injury. Epithelial damage occurs following both TO, and CA and its healing is slowed by downregulation of SOX11. Expression of SOX11 and ATF3 mRNA is reduced in Nav1.8 neurons in $Sox11^{fl/fl}$ animals, indicating the regulation of ATF3 by upstream transcription factor SOX11. These results provide support for the role of SOX11 in nerve regeneration and hypersensitivity following injury.

3.2. Introduction

Corneal nerves regulate ocular surface homeostasis and protect the eye from damage when noxious stimuli are detected. Corneal abrasions caused accidentally or through planned surgical interventions are one of the most prevalent causes of corneal nerve injury (Batra and Bali, 1977; Weissman et al., 1994; Upadhyay et al., 2001; Soong et al., 2002; Jabbur and O'Brieen, 2003; Moos and Lind, 2006; Masoudi Alavi et al., 2014; Vo et al., 2015; Hung et al., 2020). Injury to these nerves can cause sustained altered functioning and, in some cases, lead to irremediable neuropathic pain (Meng and Kurose, 2013; Galor et al., 2015; Belmonte et al., 2017). Corneal afferent terminals detect foreign insults through specialized ion channels, such as capsaicin with TRPV1 or cooling with the TRPM8 (Murata and Masuko, 2006; Robbins et al., 2012; Guerrero-Moreno et al., 2020). To maintain corneal homeostasis, axon terminals also detect subtle changes in the epithelium and tear film components. Usually, tear film is composed of regulated proportions of mucins, lipids, water, proteins, and electrolytes; any changes to the balance can shift osmolarity or trigger alternative sensors. This imbalance causes patterns of neuronal firing activity, which signals parasympathetic and sympathetic circuits to stimulate tear secreting glands which restore homeostasis (Tomlinson et al., 2006; Dartt, 2009, Meng and Kurose, 2013). In addition to the contribution of extraocular structures, corneal nerves themselves provide trophic factors that maintain homeostasis, nurture the microenvironment, and enable healing following injury (Muller et al., 2003; Mastropasqua et al., 2017; Al-Aqaba et al., 2019; Medeiros and Santhiago, 2020). Sustained damage or changes to functional properties of corneal neurons can prevent the local balance from being restored, which can lead to additional pathological features besides ocular discomfort, such as DED or corneal opacity (Song et al., 2014; Stepp et al., 2018; Hegarty et al., 2018).

Prior studies have examined corneal wound healing and nerve regeneration following graded levels of CA (Wilson et al., 2001; Song et al., 2004; Li, 2011; Ljubimov and Saghizadeh, 2015; Sacchetti and Lambiase, 2017; Xue et al., 2018; Hegarty et al., 2018; Stepp et al., 2018; Wilson, 2020; Pham and Bazan, 2021). Studies have also identified upregulation of specific markers in TG markers after CA injury, including CGRP and ATF3 (Hegarty et al., 2018). Using an ATF3 genetic deletion mouse model, an earlier study found that neurite growth and regeneration of the facial nerve was stunted following injury (Gey et al., 2016). Other studies identified the transcription factor, SOX11, as a critical upstream regulator of ATF3 expression after peripheral injury (Jankowski et al., 2008; Moore and Goldberg, 2011; Jankowski et al., 2018). This study targets this same pathway to help understand molecular triggers for the divergent mechanisms that direct the sustained pathological shift following injury. The experimental goals of this study are to 1) evaluate ATF3 regulation in *Sox11^{fl/fl}* mouse following CA 2) evaluate the impact of *Sox11^{fl/fl}* on corneal nerve regeneration and wound healing. This study hypothesizes that A) *Sox11^{fl/fl}* animals will exhibit delayed epithelial healing and decreased nerve regeneration. B) *Sox11^{fl/fl}* will influence the expression of other nerve regeneration and injury markers (SOX11, ATF3).

3.3. Materials and Methods

3.3.1. Generation of *Nav1.8*-tdTomato-*Sox11* mice

Nav1.8-Cre-C57B6/J mice originally generated by Dr. John Wood (University College London, London, UK) and obtained from Dr. Sulayman D. Dib-Hajj (Yale University, New Haven, CT, USA) were bred with B6. Cg-Gt(ROSA)26Sortm14(CAG-tdTomato)Hze/J (Stock #007914, The Jackson Laboratory, Bar Harbor, ME, USA). The resulting F1 progeny that were

heterozygous for *Nav1.8*-Cre and tdTomato were intercrossed to result in mice with specific expression of tdTomato fluorescent protein in *Nav1.8*-expressing neurons. *Nav1.8*-CreHet-tdTomatoHet progeny were intercrossed with a *Sox11*$^{fl/fl}$, previously generated using the Cre-loxP system by floxing the single *Sox11* exon. *Nav1.8*-tdtomato expression could be visualized using fluorescence microscopy (em. 581 nm). *Nav1.8*-Cre-tdTomato-*Sox11*$^{f/f}$ mice were used as experimental *Sox11* conditional downregulation (*Sox11*$^{fl/fl}$) animals and *Nav1.8*-Cre-tdTomato-*Sox11*$^{f/wt}$ animals were used as the littermate controls.

For genotyping, tissue was lysed by adding 50mM NaOH and then heated to at 95oC for 35 minutes, followed by the addition of 50mM HCl and 1M Tris HCl buffer. The sample was spun down and then stored at 4oC until processed. Polymerase chain reaction (PCR) was used to identify *Sox11* and tdTomato using Econotaq Plus 2x Buffer (Lucigen, Middleton, WI, USA). Pri-mers included: *Sox11* Forward– GTGATTGCAACAAAGGCAGA, *Sox11* Reverse – TCTGCCGATGTCTTTCAGAC, Td tomato Mutant Forward– CTGTTCCTGTACGGCATGG, Td Tomato Mutant Reverse – GGCATTAAAGCAGCGTATCC, Td Tomato Wild Type Forward – AAGGAGCTGCAGTGGAGTA, Td Tomato Wild Type Reverse – CCGAAAATCGTGG-GAAGTC. *Nav1.8*-Cre reactions were prepared with Promega GoTag Flexi-buffer (Promega, Madison, WI, USA). Primers included: *Nav1.8*-Cre Common Forward – GGAATGG-GATGGAGCTTCTTA, *Nav1.8*-Cre Mutant Reverse – CCAATGTTGCTGGA-TAGTTTTTACTGCC, *Nav1.8*-Cre Wild Type Reverse – TTACCCGGTGTGTGCTGTAGAAAG. Genotyping of all animals was conducted by the University of New England Behavioral and Genotyping Core.

3.3.2. Animals

Adult male and female mice, 8-10 weeks old, were group housed and given food ad libitum. All animal study protocols were approved by the Committee on Animal Research at the University of New England, and animals were treated in accordance to policies and recommendations of the National Institutes of Health *Guide for the Care and Use of Laboratory Animals. Nav1.8*-Cre-tdTomato-*Sox11^{f/f}* mice and *Nav1.8*-Cre-tdTomato-*Sox11^{f/wt}* mice were generated. *Nav1.8*-Cre-tdTomato-*Sox11^{f/f}* mice were used as experimental Sox11^{fl/fl} animals and *Nav1.8*-Cre-tdTomato-*Sox11^{f/wt}* animals were used as the littermate controls. Genotyping of all animals was conducted by the University of New England Behavioral and Genotyping Core.

3.3.3. Corneal Abrasion

All mice were anesthetized under isoflurane (2%) and the topical anesthetic proparacaine hydrochloride opthalamic solution (0.5%, Henry Schein, Melville, NY, USA) was applied for 1 minute to the ocular surface. A 1.5-mm dulled trephine (Katena, item #K207510, Parsippany, NJ, USA) was used to outline a central region of the cornea for creating unilateral debridement and trephine-only wounds (Stepp et al., 2018). For debridement wounds, a dulled rotating burr (Algerbrush II, Precision Vision, Woodstock, IL, US) was used to remove epithelial cells and damage axon terminals through the subbasal level of the cornea within the 1.5 mm-diameter area (Stepp et al., 2018). Naïve littermates were used as uninjured controls.

3.3.4. Retrograde Neuron Tracing

FluoroGold (FG, 3% in NaCl; Fluorochrome, Denver, CO, USA) was applied to the cornea under isoflurane anesthesia as previously described (Cassagne et al., 2016). Briefly, at 72 hours before corneal debridement, trephine-only wounding, or age-matched non-injured

littermate controls, a DC current (7 µA for 10 min) was passed between a copper wire in a capillary tube filled with FG and a copper cathode was placed in the tail. An absorbent gelatin sponge (Gelfoam 12–7 mm; Pfizer Pharmaceuticals, New York, NY) was inserted into the capillary tube so that it contacted both the cornea and the tracer solution.

3.3.5. Palpebral Opening

Palpebral opening was quantified as a sign of ocular discomfort. The height of the gap between the upper and lower eyelids and the distance separating the two canthi was measured using ImageJ/FIJI from 5 still shots taken from a 5-minute video. For each still shot, the height was divided by the distance between the canthi and these were averaged together to give an overall palpebral opening ratio.

3.3.6. Mechanical Sensitivity

Corneal mechanical sensitivity was evaluated using a Cochet-Bonnet esthesiometer, as previously described (12/100mm, Western Ophthalmics Corp., Lynnwood, WA, USA). Beginning with a length of 60 mm, the nylon filament was applied to the cornea three times. If a corneal reflex including a blink and/or eyeball retraction was observed in less than 2 of the three trials, then the length of the filament was decreased by a 5mm increment. The length of the filament was converted to the amount of pressure (g/mm^2) using the filament specific conversion chart provided by Western Ophthalmics.

3.3.7. Tear Production

Tearing was quantified using phenol red threads inserted into the lateral canthus of the eye for 15 s in unanesthetized animals (Zone-Quick, FCI Ophthalmic, Pembroke, MA, USA), as

previously described (Meng et al., 2015). The length of the red portion of the thread was measured under a dissecting microscope.

3.3.8. Corneal Fluorescein Staining

Fluorescein staining was used to assess corneal epithelial damage. The staining was performed prior to and 24 hours, 48 hours, 7 days and 14-days following trephine-only, corneal debridement and in naïve controls. A fluorescein solution (1%, 10uL; Sigma-Aldrich Corp., St. Louis, MO, USA) was applied to the cornea while animals were under isoflurane anesthesia. After 1 minutes, the eye was rinsed with artificial tears and was visualized with a cobalt blue light as previously described (Meng et al., 2015) (16 LED Blue Flashlight, 464 nm, LDP LLC, Carlstadt, NJ, USA). The area of staining was imaged using a Sony Cybershot RX100 III with Zeiss Vario-Sonnar T* f/1.8-2.8 lens and a no.10 f100 Kenko magnification filter. The percent area of staining within the wounding area was calculated using ImageJ/FIJI.

3.3.9. Corneas

At 1, 2, 7, and 14-days post-corneal debridement, trephine-only injury or in age-matched littermate controls, animals were deeply anesthetized with Euthasol (Henry Schein, Melville, NY, USA) and eyeballs were removed using curved blade fine scissors (Item # 14061-10, Fine Science Tools, Foster City, CA, USA). Eyeballs were briefly fixed with 10% formalin and transferred into PBS before dissection. Corneas were dissected out and washed three times in PBS on a shaker at room temperature for 10 min. After making 3 pie cuts along the periphery to allow the corneas to lie flat, corneas were whole-mounted onto slides with DAPI infused mounting media (ProLong Gold Antifade with Dapi, ThermoFisher Scientific, Waltham, MA, USA). Corneas were imaged at 40x using a Keyence BZ-X series fluorescence microscope.

Five images were taken, in a z-stack in 1 mm steps, with one in the central and four in the peripheral regions of the cornea. The center was selected based on the converged spiral of subbasal axons and the peripheral areas were chosen diagonal from the center image along the periphery of the 1.5 mm injury zone. Images were split into free nerve ending and sub basal layers and were analyzed using FIJI/IMAGEJ. The maximum projection of each z-stack was converted to a mask and the Sholl Analysis plugin was used to quantify innervation density.

3.3.10. Fluorescence In Situ Hybridization

After eyeball extraction, at 1, 2, 7, and 14-days post-CA, TO or naive animals were perfused with heparinized saline and 10% neutral buffered formalin on ice. TG were dissected out and postfixed in 10% formalin for 24 hours at 4°C before submerging in 30% sucrose. TG were cut using a cryostat at 12 µm using serial sectioning such that every fifth section could be counted. Fluorescent in situ hybridization studies were performed according to the protocol for fresh frozen tissue using the RNAscope Fluorescent Multiplex Reagent kit (Advanced Cell Diagnostics, Newark, CA) with minor modifications.

After dehydration of sections in ethanol, sections were treated with protease IV (ref. no. 322340, RNAscope) and incubated for 30 min at room temperature and washed in PBS. Species-specific target probes for SOX11, ATF3, CGRP and GAP43 were used (Stock #'s 440811, 426891, 417961, 318621, Advanced Cell Diagnostics, Newark, CA, USA). Sections were treated with the probe mixture and negative (ref. no. 320871) or positive (ref. no. 320891) controls and were hybridized for 2 hours at 40°C in a humidified oven (RNAscope HybEZ oven with HybEZ humidity control tray, Advanced Cell Diagnostics). A series of incubations were then performed to amplify the hybridized probe signals and label target probes with the assigned fluorescence detection channels (C1-Alexa488, C2-Atto550). Nuclei were stained using a Cy5

nuclear stain (NucRed Live 647; Invitrogen, Carlsbad, CA) for 20 min and washed with PBS. Slides were glass coverslip mounted with Fluoromount-G (SouthernBiotech, Birmingham, AL) mounting media and sealed.

Sections were imaged at 20x using a Keyence BZ-X series fluorescent microscope (Keyence, Itasca, IL) using filter cubes for DAPI (excitation (ex): 340–400 nm; emission (em): 435–485 nm), GFP (ex: 450–490 nm; em: 500–550 nm), Cy3 (ex: 530–560 nm; em: 570–640 nm), and Cy5 (ex: 590–650 nm; em: 665–735 nm). Keyence Analyzer software was used to stitch images of each section in each channel. ImageJ software (National Institutes of Health, Bethesda, MD) was used to merge each fluorescent channel into a final composite. Images were randomized and blinded before counting. Cells positive for fluorescent markers were manually counted and marked using the Cell Counter plugin in ImageJ. Cells were counted as positive if the fluorescent marker was present in the channel specific image and if it corresponded to a cell containing nuclei when viewed as a merged composite. Co-labeled cells were counted as positive if they were determined to be within the same cell that contained a nucleus and exhibited at least three fluorescent puncta using individual and composite channel images (Kramer et al.,2018). Percent of tracer positive cells were calculated out of the total tracer positive cells labeled for each animal. All images were blinded prior to quantification.

3.3.11. Data Analysis

Statistical analyses for palpebral opening, tear production, cell counts and diameters were performed with a two-way ANOVA and Tukey post-hoc test. For non-parametric data (mechanical sensitivity and fluorescein staining) a Kruskal-Wallis one-way ANOVA with Dunn's post hoc test was performed. Statistical analyses were performed using R and the 'dplyr'

package.   Statistical significances were accepted as $p < 0.05$. Plots, tables and diagrams were created using R and Excel and PowerPoint, and data are presented as mean ± SEM.

3.4. Results

3.4.1. Development and evaluation of transgenic mouse model: *Nav1.8*-Cre-tdTomato-Sox11[f/f]

Prior studies have identified the influence of SOX11 on peripheral nerve regeneration but have not yet assessed its role in corneal nerve injury (Jankowski et al., 2008; Moore and Goldberg, 2011; Jankowski et al., 2018). Corneas have the unique property of transparency which allows for visualization of axons within whole corneal tissue without potentially damaging clearing methods, corneal composition and thickness yield practical challenges in using traditional immunofluorescence methods. Transgenic reporters have been used to create mouse models in which corneal nerve morphology and regeneration could be visualized in the absence of tissue destructing experimental protocols (Yu et al., 2007). Distinctively, this study developed and characterized a mouse model that would isolate the contribution of SOX11 in corneal nerve regeneration and in which nerve morphology and the Nav1.8 positive subpopulation could be consistently and reliably visualized. A transgenetic mouse was created by breeding *Nav1.8*-CreHet-tdTomatoHet mice on a C57B6/J background with other C57B5/J mice, flox a single *Sox11* exon which is selectively silenced by the Cre-loxP system following the *Nav1.8* promoter (Figure 3.1.A). This mouse model uses a robust fluorescent reporter to visualize Nav1.8 axon terminals within the cornea and Nav1.8 cell bodies in the TG. This transgenic model, combined with a newly optimized method for innocuously applying retrograde tracer FluoroGold to the cornea, further identifies the corneal nerve subpopulation within the TG

(Figure 3.1.A). This method provides this study with two robust markers for the visualization categorization of corneal neurons. As this is the first study to use this model, naïve animals *Sox11$^{fl/fl}$* and littermate controls were evaluated in terms of innervation density, tearing, mechanical, and fluorescein scores. Across all tests, there were no significant differences between *Sox11$^{fl/fl}$* and controls (Figure 3.1.B-C, t-test). Although not statistically significant with the measures used, it should be noted that axon morphology of naïve *Sox11$^{fl/fl}$* animals often appeared to lack an organized whorl pattern, usually a subbasal hallmark in rodents and humans. Subbasal axons and intraepithelial terminals appeared to cluster in areas and be absent in others. Additionally, in naïve *Sox11$^{fl/fl}$* animals, fluorescein slight staining to indicate areas of epithelial injury was noted in many animals.

3.4.2. Impact of graded corneal abrasions on innervation density and influence of SOX11 in reinnervation

TO and CA were used to directly injure corneal neurons in moderate and severe grades (Figure 3.2.A). A tdTomato fluorescent reporter labeled Nav1.8 neurons and visualized and quantified innervation density in whole-mounted corneas (Figure 3.2.B). Prior experiments from this lab confirmed approximately 87% overlap of *Nav1.8*-are;tdTomato with immunolabelled PGP9.5. As the tdTomato reporter labels most corneal neurons, it is adequate to base innervation quantification on tdTomato labeled axons, and uniformity in labeling can be assumed across samples. Innervation density was assessed using Sholl-quantification analysis in ImageJ, which overlayed concentric circles on five separate z-stacks of one central and four peripheral locations on the cornea as previously reported (Mecum et al., 2020). Total innervation was quantified as an average of all five sections across the genotype and injury group. The results showed that following TO injury, at 24-hours and 14-days post-injury,

Sox11^{fl/fl} animals had significantly less total innervation density when compared to controls at the same time point (Figure 3.2.C, left plot, two-way ANOVA, Tukey post hoc, p<0.001, Table 3.1.). Between 24-hours and 48-hours following TO injury, *Sox11^{fl/fl}* animals significantly increased total innervation density (Figure 3.2.C, left plot, two-way ANOVA, Tukey post hoc, p<0.0001, Table 3.1.). Unexpectedly, innervation density significantly decreased between 48-hours and 14-days post TO in *Sox11^{fl/fl}* groups (Figure 3.2.C, left plot, two-way ANOVA, Tukey post hoc, p<0.0001, Table 3.1.). This pattern was not seen in control animals following TO injury. Comparatively, significantly worse denervation was seen in *Sox11^{fl/fl}* following CA when compared to controls at 24-hours, 48-hours, and 7-days following injury (Figure 3.2.C, right plot, two-way ANOVA, Tukey post hoc, p<0.01, Table 3.1.). While no significant difference in total innervation density was observed in controls between 24- and 48-hours, reinnervation was significantly increased between 24- and 48-hours and 14-days (Figure 3.2.C, right plot, two-way ANOVA, Tukey post hoc, p<0.001, Table 3.1). Significant increases in total innervation also occurred between 7- and 14-days in control groups (Figure 3.2.C, right plot, two-way ANOVA, Tukey post hoc, p<0.01, Table 3.1). Conversely, innervation density was significantly increased between 24- and 48-hours and again between 7- and 14-days in *Sox11^{fl/fl}* animals (Figure 3.2.C, right plot, two-way ANOVA, Tukey post hoc, p<0.001, Table 3.1.) and then significantly decreased between 48-hours and 7-days following CA (Figure 3.2.C, right plot, two-way ANOVA, Tukey post hoc, p<0.01, Table 3.1.). Overall, total innervation density was increased between 24-hours and 14-days following CA in *Sox11^{fl/fl}* with evidence of cyclical changes in total axonal density (Figure 3.2.C, right plot, two-way ANOVA, Tukey post hoc, p<0.0001, Table 3.1.).

3.4.3. SOX11 downregulation influences central subbasal and overall intraepithelial terminal reinnervation density following trephine only

To understand the cyclical changes in reinnervation following direct corneal injury, z-stack images of peripheral and central corneal regions were analyzed separately. Additionally, z-stacks were vertically divided into sub-stacks of the subbasal nerve plexus and intraepithelial terminals. The demarcation of these layers is evident by the apparent horizontal arrangement of nerve fibers in the subbasal plexus, which shift in more superficial layers of the corneal epithelium and present as upward projections signaling the branching intraepithelial terminals (Figure 3.2.B). Sholl analysis of corneal regions within these distinct corneal layers was performed using the same parameters as total innervation analysis. With TO injury, $Sox11^{fl/fl}$ groups showed a significant decrease in central subbasal innervation density between 48-hours and 14-days (Figure 3A, left plot, two-way ANOVA, Tukey post hoc, p<0.001, Table 3.1.). While not significant, central subbasal terminals appear to increase in $Sox11^{fl/fl}$ even more than in control animals at 48-hours following TO injury. These findings match trends seen in total innervation analysis and further support initiating a compensatory nerve regeneration mechanism between 24- and 48-hours. While not significant, similar patterns to what was observed in total innervation analysis were observed in peripheral regions of the subbasal plexus displaying innervation increases at 48-hours followed by decreased levels of innervation at 14-days in TO $Sox11^{fl/fl}$ groups (Figure 3.3.A, right plot, two-way ANOVA, Tukey post hoc, Table 3.1.). More differences were seen in superficial corneal layers when quantifying intraepithelial terminal nerve density following TO injury. Control groups did not show significant changes in innervation regeneration in central intraepithelial terminals through 7-days following injury. However, between 7- and 14-days, central intraepithelial terminal density significantly increased (Figure 3.3.B, left plot, two-way ANOVA, Tukey post hoc, p<0.01, Table 3.1.).

Sox11$^{fl/fl}$ animals showed significantly lower central intraepithelial density at 14-days versus controls after TO injury significantly increased (Figure 3.3.B, left plot, two-way ANOVA, Tukey post hoc, p<0.0001, Table 3.1.). Central intraepithelial density significantly decreased from 24- and 48-hours to 14-days following injury in *Sox11$^{fl/fl}$* groups (Figure 3.3.B, left plot, two-way ANOVA, Tukey post hoc, p<0.01, Table 3.1.). Similarly, peripheral intraepithelial density also significantly decreased between 24-hours and 14-days in *Sox11$^{fl/fl}$* animals. (Figure 3.3.B, right plot, two-way ANOVA, Tukey post hoc, p<0.01, Table 3.1.). Unexpectedly, significant decreases were quantified between 24-hours and 48-hours and 7-days for control animals, followed by a non-significant increase at 14-days (Figure 3.3.B, right plot, two-way ANOVA, Tukey post hoc, p<0.01, Table 3.1.).

3.4.4. SOX11 downregulation influences overall subbasal and intraepithelial terminal reinnervation density following corneal abrasion

When examining changes to regional innervation density following CA, the influence of SOX11 in regeneration after severe injury appeared more significant. Central subbasal innervation was significantly reduced in *Sox11$^{fl/fl}$* groups compared to controls at 24-hours and 14-days following CA (Figure 3.4.A, left plot, two-way ANOVA, Tukey post hoc, p<0.0001, p<0.01, Table 3.1.). While control animals did not exhibit any significant changes in central subbasal innervation density between 24-hours and 14-days, a general trend of increased innervation over time was noted. Similarly, a general upward trend in central subbasal innervation density was also observed in *Sox11$^{fl/fl}$* groups, with significant increases between 24- and 48-hours and between 24-hours and 7-days (Figure 3.4.A, left plot, two-way ANOVA, Tukey post hoc, p<0.01, Table 3.1.). Peripheral subbasal innervation was significantly less in *Sox11$^{fl/fl}$* animals at 24-hours when compared to controls (Figure 3.4.A, right plot, two-way

72

ANOVA, Tukey post hoc, p<0.01, Table 3.1.). A significant increase was identified between 24-hours and 14-days and between 7-days and 14-days in *Sox11*^{fl/fl} groups, while a significant decrease in innervation between 48-hours and 7-days (Figure 3.4.A, right plot, two-way ANOVA, Tukey post hoc, p<0.01, Table 3.1.). This difference in central and peripheral innervation density trends reveals physical, morphological changes to axon terminals following severe injury and understand trends observed in total innervation analysis. Examining intraepithelial terminals after CA shows a similar trend of gradual density increases in *Sox11*^{fl/fl} groups, although not statistically significant over time. Similar to previously described trends, central intraepithelial terminals were significantly decreased in *Sox11*^{fl/fl} animals when compared to controls at 24-hours after CA but unexpectedly were also increased at 14-days compared to controls (Figure 3.4.B, left plot, two-way ANOVA, Tukey post hoc, p<0.0001, Table 3.1.). At the same time, control groups showed significant increases between 24-hours (p<0.001) and 48-days (p<0.01) with 7-days, respectively, there was a notable decrease in central intraepithelial terminal density in controls between 7- and 14-days (Figure 3.4.B, left plot, two-way ANOVA, Tukey post hoc, p<0.001, Table 3.1.). Although not statistically significant, this was in contrast to overall increases in peripheral intraepithelial terminal density observed in controls. In *Sox11*^{fl/fl} groups, peripheral intraepithelial density significantly increased between 24-hours and 14-days and between 7- and 14-days (Figure 3.4.B, right plot, two-way ANOVA, Tukey post hoc, p<0.01, Table 3.1.).

3.4.5. Epithelial wound healing following graded injury and influence of SOX11

Epithelial damage was evaluated using a fluorescein stain on the corneal surface, applied directly after injury (i.e., 0 hours) and at subsequent time points of 24-hours, 48-hours, 7-days, and 14-days (Figure 3.5.A). Images were taken at each time point and were analyzed

using a new method of fluorescein scoring in which the percent area of corneal stain is quantified in ImageJ. This new method was developed and optimized for this study to detect subtle changes that may not be as precisely captured using traditional subjective scoring methods. Genotype and injury type were evaluated in this analysis. The TO injury caused moderate epithelial damage in the circle made by the sharp trephine blade, as shown directly after injury at 0-hours. Visually apparent (Figure 3.5.A) *Sox11* downregulation causes significantly greater injury to a larger epithelial area at all time points when compared to controls in both TO and CA injuries (Figure 3.5.B, two-way ANOVA, Tukey post hoc, $p<0.01$, Table 3.1.). Epithelial damage, as measured by percent area of fluorescein stain, control groups presented with significantly decreased staining over time, specifically between 0-hours and 14-days ($p<0.0001$), 0-hours and 24-hours ($p<0.0001$), and between 48-hours and 14-days (Figure 3.5.B, left plot, two-way ANOVA, Tukey post hoc, $p<0.01$, Table 3.1.). Following CA, controls exhibited significantly decreased fluorescein staining between 0- and 24-hours and between 0-hours and 14-days (Figure 3.5.B, right plot, two-way ANOVA, Tukey post hoc, $p<0.0001$, Table 3.1.). No significant differences were noted in *Sox11$^{fl/fl}$* groups at early time points, but a significant decrease in fluorescein staining was observed between 0-hours and 7-days (Figure 3.5.B, right plot, two-way ANOVA, Tukey post hoc, $p<0.001$, Table 3.1.).

3.4.6. Expression changes after corneal abrasion/trephine only

Expression changes in corneal somas in the TG were analyzed using targeted SOX11 and ATF3 FISH probes. Corneal neurons were identified within the TG using a previously optimized innocuous retrograde tracing process where FluoroGold is applied to the cornea from which it is transported up axons and resides in lysosomes within corneal neurons for months following application—using a transgenic fluorescent reporter on Nav1.8 neurons combined with

FluoroGold tracer identifying corneal neurons allowed for downstream expression analysis (Figure 3.6.). Expression changes of SOX11 and ATF3 in TO injury groups were generally unremarkable at 24-hours post-injury. At 24-hours following CA, significant increases in SOX11 have been noted in *Nav1.8*-tdTomato negative neurons in control and *Sox11^{fl/fl}* animals (p<0.01). Additionally, SOX11 has significantly increased in *Nav1.8*-tdTomato positive neurons in littermate controls compared to *Sox11^{fl/fl}* animals (Figure 3.7.A, right plot, two-way ANOVA, Tukey post hoc, p<0.0001, Table 3.1.). Additionally, ATF3 expression did not exhibit any significant changes in expression at 24-hours following injury (Figure 3.7.B, two-way ANOVA, Tukey post hoc, Table 3.1.). At 48-hours following CA, controls presented significantly higher SOX11 and ATF3 expression in *Nav1.8*-tdTomato positive neurons compared to *Sox11^{fl/fl}* groups (Figure 3.8., two-way ANOVA, Tukey post hoc, p<0.001, Table 3.1.). Accordingly, at 48-hours, ATF3 was significantly increased in *Sox11^{fl/fl}* *Nav1.8*-tdTomato negative neurons compared to expression levels of controls (Figure 3.8.B, two-way ANOVA, Tukey post hoc, p<0.001, Table 3.1.).

3.5. Discussion

Prior studies have used trephine and corneal burr abrasion injuries to characterize corneal healing and regeneration after injury (Stepp et al., 2014, Kalha et al., 2018). This study used a transgenic mouse model with these graded injury types to characterize the role of SOX11 in axon regeneration, epithelial healing, and molecular marker expression changes in corneal somas in the TG. Using a novel transgenic model and newly optimized tracing method, corneal neurons could be visualized from axon terminals embedded in corneal epithelium to cell bodies in TG. Using these neuron visualization methods, the results of this study indicate TO and CA injury causes acute denervation followed by regeneration of terminals in minor and

severe levels, respective to injury type. The genetic downregulation of *Sox11* causes more

severe denervation and slower regeneration in both injury types when compared to controls.

Characterization of mRNA expression shows that the transgenic model effectively down

regulates SOX11 in Nav1.8 corneal neurons. FISH results also show that ATF3 appears to be

regulated, at least in part, by SOX11.

Studies have shown the critical role of SOX11 in successful neuronal development and,

in the absence of a normal *Sox11* allele, will die before birth (Bhattaram et al., 2010; Thein et

al., 2010). Using the targeted downregulation of *Sox11* in Nav1.8 neurons was critical for the

success of this study. Thus, the *Nav1.8* promoter was carefully selected, as it is known to be

highly expressed in the cornea (Black, 2002; Mecum, 2020). Nav1.8 is in a unique class of

voltage-gated sodium TTX-R channels (Gauron et al., 2011; Black and Waxman, 2002).

Substantial Nav1.8 corneal expression in unmyelinated neurons provided a useful transgenic

target to label most corneal neurons with a robust and consistent fluorescent reporter. Corneal

Aδ mechanoreceptors have been previously characterized as TTX-S and are likely not labeled

by the *Nav1.8*-tdTomato reporter (De Armentia et al., 2002; Moreira et al., 2007). This provides

information regarding the corneal subclassification of the Nav.18-tdTomato labeled cell

population and the results' interpretations.

Earlier studies have identified SOX11 as a transcription factor initially expressed during

development with an integral role in neurogenesis and upstream regulator of neuronal traits

(Jing et al., 2006). SOX11 has also been identified as influencing dendritic morphogenesis

within the cerebral cortex, influencing the branch of neurons, and influencing migration patterns

(Hoshiba et al., 2016). Observations of innervation morphology and density within the present

study put into the context of the known role of SOX11 suggests this transcription factor may play

a role in corneal axon structure during development, as seen in naïve animals and after both TO

and CA injury. The patterning changes observed in even naïve *Sox11^{f/f}* animals might result from the downstream effectors that SOX11 has a known influence, including GAP43 and SPRRP1A. Prior studies have identified GAP43 as a factor in growth cones of regenerating axons and in early development (Strittmatter et al., 1995; Sretavan and Kruger, 1998). Likely, the absence of SOX11 in the majority of corneal axon terminals is enough to cause abnormal naïve morphology in the subbasal and intraepithelial terminals. Detailed analysis of this morphology should be explored in the future.

Innervation density experiments in this study revealed unexpected cyclical patterns of denervation followed by regeneration with subsequent denervation in *Sox11^{fl/fl}* groups. These results suggest that the absence of SOX11 may have a more profound impact on nerve healing than simply slowing regeneration. The pattern of cyclic denervation, reinnervation was observed in both moderate trephine and severe CA injuries. It appears that at 48-hours following injury, there is some compensatory molecular switch that aids rapid but temporary reinnervation. At timepoints following, terminals are likely to retract due to the absence of the SOX11 RAG pathway. Cyclical reinnervation observed at 14-days in CA could indicate the compensatory pathway again turning on to assist corneal neurons under stress. Prior studies have found that normally, SOX11 expression increases directly after injury and decreases once regeneration has completed (Boeshore et al., 2004; Patodia and Raivich, 2012). The sinusoidal pattern observed in axon reinnervation may be a product of a compensatory nerve regeneration mechanism that takes over for SOX11 in its absence but should be explored further.

Severe injury and delayed healing observed in the corneal epithelium were identified in this study following TO and CA in *Sox11^{fl/fl}* groups. This effect could result from reduced neuromediator release from SOX11 deficient axon terminals, which are no longer providing the necessary trophic factors required for epithelial healing. The significant reduction of innervation

density through 7-days post-injury with *Sox11^{fl/fl}* aligns with sustained epithelial damage seen through the same time period. Previous studies have identified the regulatory control of neurotrophic factor release and SOX11 expression (Salerno et al., 2012; Jankowski et al., 2018). BDNF expression was elevated, has SOX binding sites on 5' exons, and was correlated with increases in SOX11 expression in prior days in DRG cells following sciatic nerve axotomy in mice (Salerno et al., 2012). Additionally, the same study found a 7-fold increase in BDNF with overexpression of SOX11 using an HSV-vector in cultured Neuro2a cells (Salerno et al., 2012). Another study using cultured DRGs linked SOX11 with increased GDNF receptor expression, increased response to GDNF, and artemin application, which resulted in enhanced terminal branching (Jankowski et al., 2018).

In summary, CA injury caused severe denervation of axon terminals within the corneal, made worse with the genetic deletion of SOX11. The regeneration of those terminals occurred within the first week of injury, but overall regeneration at 14-days following injury was less in *Sox11^{fl/fl}* when compared to controls. TO injury caused moderate epithelial damage, as visualized with fluorescein, exacerbated in *Sox11^{fl/fl}* animals. Healing of even minor trephine injury was slowed without SOX11 expression in Nav1.8 neurons. CA caused severe epithelial damage, which was made worse at 24-hours following injury and was slowed 14-days after injury in *Sox11^{fl/fl}* compared to controls. Expression of SOX11 and ATF3 increased after TO and CA, but genetic deletion of SOX11 decreased expression of these markers in Nav1.8. Together, these results suggest that SOX11 regulates ATF3, and this molecular pathway plays a vital role in nerve regeneration and epithelial healing following direct corneal injury.
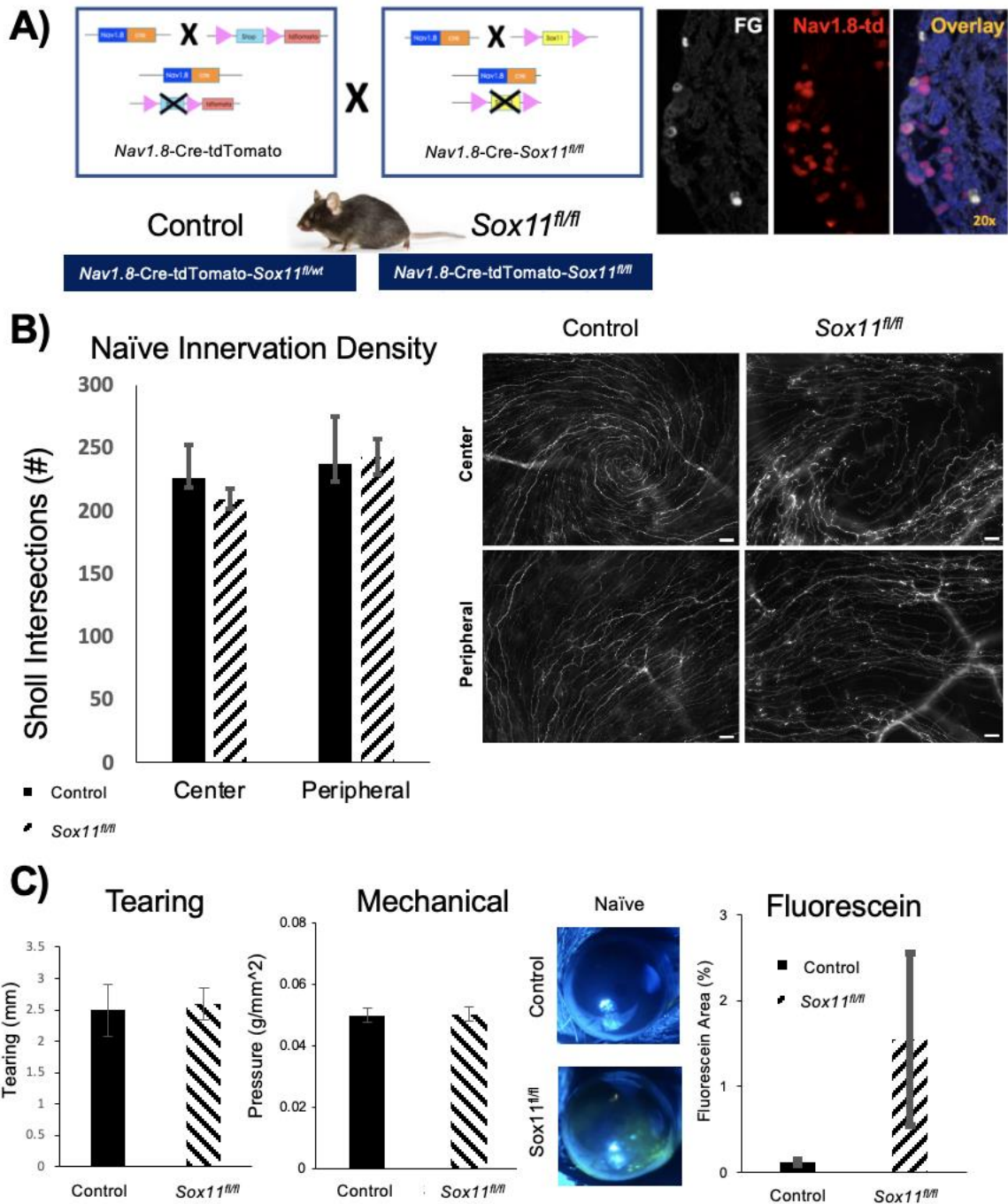
Figure 3.1. Characterization of *Nav1.8*-Cre-tdTomatot-*Sox11* transgenic model. A)

Development and evaluation of the transgenic *Nav1.8*-Cre-tdTomato- *Sox11^{fl/fl}* Model B) Naïve

innervation density quantified (left) with representative images (left) C) Tearing, mechanical and

fluorescein scores of naïve control versus $Sox11^{fl/fl}$ animals. Two-Way ANOVA, Tukey Post-Hoc. * p <0.05 ** p < 0.01 Scale bar 20 µm.
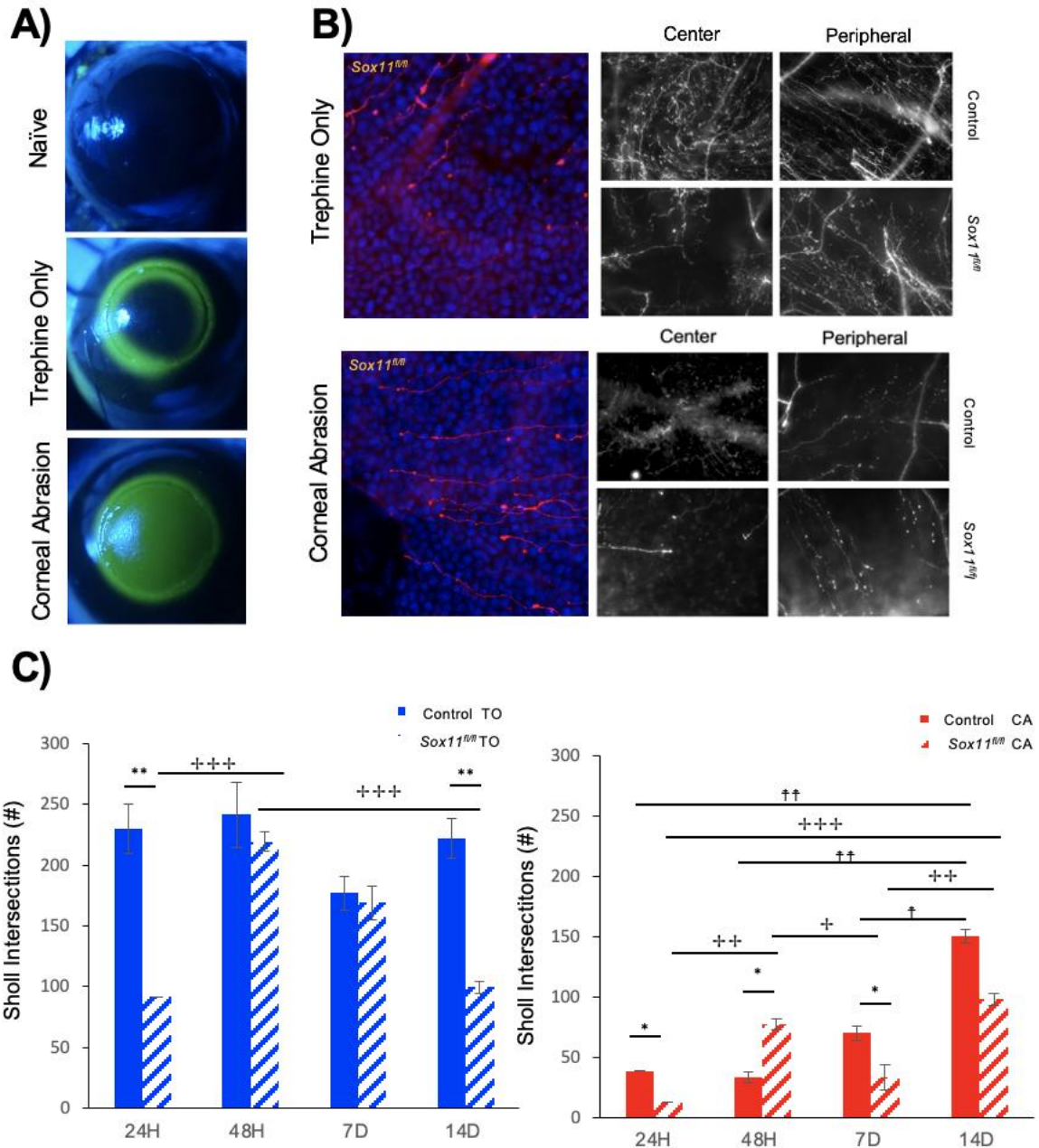
Figure 3.2. Direct corneal injury on epithelium and innervation density. A) Fluorescein stain on naïve immediately before injury (top), TO (bottom), CA immediately following injury (i.e. 0 hours post-injury). B) Representative images of epithelium damage and innervation density (left top panel) at 24 hours following TO (right top panels) and CA (right bottom panels) in control and *Sox11*^{fl/fl} animals (40x). C) Quantification of innervation density at 24 hours, 48 hours, 7 days

and 14 days following TO and CA injury in control and $Sox11^{fl/fl}$ animals. Two-Way ANOVA,

Tukey Post-Hoc, Control vs $Sox11^{fl/fl}$ * p <0.05 ** p < 0.01, *** p < 0.001; Timepoint vs Control †

p <0.05 †† p < 0.01, ††† p < 0.001; Timepoint vs $Sox11^{fl/fl}$ ✝ p <0.05 ✝✝ p < 0.01, ✝✝✝ p <
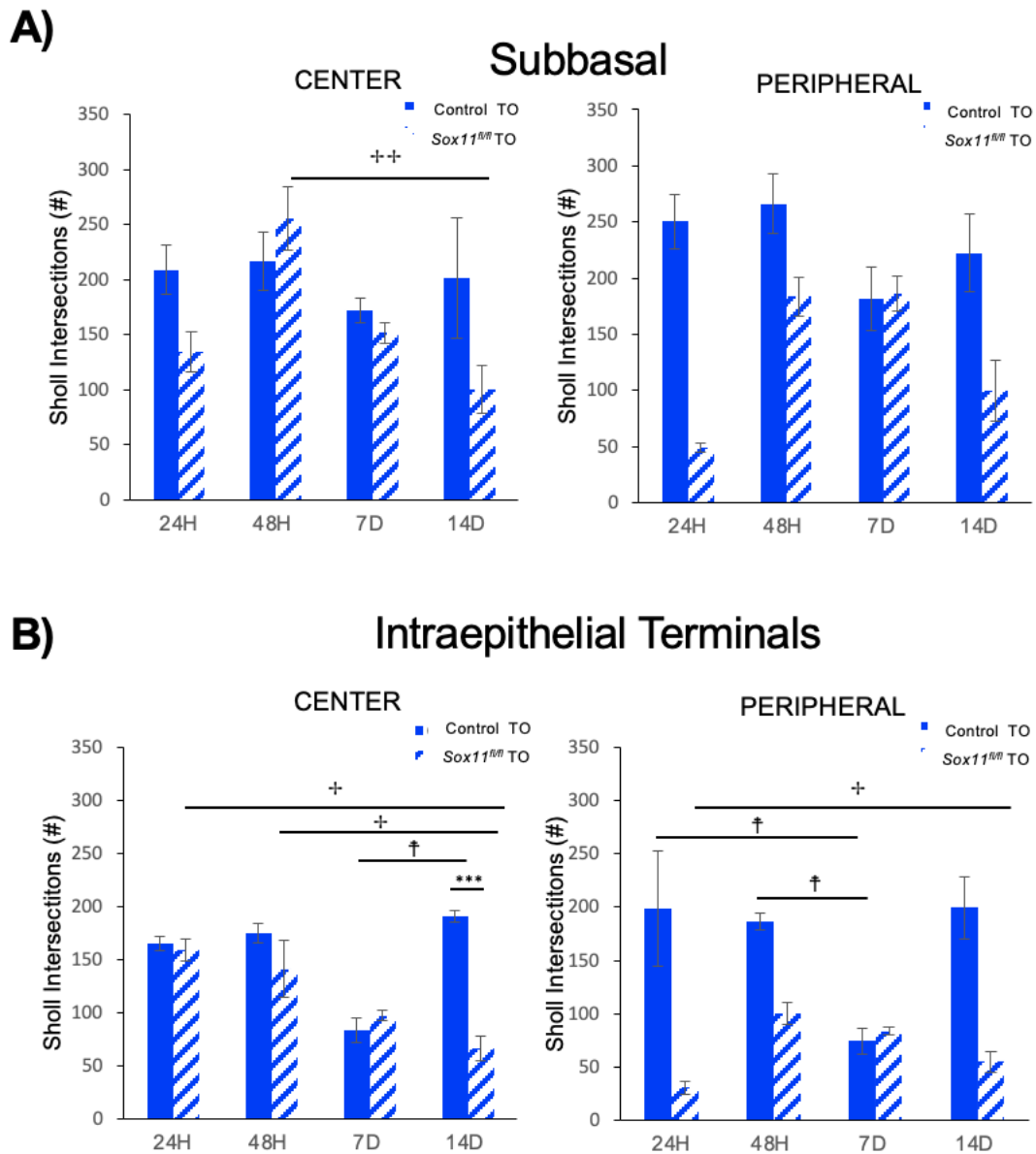
0.001

Figure 3.3. Innervation Density of center and peripheral corneal regions. A) subbasal and B) intraepithelial terminals following TO injury. Two-Way ANOVA, Tukey Post-Hoc, Control vs *Sox11fl/fl* * p <0.05 ** p < 0.01, *** p < 0.001; Timepoint vs Control † p <0.05 †† p < 0.01, ††† p < 0.001; Timepoint vs *Sox11fl/fl* ╬ p <0.05 ╬╬ p < 0.01, ╬╬╬ p < 0.001
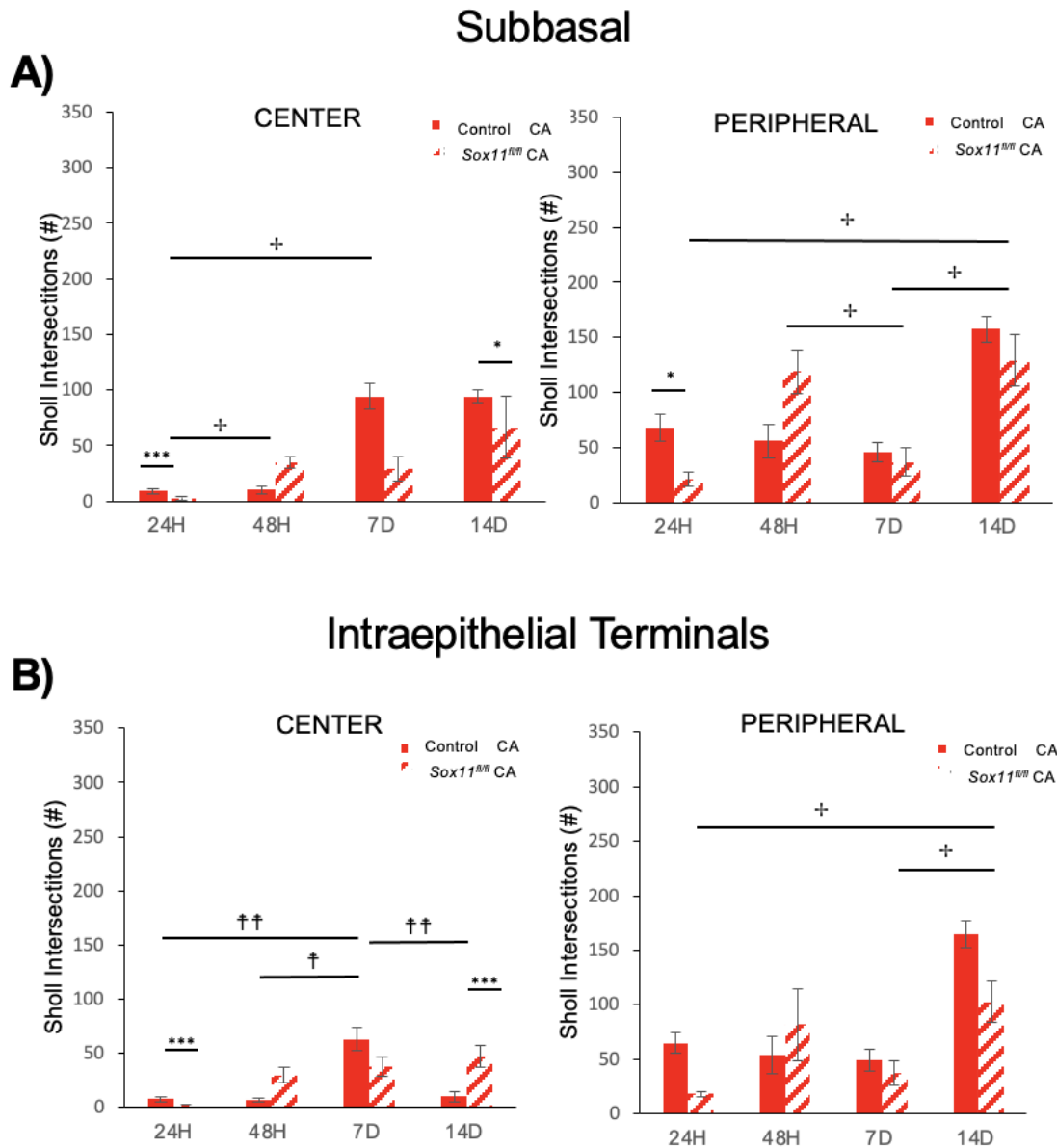
Figure 3.4. Innervation Density of center and peripheral corneal regions. A) subbasal and B) intraepithelial terminals following CA injury. Two-Way ANOVA, Tukey Post-Hoc, Control vs *Sox11^{fl/fl}* * p <0.05 ** p < 0.01, *** p < 0.001; Timepoint vs Control † p <0.05 †† p < 0.01, ††† p < 0.001; Timepoint vs *Sox11^{fl/fl}* ✝ p <0.05 ✝✝ p < 0.01, ✝✝✝ p < 0.001
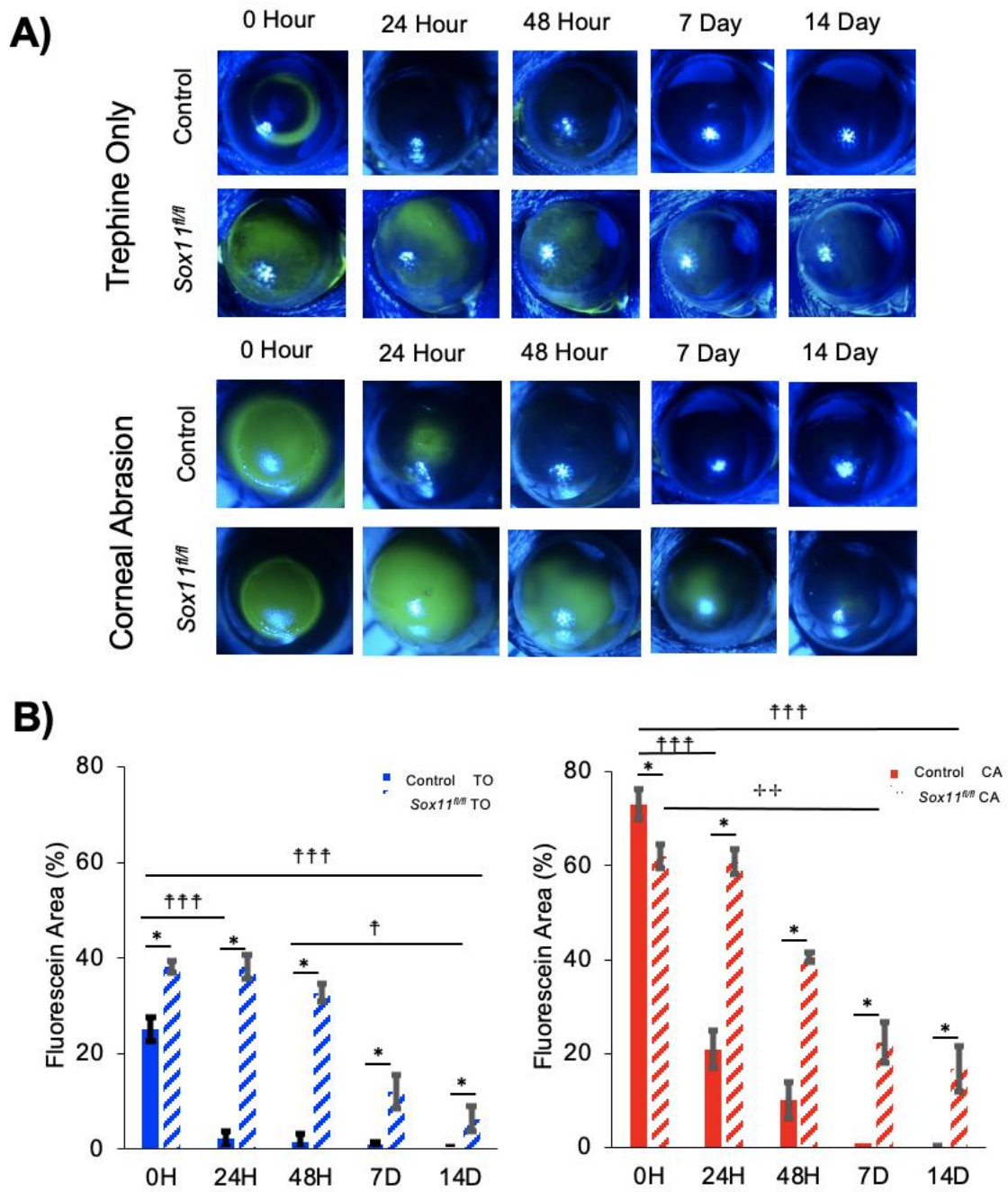
Figure 3.5. Epithelial wound healing. A) Representative images of CA at 24-hours, 48-hours, 7

days and 14 days injury. B) Quantification of percent area showing fluorescein stain at the same

time points following injury. Two-Way ANOVA, Tukey Post-Hoc Control vs $Sox11^{fl/fl}$ * p <0.05 **

p < 0.01, *** p < 0.001; Timepoint vs Control † p <0.05 †† p < 0.01, ††† p < 0.001; Timepoint

vs $Sox11^{fl/fl}$ ┿ p <0.05 ┿┿ p < 0.01, ┿┿┿ p < 0.001
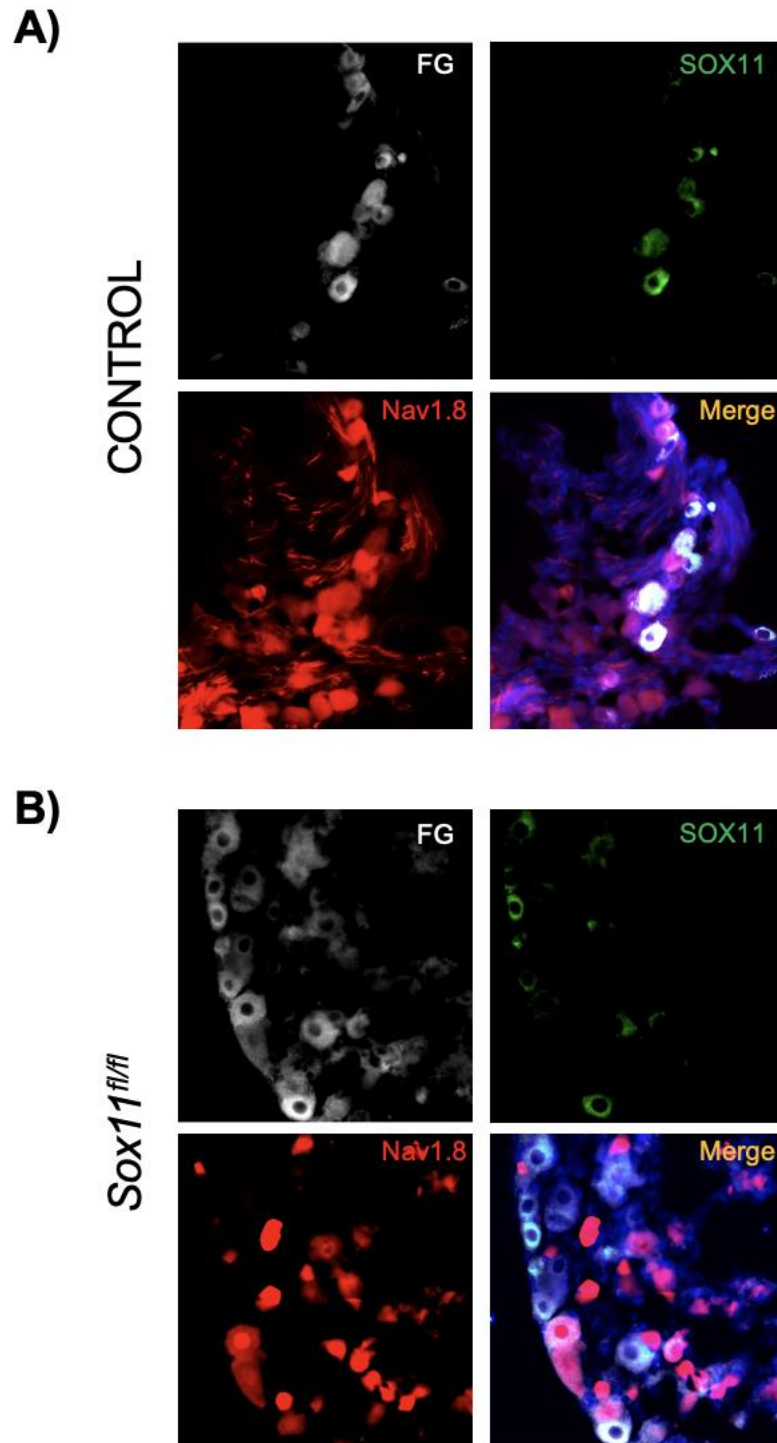
Figure 3.6. Representative images of *Sox11fl/fl* and littermate controls with FluoroGold in TG.

control (A) and *Sox11fl/fl* SOX11 expression 24 hours following CA injury. Scale 20x
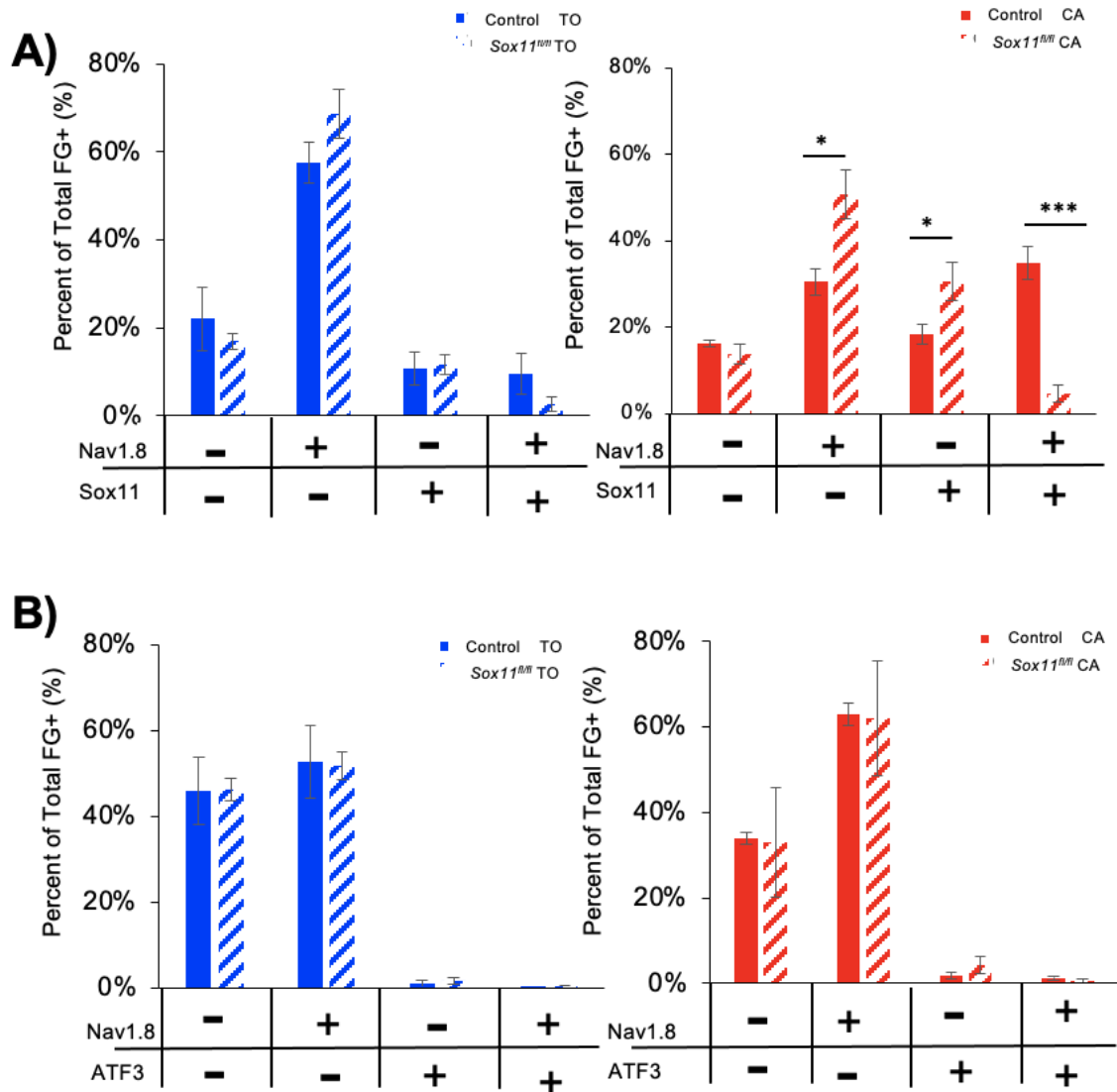
Figure 3.7. Expression 24 hours following TO injury and CA injury A) SOX11 expression B) ATF3 expression. Student t-test, * p <0.05   ** p < 0.01 * p <0.05   ** p < 0.01
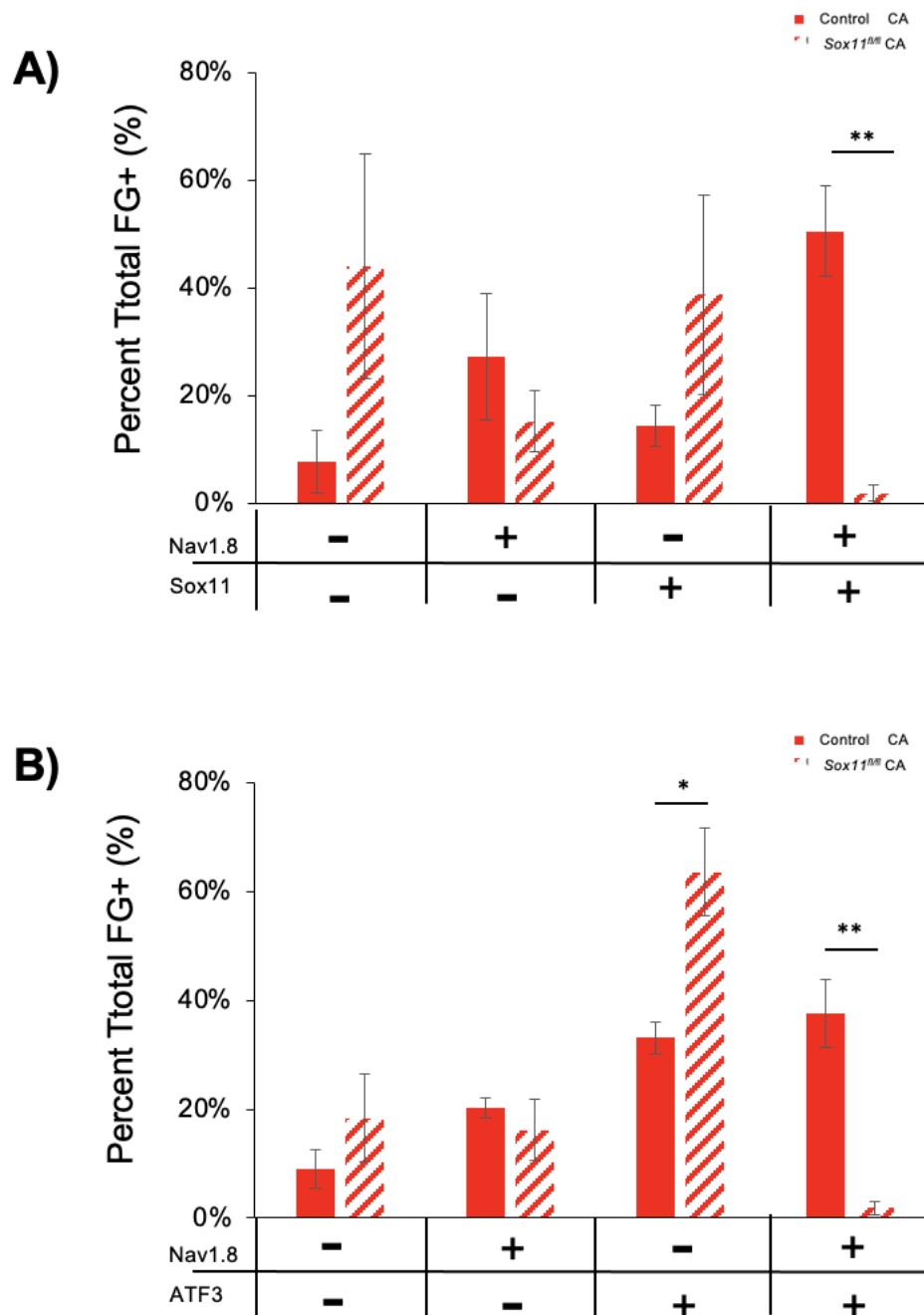
Figure 3.8. Expression 48 hours following CA injury A) SOX11 expression B) ATF3 expression.

Student t-test, * p <0.05   ** p < 0.01

Table 3.1. Results for ANOVA for all presented data.

Figure	Metric	Measurement	Genotype				Time				Genotype:Time			
			DF-V	DF-R	F	P	DF-V	DF-R	F	P	DF-V	DF-R	F	P
2C	ANOVA (2W)	Intersections (#) TO	1	23	25.343	4.29E-05	3	23	10.15	0.000189	3	23	6.102	0.00328
2C	ANOVA (2W)	Intersections (#) CA	1	23	0.086	0.7719	3	23	16.6	5.86E-06	3	23	4.843	0.00934
3A	ANOVA (2W)	Intersections (#) TO-SB-Center	1	23	2.965	9.85E-02	3	23	6.739	2.00E-03	3	23	2.54	0.0814
3A	ANOVA (2W)	Intersections (#) TO-SB-Peripheral	1	23	27.625	2.48E-05	3	23	4.388	1.40E-02	3	23	5.083	0.0076
3B	ANOVA (2W)	Intersections (#) TO-IT-Center	1	23	10.86	0.00316	3	23	6.752	0.00198	3	23	5.768	0.0043
3B	ANOVA (2W)	Intersections (#) TO-IT-Peripheral	1	23	45.295	7.27E-07	3	23	3.182	0.043	3	23	7.502	0.00113
4A	ANOVA (2W)	Intersections (#) CA-SB-Center	1	23	0.231	6.36E-01	3	23	5.014	8.07E-03	3	23	2.159	0.12037
4A	ANOVA (2W)	Intersections (#) CA-SB-Peripheral	1	23	1.038	0.318895	3	23	8.589	0.000524	3	23	1.598	0.21709
4B	ANOVA (2W)	Intersections (#) CA-IT-Center	1	23	1.268	2.72E-01	3	23	7.642	1.02E-03	3	23	3.48	0.03228
4B	ANOVA (2W)	Intersections (#) CA-IT-Peripheral	1	23	0.116	0.736286	3	23	8.888	0.000428	3	23	1.55	0.22854
5B	ANOVA (2W)	Area (%) TO-Fluorescein	1	42	50.83	9.50E-09	3	42	14.72	1.08E-06	1	42	0.2	0.657
5B	ANOVA (2W)	Area (%) CA-Fluorescein	1	101	0.429	0.51413	4	101	21.69	6.16E-13	3	101	7.716	0.00011

CHAPTER 4

CHRONIC CORNEAL NERVE INJURY

DELAYED NAV1.8 REINNERVATION FOLLOWING LACRIMAL GLAND EXCISION WITH

Sox11 DOWNREGULATION

4.1. Abstract

Reduced innervation and altered sensitivity are often reported in severe dry eye. The aim of this study was to investigate the role of transcription factor SOX11 in sensitivity, innervation, and healing in a *Nav1.8-Sox11* conditional downregulation within the context of a severe aqueous tear deficient mouse model. Severe chronic dry eye was created by ipsilateral excision of the extra- and intraorbital lacrimal glands in both sexes of transgenic *Sox11$^{fl/fl}$* and littermate controls. Tearing was quantified before and timepoints after LGE surgery using a phenol-coated thread. Corneal epithelial damage was assessed by applying fluorescein dye, and changes to mechanical sensitivity were measured using a Cochet-Bonnet esthesiometer. Ocular sensitivity, indicative of peri-ocular pain, was quantified by measuring palpebral opening before and at times following LGE. Corneal axons were visualized, and Sholl analysis was performed to quantify innervation density across groups. Fluorescence In Situ Hybridization was used to visualize mRNA of molecular markers (SOX11, ATF3, GAP43) at timepoints following LGE. The LGE model decreased tearing and palpebral opening while increasing fluorescein staining. Mechanical sensitivity was decreased in all surgery group females, with less drastic change observed across male groups. Changes were observed to comparable levels over the 4-week observation period in *Sox11$^{fl/fl}$* and littermate controls. Innervation density significantly decreased in timepoints following LGE, with *Sox11$^{fl/fl}$* animals exhibited slower reinnervation than controls. Corneal neurons expressed SOX11 in the highest levels in the acute 7-day period following LGE in controls, while that effect was absent in the *Sox11$^{fl/fl}$* animals during the same

period. Accordingly, ATF3 and GAP43 expression was upregulated following LGE-induced

injury in controls but not in *Sox11^{fl/fl}* animals. These results indicate that LGE-induced corneal

injury results in activating nerve injury and regeneration pathways under SOX11 regulation.

4.2. Introduction

The cornea is specialized epithelial tissue with unique sensory features that aid its ability

to protect the visual system (Lele and Weddell, 1959; Galler et al., 1993; Beuerman and

Pedroza, 1996; DelMonte and Kim, 2011; Marfurt et al., 2010; Sridhar, 2018). One of the few

transparent tissues found in the body, the cornea relies on tear film to replace vascular functions

(i.e., trophic factors, oxygen, waste removal) used in other epithelial tissue. The avascular

nature of the cornea enables its transparency, but in hypoxic pathologies, such as DED,

neovascularization of the cornea is prevalent and often alters structural and molecular aspects

of the corneal microenvironment (Cho et al., 2014; Sharif and Sharif, 2019). Reduced tear film

severely impacts axonal morphology and functioning, resulting in altered responses to a range

of stimuli, retracted axon terminals, and transcriptomic changes (Gallar et al., 2005; Benítez-del-

Castillo et al., 2007; Lemp et al., 2011; Vehof et al., 2013; Stephens and McNamara, 2015;

Belmonte et al., 2017; Piña et al., 2019, Liu et al., 2020). Identifying specific transcription

factors that influence these changes is needed to inform targeted molecular treatments that can

reverse or prevent chronic pathology and pain associated with DED.

Animal models have replicated acute and chronic forms of DED pathology through

temporary inactivation of lacrimal glands, nerve ligation, or through the removal of lacrimal

glands (Park et al., 2007; Kurose and Meng, 2013; Meng and Kurose, 2013; Bannai et al., 2015;

Aicher et al., 2015**;** Kovács et al., 2016; Dietrich et al., 2018; Mecum et al., 2019; Fakih et al.,

2019; Honkanen, 2020; Chang, 2021; Singh, 2021). This study chose an ipsilateral LGE model

to create chronic DED that only causes injury to corneal nerves through the removal of the lacrimal-generated aqueous tear film. This model most accurately recreates chronic corneal surface conditions and mimics corneal nerve injury in the way experienced by many DED patients.

Normally, nerve injury and repair cascades initiate rapidly and restore corneal homeostasis in the acute period following injury (Di et al., 2017; Labetoulle et al., 2018; Al-Aqaba et al.,2019). However, in aberrant chronic corneal injury cases, neuroprotective mechanisms become maladaptive when neovascularization and inflammation persist in a normally avascular, immune-privileged structure (Azar, 2006; Beebe, 2007; Dartt, 2009; McDougal and Gamlin, 2015; Paunicka et al., 2015; Sharif and Sharif,2019). Immediately following injury, peripheral axon terminals retract or degenerate, and nerve regeneration programs are activated (Lagli et al., 2015; Tepelus et al., 2017; Wang et al., 2018; Fakih et al., 2019; Ma et al., 2019). Upregulated expression of nerve regeneration-associated transcription factors, such as ATF3, correlate with successful axon repair and elongation following peripheral nerve injury (Seijffers et al., 2006; Hegarty et al., 2018; Guerrero-Moreno et al., 2020). Unlike in acute injury models (Hegarty et al., 2018). While RAG network activation normally occurs acutely after injury, aberrant changes to this cascade may contribute to sustained peripheral neuropathology (Schmitt et al., 2003; Zujovic et al., 2005; Gey et al., 2016; Norsworthy et al., 2017; Shin et al., 2019; Shin et al., 2021). SOX11 has been attributed to upstream regulation of RAGs and specifically in peripheral nerve regeneration following injury (Jankowski et al., 2009; Jing et al., 2012; Norsworthy et al., 2017). SOX11, in addition to other well-known injury and regeneration markers, such as ATF3 and GAP43, are part of a complex regeneration signaling network that promotes nerve healing and regeneration following injury (Schreyer et al., 1991; Chaudhary et al., 2012; Gey et al., 2016; Norsworthy et al., 2017; Wang et al., 2018; Shin et al.,

2019). Examining the effect of SOX11 deletion on corneal nerve regeneration following LGE has not been reported to date but has been evaluated in the present study.

This study investigated the role of SOX11 expression after DED-induced corneal injury. Selecting an upstream regulator within the RAG peripheral nerve injury pathway will provide insight into the role of critical molecular targets within this pathway that can be further investigated in whole transcriptome analysis or through targeted molecular treatments.

4.3. Materials and Methods

4.3.1. Generation of *Nav1.8*-tdTomato-*Sox11* mice

Nav1.8-Cre-C57B6/J mice generated initially by Dr. John Wood (University College London, London, UK) and obtained from Dr. Sulayman D. Dib-Hajj (Yale University, New Haven, CT, USA) were bred with B6. Cg-Gt(ROSA)26Sortm14(CAG-tdTomato)Hze/J (Stock #007914, The Jackson Laboratory, Bar Harbor, ME, USA). The resulting F1 progeny that was heterozygous for *Nav1.8*-Cre and tdTomato were intercrossed to result in mice with specific expression of tdTomato fluorescent protein in Nav1.8-expressing neurons. *Nav1.8*-CreHet-tdTomatoHet progeny were intercrossed with *Sox11* conditional downregulation, previously generated using the Cre-loxP system by floxing the single *Sox11* exon. *Nav1.8*-tdtomato expression could be visualized using fluorescence microscopy (em. 581 nm). *Nav1.8*-Cre-tdTomato-*Sox11*$^{fl/fl}$ mice were used as experimental *Sox11*$^{fl/fl}$ animals, and *Nav1.8*-Cre-tdTomato-*Sox11*$^{fl/wt}$ animals were used as the littermate controls.

For genotyping, tissue was lysed by adding 50mM NaOH and then heated to at 95°C for 35 minutes, followed by the addition of 50mM HCl and 1M Tris HCl buffer. The sample was spun down and then stored at 4°C until processed. Polymerase chain reaction (PCR) was used

to identify *Sox11* and tdTomato using Econotaq Plus 2x Buffer (Lucigen, Middleton, WI, USA). Primers included: *Sox11* Forward– GTGATTGCAACAAAGGCAGA, *Sox11* Reverse – TCTGCCGATGTCTTTCAGAC, Td tomato Mutant Forward– CTGTTCCTGTACGGCATGG, Td Tomato Mutant Reverse – GGCATTAAAGCAGCGTATCC, Td Tomato Wild Type Forward – AAGGAGCTGCAGTGGAGTA, Td Tomato Wild Type Reverse – CCGAAAATCGTGG-GAAGTC. *Nav1.8*-Cre reactions were prepared with Promega GoTag Flexi-buffer (Promega, Madison, WI, USA). Primers included: *Nav1.8*-Cre Common Forward – GGAATGG-GATGGAGCTTCTTA, *Nav1.8*-Cre Mutant Reverse – CCAATGTTGCTGGA-TAGTTTTTACTGCC, *Nav1.8*-Cre Wild Type Reverse – TTACCCGGTGTGTGCTGTAGAAAG. Genotyping of all animals was conducted by the University of New England Behavioral and Genotyping Core.

4.3.2. Animals

Adult male and female mice were group-housed and given food ad libitum. Animals used in experiments were between 8-10 weeks old. All animal study protocols were approved by the Committee on Animal Research at the University of New England. Animals were treated according to policies and recommendations of the National Institutes of Health Guide for the Care and Use of Laboratory Animals.

4.3.3. Lacrimal Gland Excision

Moderate-to-severe dry eye was created by removing the left exorbital and infraorbital lacrimal glands under isoflurane anesthesia. Sham surgery was performed on control animals by making incisions over the left exorbital and infraorbital gland sites. Animals were monitored daily for 5 days post-surgery (Figure 4.1.B).

4.3.4. Retrograde Neuron Tracing

FluoroGold (FG, 3% in NaCl; Fluorochrome, Denver, CO, USA) was applied to the cornea under isoflurane anesthesia as previously described. Briefly, at 72 hours before LGE or sham surgery, a DC current (7 µA for 10 min) was passed between a copper wire in a capillary tube filled with FG, and a copper cathode was placed in the tail. An absorbent gelatin sponge (Gelfoam 12–7 mm; Pfizer Pharmaceuticals, New York, NY) was inserted into the capillary tube to contact both the cornea and the tracer solution.

4.3.5. Palpebral Opening

Palpebral opening was quantified as a sign of ocular discomfort as previously described. The height of the gap between the upper and lower eyelids and the distance separating the two canthi was measured using ImageJ/FIJI from 5 still shots taken from a 5-minute video. For each still shot, the height was divided by the distance between the canthi, and these were averaged together to give an overall palpebral opening ratio.

4.3.6. Mechanical Sensitivity

Corneal mechanical sensitivity was evaluated using a Cochet-Bonnet esthesiometer (12/100mm, Western Ophthalmics Corp., Lynnwood, WA, USA). Beginning with a length of 60 mm, the nylon filament was applied to the cornea three times. If a corneal reflex including a blink and/or eyeball retraction was observed in less than 2 of the three trials, then the filament length was decreased by a 5mm increment. The filament length was converted to the amount of pressure (g/mm2) using the filament-specific conversion chart provided by Western Ophthalmics.

4.3.7. Tear Production

Tearing was quantified using phenol red threads inserted into the lateral canthus of the eye for 15 seconds in unanesthetized animals (Zone-Quick, FCI Ophthalmic, Pembroke, MA, USA). The length of the red portion of the thread was measured under a dissecting microscope.

4.3.8. Corneal Fluorescein Staining

Fluorescein staining was used to assess corneal epithelial damage. The staining was performed before and 3-days, 7-days, 14-days, and 28-days following LGE. A fluoresce-in solution (1%, 10uL; Sigma-Aldrich Corp., St. Louis, MO, USA) was applied to the cornea while animals were under isoflurane anesthesia. After 2 minutes, the eye was rinsed with artificial tears and was visualized with a cobalt blue light (16 LED Blue Flashlight, 464 nm, LDP LLC, Carlstadt, NJ, USA). The area of staining was evaluated on a 0 to 4 scale. The total absence of staining was scored a 0, less than 1/8 of total area stained a 1, 1/8-1/4 was given a 2, 1/4-1/2 scored as 3, and any fluorescein staining greater than 50% of the total corneal area was given a 4. For a subset of animals, the area of staining was imaged using an iPhone X with a Kaiess 20x macro lens attachment. The percent area of staining within the wounding area was calculated using ImageJ/FIJI.

4.3.9. Corneas

At 3, 7, 14, and 28 days post-LGE or sham surgery, animals were deeply anesthetized with Euthasol (Henry Schein, Melville, NY, USA), and eyeballs were removed using curved blade fine scissors (Item # 14061-10, Fine Science Tools, Foster City, CA, USA). Eyeballs were briefly fixed with 10% formalin and transferred into PBS before dissection. Corneas were

dissected and washed three times in PBS on a shaker at room temperature for 10 minutes. After making 3 cuts along the periphery to allow the corneas to lie flat, corneas were whole-mounted onto slides with DAPI infused mounting media (ProLong Gold Antifade with Dapi, ThermoFisher Scientific, Waltham, MA, USA). Corneas were imaged at 40x using a Keyence BZ-X series fluorescence microscope. Five images were taken in a z-stack in 1 mm steps, with one in the central and four in the peripheral regions of the cornea. The center was selected based on the converged spiral of subbasal axons, and the peripheral areas were chosen at least 0.92 mm diagonal from the central image. Images were split into free nerve ending and subbasal layers and analyzed using FIJI/IMAGEJ. The maximum projection of each z-stack was converted to a mask, and the Sholl Analysis plugin was used to quantify innervation density.

4.3.10. Fluorescence In Situ Hybridization

After corneas were extracted at 3, 7, 14, and 28-days post-LGE or sham surgery, animals were perfused with heparinized saline and 10% neutral buffered formalin on ice. TG was harvested and postfixed in 10% formalin for 24 hours at 4°C before submerged in 30% sucrose. TG were cut using a cryostat at 12 μm using serial sectioning to count every fifth section. Fluorescent in situ hybridization studies were performed according to the protocol for fresh frozen tissue using the RNAscope Fluorescent Multiplex Reagent kit (Advanced Cell Diagnostics, Newark, CA) with minor modifications.

After dehydration of sections in ethanol, sections were treated with protease IV (ref. no. 322340, RNAscope), incubated for 30 min at room temperature, and washed in PBS. Species-specific target probes for SOX11, ATF3, CGRP, and GAP43 were used (Stock #'s 440811, 426891, 417961, 318621, Advanced Cell Diagnostics, Newark, CA, USA). Sections were treated with the probe mixture and negative (ref. no. 320871) or positive (ref. no. 320891)

controls and were hybridized for 2 hours at 40°C in a humidified oven (RNAscope HybEZ oven with HybEZ humidity control tray, Advanced Cell Diagnostics). A series of incubations were then performed to amplify the hybridized probe signals and label target probes with the assigned fluorescence detection channels (C1-Alexa488, C2-Atto550). Nuclei were stained using a Cy5 nuclear stain (NucRed Live 647; Invitrogen, Carlsbad, CA) for 20 min and washed with PBS. Slides were glass coverslip mounted with Fluoromount-G (SouthernBiotech, Birmingham, AL) mounting media and sealed.

Sections were imaged at 20x using a Keyence BZ-X microscope using filter cubes for DAPI (ex-citation (ex): 340–400 nm; emission (em): 435–485 nm), GFP (ex: 450–490 nm; em: 500–550 nm), Cy3 (ex: 530–560 nm; em: 570–640 nm), and Cy5 (ex: 590–650 nm; em: 665–735 nm). Keyence Analyzer software was used to stitch together images from each section in each channel. ImageJ software (National Institutes of Health, Bethesda, MD) was used to merge each fluorescent channel into a final composite. Images were randomized and blinded before counting. Cells with at least 3 puncta were considered positive for fluorescent markers were manually counted and marked using the Cell Counter plugin in ImageJ. Cells were counted as positive if the fluorescent marker was present in the channel-specific image and corresponded to a cell containing nuclei when viewed as a merged composite. Percent of tracer-positive cells was calculated using the number of total tracer labeled cells per animal. All images were blinded before analysis. Co-labeled cells were counted as positive if they were determined to be within the same cell that contained a nucleus and exhibited at least three fluorescent puncta using individual and composite channel images.

4.3.11. Data Analysis

Statistical analyses for palpebral opening, tear production, cell counts, and diameters were performed with a two-way ANOVA and Tukey post-hoc test. For non-parametric data (mechanical sensitivity and fluorescein staining), a Kruskal-Wallis one-way ANOVA with Dunn's post hoc test was performed. Statistical analyses were performed using R and the 'dplyr' package.   Statistical significances were accepted as $p < 0.05$. Plots, tables, and diagrams were created using R and Excel and PowerPoint, and data are presented as mean ± SEM.

4.4. Results

4.4.1. Lacrimal gland excision reduces tearing in *Sox11$^{fl/fl}$* and controls

Retrograde tracer was applied to the cornea 72 hours prior to LGE surgery in which both ipsilateral lacrimal glands were removed (Figure 4.1.A-B). Transgenic mice were bred to express tdTomato in Nav1.8 expressing neurons and in a subset of animals inhibit expression of *Sox11* in tdTomato-*Nav1.8* neurons (Figure 4.2.B). Tearing was measured at time points following LGE to evaluate the reduction of aqueous tear film in response to removing the aqueous tear-producing lacrimal glands. Tearing was reduced across all groups, as measured by a phenol thread inserted into the lateral canthus (Figure 4.1.C, p<0.0001, 3-way ANOVA). The comparison of naïve *Sox11$^{fl/fl}$* and naïve littermate controls showed no significant difference in tear production.

4.4.2. Lacrimal gland excision alters mechanical sensitivity and causes ongoing pain-like behavior

Mechanical thresholds were determined according to the length of a nylon monofilament elicited a corneal reflex (Figure 4.2.). Animals showed decreased responses to mechanical stimuli, with control females exhibiting significant hyposensitivity at all time points following LGE. This effect was blunted in female *Sox11^{fl/fl}* animals compared to baseline and sham animals (Figure 4.2.B, left plot, 3-way ANOVA). While reduced mechanical responses indicate hyposensitivity, ongoing pain-like behavior was observed through squinting behavior (Figure 4.3.A, 3-way ANOVA). Reduced palpebral opening was observed ipsilaterally, accompanied by acute ocular hair loss and grimace on the same side (Figure 4.3.A, right). Epithelial damage was observed at all times following LGE in both control and *Sox11^{fl/fl}* animals, evidenced by more than 50% of the surface area displaying fluorescein staining under a cobalt blue light (Figure 4.3.B).

4.4.3. Corneal afferent regeneration is slowed in *SOX11^{fl/fl}*

Innervation density was measured using a unique tdTomato fluorescent protein reporter expressed by the *Nav1.8*-cre promoter (Figure 4.4.). Unlike in many other innervation studies, which rely on immunofluorescence to visualize corneal neurons, through the use of transgenic models, this study eliminates experimental variability and confounds seen in traditional studies. This combined with a traditional Sholl analysis (Causey and Palmer, 1953) quantification of nerve density, using ImageJ to total intersections averaged across varying diameter concentric circles, overlayed on four peripheral and one center corneal z-stacked images (Figure 4.4.B). Comparison of groups found that axonal regeneration slowed at 3-,7- and 14-days following

LGE in *Sox11*^{fl/fl} animals compared to littermate controls following LGE and sham groups (Figure 4.4.C).

4.4.4. LGE increased expression of regeneration association genes in Nav1.8 corneal afferents but with blunted effect with *SOX11*^{fl/fl}

LGE-induced corneal dryness resulted in epithelial injury, sensitivity changes, and decreased axonal innervation in both *Sox11*^{fl/fl} and littermate controls. Using iontophoretic application of a retrograde tracer, corneal cell bodies were labeled by FluoroGold, and mRNA expression was evaluated at timepoints up to 28-days following LGE across groups. Genetic downregulation of *Sox11* in Nav1.8 neurons significantly reduced SOX11 (Figure 4.5.), ATF3, and GAP43 (Figure 4.6.) in Nav1.8 expressing corneal afferents following LGE when compared to littermate controls which saw an increase in all of these molecular markers at the same time points following injury. The percentage of SOX11 in control corneal neurons was elevated at 3-days following LGE, an increase that nearly doubled at 7-days post-LGE (Figure 4.5.B). This pattern of this effect was seen in both genetic control and *Sox11*^{fl/fl} groups, but with a muted effect in the latter. At 14-days following injury, SOX11 expression was at its lowest across all groups, following at 28-day with a near doubling of that expression (Figure 4.5.B). ATF3 and GAP43 were also increased at 3- and 14-days following LGE, but expression increases post-LGE were not statistically significant at later timepoints. The chronic injury which creates sustained damage to the corneal microenvironment may induce cyclical increases in this peripheral nerve regeneration pathway.

4.5. Discussion

Prior studies have validated the use of ipsilateral LGE to create a chronic and severe DED model that adequately replicates symptoms found in clinical populations (Kurose and Meng, 2013; Meng et al., 2015; Shinomiya et al., 2018; Hatta et al., 2019; Skryzypecki et al., 2019; Mecum et al., 2020). Chronic DED is often associated with ocular discomfort, pain, and corneal morphology changes in clinical populations. Physical findings of corneal pathology and psychophysical experiences of corneal have been well characterized by these studies. This study examined these same components of DED, in addition to molecular changes in corneal neuron somas in the TG, within the context of a *Sox11* genetic downregulation and LGE. The present study results identify the role of SOX11 in the speed and morphological organization of axonal reinnervation of the cornea following LGE-induced DED. These results also identify other molecular markers (e.g., ATF3, GAP43), presumably regulated at least in part by SOX11, which contribute to corneal nerve recovery after aqueous-deficient DED onset.

According to other studies (Kurose and Meng, 2013; Meng et al., 2015; Shinomiya et al., 2018; Mecum et al., 2020), all groups presented with nearly total elimination of ipsilateral tearing at all time points following LGE. Tear reduction confirms that LGE sufficiently removed both ipsilateral lacrimal glands and eliminated the contribution of aqueous tear film to ipsilateral eyes across all groups. Unremarkably, these results show that SOX11 has no auxiliary role in increasing tearing in the absence of lacrimal glands. Pain-like behaviors have been observed in aqueous deficient DED rodent models (Hirata et al., 2014; Fakih et al., 2019, Mecum et al., 2020) and are considered a hallmark symptom of DED reported in clinical populations (Gowrisankaran et al., 2007; Galor et al., 2015; Kalangara et al., 2017; Vehof et al., 2018; Galor et al., 2018; Elhusseiny et al., 2019; Donthineni et al., 2021). Similarly, this study observed decreased palpebral opening on the ipsilateral side of LGE. This further supports this model as

an accurate representation of severe chronic DED, with mice specifically displaying irritation in the eye lacking tears. Concordantly, fluorescein staining of the cornea was maintained at least in excess of 50% of the total corneal surface through 28 days following LGE-induced dry eye. The absence of SOX11 did not yield a measurable effect on either eye closure or fluorescein score. While epithelial SOX11 has been documented to regulate eye closure ability during development (Nunomura et al., 2021), there have not been any documented reports in the literature characterizing the role of SOX11 in chronic pain-like behaviors.

Corneal mechanical sensitivity has been reported to be altered in dry eye patients, yet with some subsets of patients reporting corneal hypo- or hypersensitivity. Some populations appear to exhibit corneal mechanical hypoesthesia (Xu et al., 1996; Adatia et al., 2004; Bourcier et al., 2005; Benitez-Del-Castillo et al., 2007; Labbe et al., 2012), while others present with mechanical hypersensitivity (De Paiva et al., 2004; Situ et al., 2008; Tuisku et al., 2008; Spierer et al., 2015). The variability seen in the clinical population seems to parallel findings in animal studies. Mechanical hypersensitivity was observed following LGE in male rats (Meng et al., 2015; Meng et al., 2019) and following unilateral excision of the extraorbital lacrimal gland and harderian gland in female and male mice (Fakih et al., 2019). In contrast, extraorbital LGE in female mice appeared to decrease corneal mechanical sensitivity (Yamakazi et al., 2017). This study observed cohorts of animals that displayed hyper- or hyposensitivity to mechanical stimuli following LGE, with a majority of female mice becoming less sensitive than their male counterparts. SOX11 appeared to have a moderate impact on diminishing this effect in females. Since this response cannot be explained by innervation density, it is likely that the elimination of SOX11 may change these neurons' sensory properties. These results highlight complex divergence in mechanical sensitivity responses within dry eye conditions across sex, model, and injury type, thus requiring further investigation.

Healthy corneas have characteristic spiral innervation organizational patterns which maximize space and create a uniform dispersion of axonal fibers throughout each epithelial layer (McKenna and Lwigale, 2011; He et al., 2016; Yang et al., 2018; Al-Aqaba et al., 2019; Labetoulle et al., 2019). Strikingly, we also observed in many LGE genetic control animals and both sham and LGE *Sox11^{fl/fl}*. Typically, the corneal subbasal plexus is organized in a constricted whorl pattern (Shaheen et al., 2014; Cruzat et al., 2017; Marfurt et al., 2019; Bouheraoua et al., 2019). The loss of the whorl was evident in many LGE animals at 28-days following LGE, with even more pronounced aberrant morphology accompanying the *Sox11^{fl/fl}*, which only becomes more apparent in timepoints following injury. Further characterization of the morphological changes in axon terminals is needed to see if a whorl ever develops or if innervation remains disorganized.

Disruptions to the corneal microenvironment, including reducing aqueous tears, can dramatically alter innervation density and morphology. This study supported prior findings that hypoxic dry eye conditions induce denervation of axon terminals (Chao et al., 2014; Chao et al., 2015; Ferdousi et al., 2018; Labetoulle et al., 2019; Liu et al., 2019; Lyu et al., 2019) which recover in density to near-normal levels. Following earlier studies, corneal reinnervation occurs even in the continued absence of tears, neurotrophic factors, and their ability to remove waste byproducts. Downregulation of *Sox11* does reveal its role in reinnervation of the cornea after LGE injury by significantly slowing nerve density regeneration within the cornea. Interestingly, in naïve *Sox11^{fl/fl}* animals, the morphology appears irregular, especially apparent in the center subbasal region where the typical spiral is absent or notably irregular. Studies have identified the role of SOX11 in axon guidance and could explain aberrant morphology even in naïve animals prior to injury (Norsworthy et al., 2017). Additionally, the lack of other intrinsic factors that normally support corneal homeostasis processes likely impairs organizational guidance

105

during the regeneration process. Altered corneal sensitivity observed in dry eye clinical populations, and animal studies may be in part explained by disorganized fiber distribution (Herrmann et al., 2005; Chao et al.,2014; Labbe et al., 2013; Dienes et al., 2015; Tepelus et al., 2017, Liu et al., 2020).

Immediately following injury, peripheral axon terminals retract, or degenerate, and nerve regeneration programs are activated (Lagli et al.,2015; Tepelus et al., 2017; Wang et al., 2018; Fakih et al., 2019; Ma et al., 2019). To evaluate genetic expression changes occurring in the cell bodies of these neurons following injury, FluoroGold was applied as a retrograde tracer in order to clearly and consistently identify the corneal nerve population within the TG. This study evaluated expression changes within this corneal subpopulation. Upregulated expression of regeneration-associated transcription factors (SOX11, ATF3, GAP43) correlates with successful axon repair and elongation following corneal injury (Saito et al., 2008; Hegarty et al., 2018). Upregulated RAGs promote robust axon regeneration, even within the context of severe chronic corneal injury. Thus, chronic conditions which perpetuate corneal dysfunction, such as DED, promote neuroprotective adaptations, which shift sensory thresholds and response properties of injured corneal neurons (Belmonte et al., 2004; Hatta et al., 2019). Morphological and functional changes of axonal afferents are hallmark symptoms seen in many cases of severe clinical DED (Labbe et al., 2013). Altered sensitivity can likely be attributed to receptor expression changes in corneal neurons following injury.

The present study reveals molecular changes occurring to corneal neurons within severe dry eye models. Our results indicate that neuroprotective plasticity occurs to broaden the sensory properties of corneal neurons. Even in chronic injury, and perhaps even more imperatively, the cornea requires adequately functioning corneal sensory processing to protect the cornea and eye from further injury or impairment.
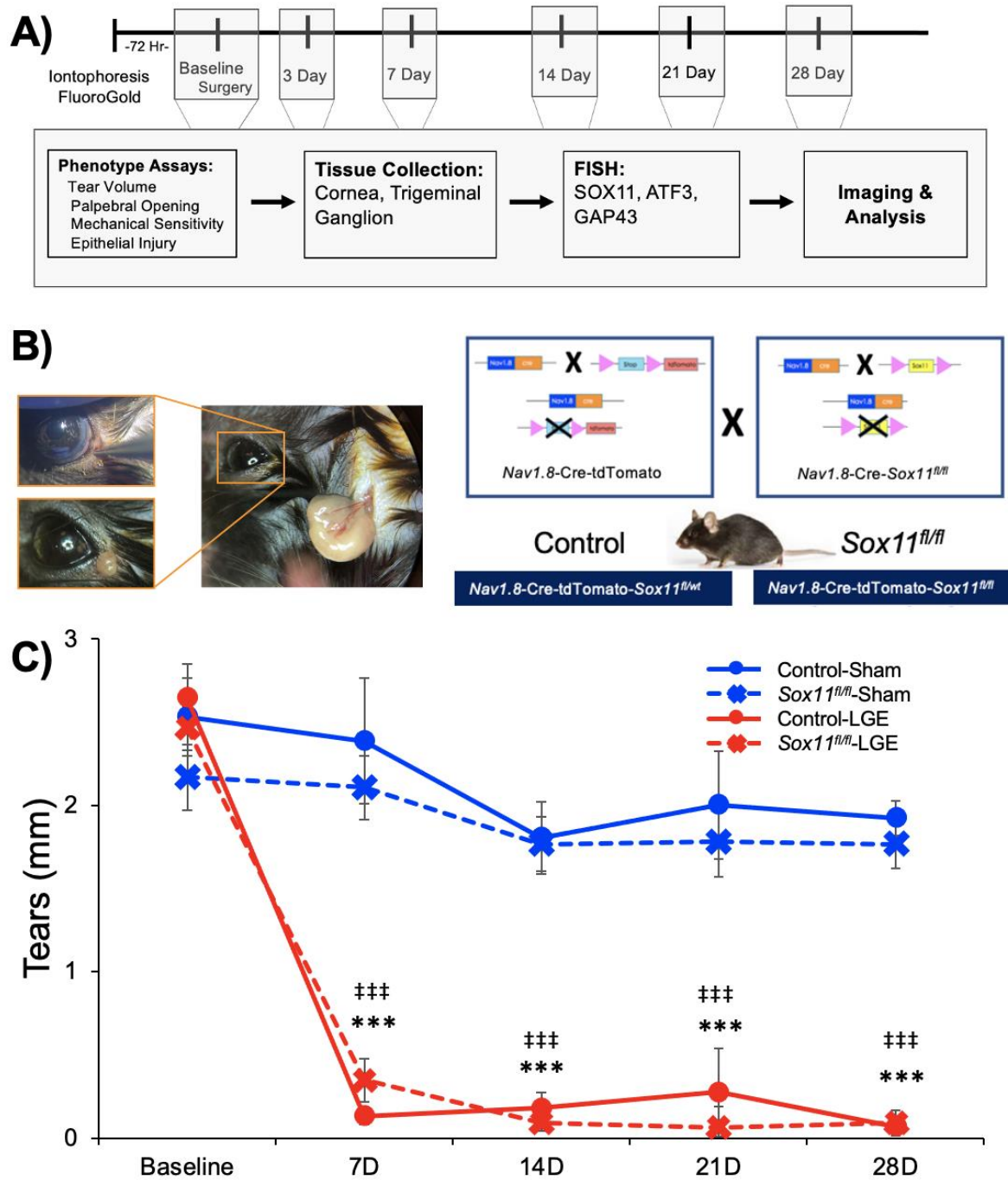
Figure 4.1. Experimental overview and tearing. A) Development and evaluation of the transgenic *Nav1.8*-Cre-tdTomato- *Sox11^{fl/fl}* Model B) Naïve innervation density quantified (left) with representative images (left) C) Tearing, mechanical and fluorescein scores of naïve control

versus *Sox11^{fl/fl}* animals. Two-Way ANOVA, Tukey Post-Hoc. * p <0.05 ** p < 0.01 Scale bar

20 μm.
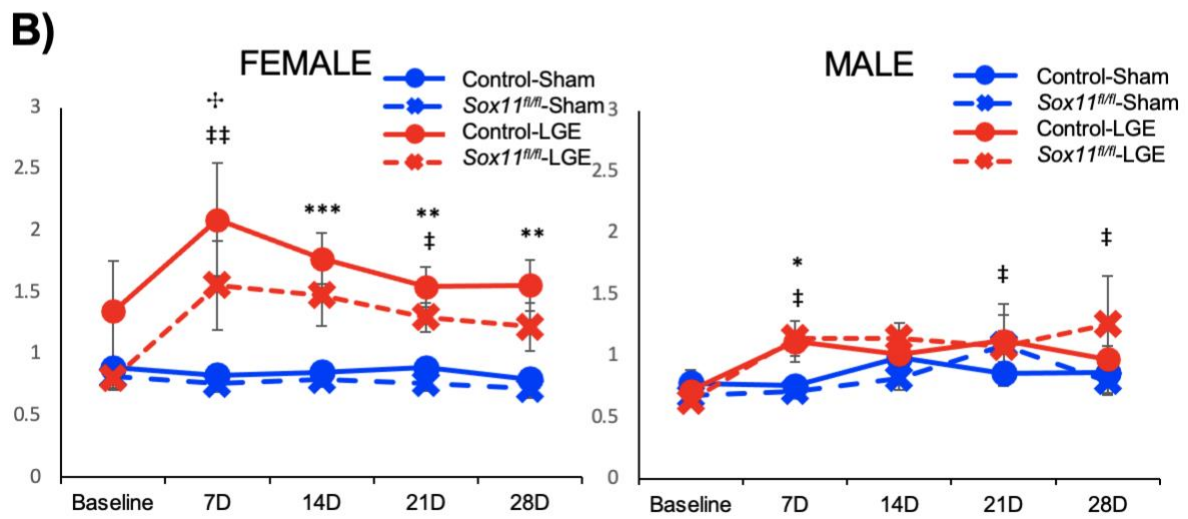
Figure 4.2. Sex differences in mechanical sensitivity. A) Mechanical sensitivity measured by restraining mouse in hand (left) with 12/100mm Cochet-Bonnet esthesiometer (right) B) Mechanical sensitivity Kruskal Wallis (* p <0.05, ** p < 0.001, *** p < 0.0001) (Sham/LGE n= 24,12m/12f). * - significant difference between control sham and control LGE, ‡ - significant difference between *Sox11^{fl/fl}* sham and *Sox11^{fl/fl}* LGE, ÷ - Significant difference between *Sox11^{fl/fl}* and control, 1-Way ANOVA, Tukey Post-Hoc (* p <0.05, ** p < 0.001, *** p < 0.0001)
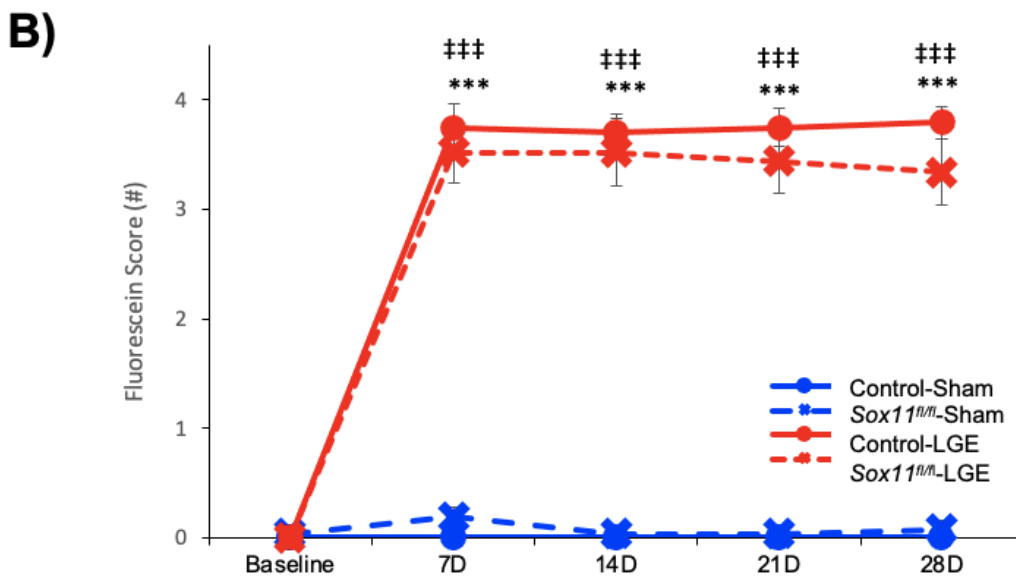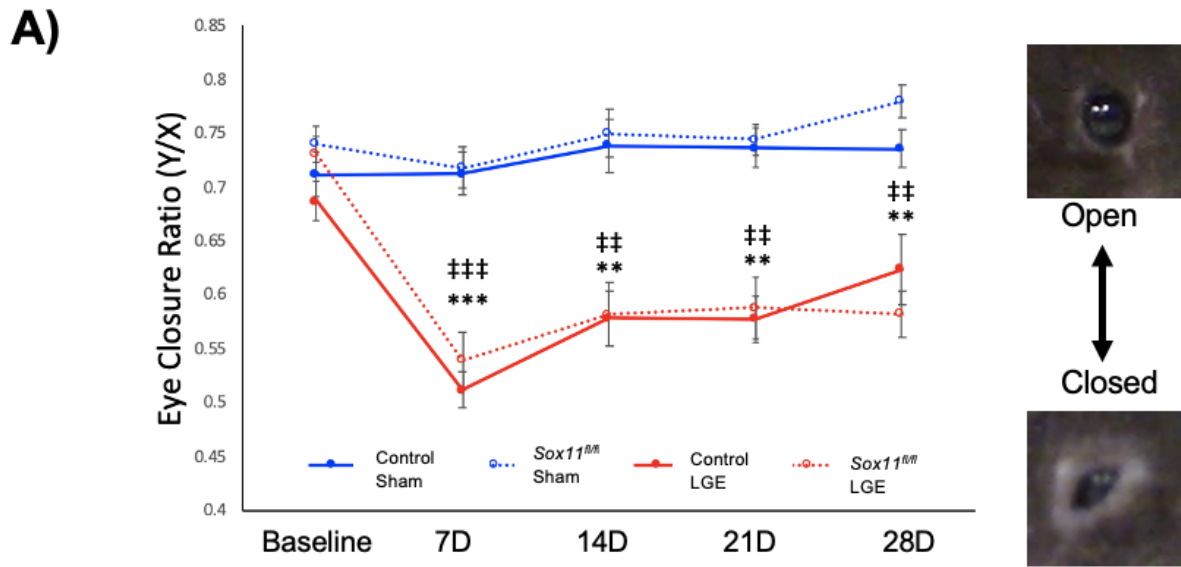
Figure 4.3. Palpebral opening eye closure ratio (Y/X) (Sham/LGE n= 24,12m/12f). 3-Way

ANOVA collapsed to 2-Way ANOVA, Tukey post hoc test) * - significant difference between

control sham and control LGE, ‡ - significant difference between *Sox11$^{fl/fl}$* sham and *Sox11$^{fl/fl}$*

LGE, (*/ ‡ p <0.05, **/ ‡ ‡ p < 0.001, ***/ ‡ ‡ ‡ p < 0.0001) (B), 7-day (7D), 14-day (14D), 28-

day (28D). B) Mean fluorescein score for sham and LGE *Sox11$^{fl/fl}$* and littermate controls.

(Sham/LGE n= 24,12m/12f). Kruskal Wallis (* p <0.05,** p < 0.001,*** p < 0.0001)
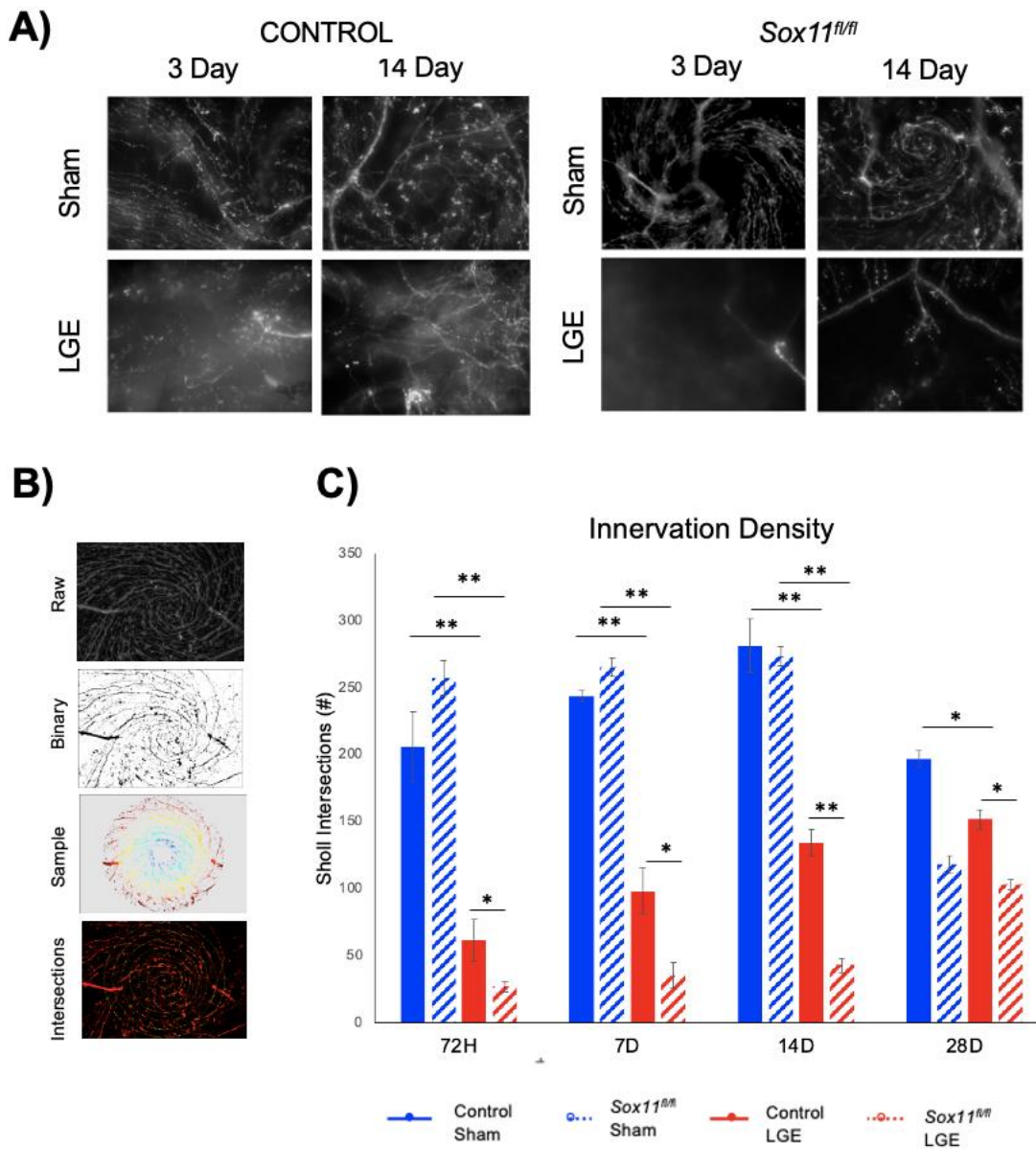
Figure 4.4. Innervation density analysis. A) Representative images of innervation density at 3- and 14-days in sham and LGE control and *Sox11^{fl/fl}* animals. B) Representative images of Sholl analysis quantification process C) Total innervation density quantified by number of Sholl intersections, 7-day (7D), 14-day (14D), 28-day (28D). (Sham/LGE n= 24,12m/12f). 2-ANOVA, Tukey post-hoc (* p <0.05, ** p < 0.001, *** p < 0.0001)
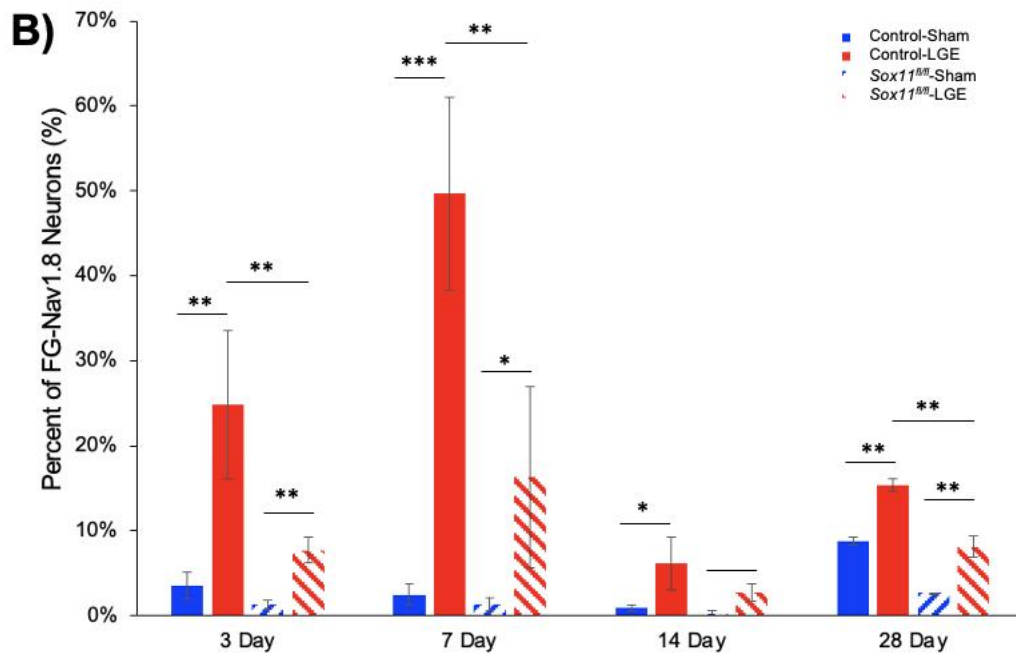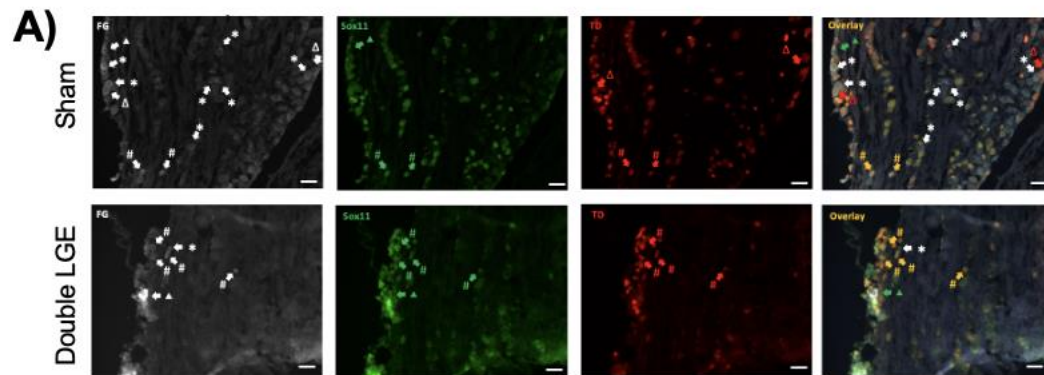
Figure 4.5. mRNA expression following LGE A) Representative images of SOX11 mRNA

expression 3-days following LGE. B) SOX11 at 3-, 7-, 14-, 28-days post-LGE. (Sham/LGE n=

12, 4 control/4 *Sox11$^{fl/fl}$*). 2-Way ANOVA, Tukey post-hoc (* p <0.05, ** p < 0.001, *** p <
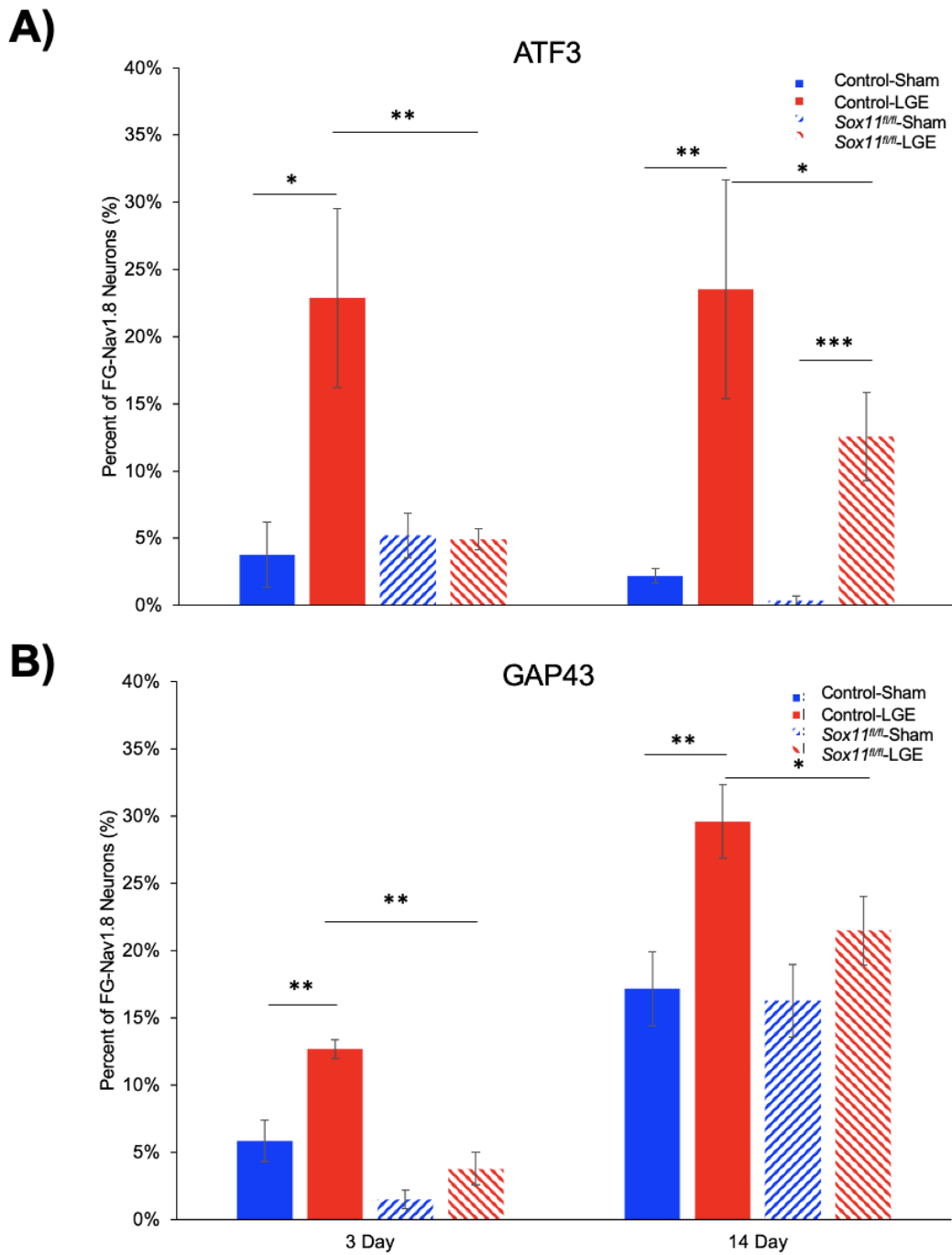
0.0001)

Figure 4.6. mRNA expression of ATF3 and GAP43 following LGE A) ATF3 (left) and B) GAP43 (right) at 3- and 14-days post-LGE. (Sham/LGE n= 12, 4 control/4 *Sox11*^{fl/fl}). 2-Way ANOVA, Tukey post-hoc (* $p < 0.05$,** $p < 0.001$,*** $p < 0.0001$)
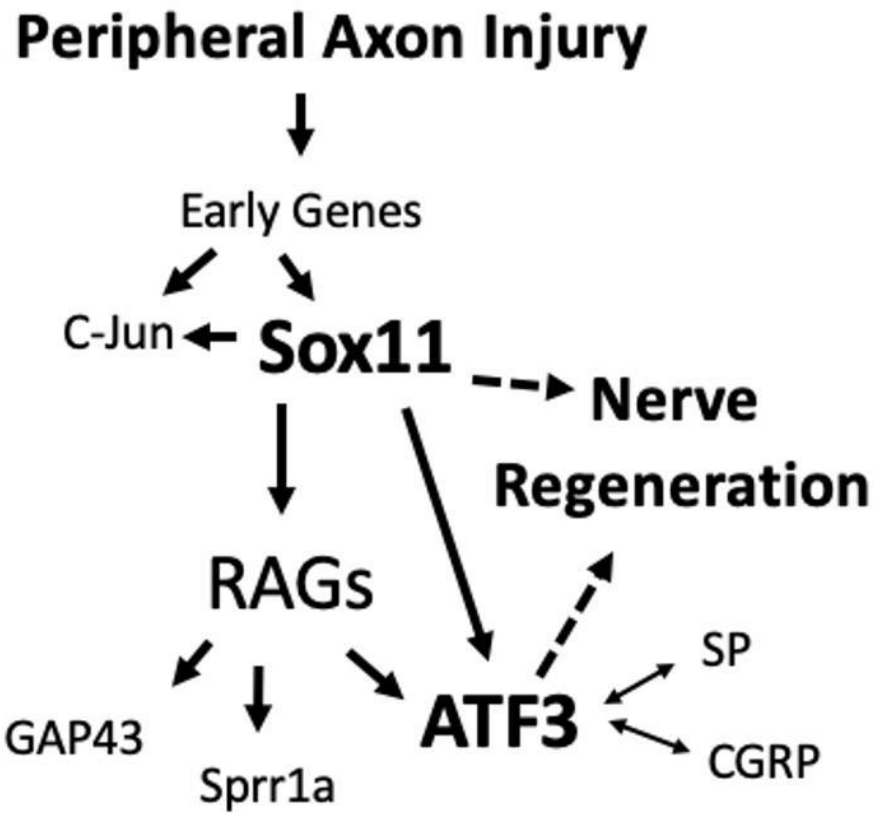
Figure 4.7. Regeneration Associated Gene Network. Schematic depiction of proposed RAG network activation in corneal nerve injury.

5. DISCUSSION OF FINDINGS

This body of work reveals that the cornea adapts a neuroprotective phenotype to speed recovery and continue to function in the face of severe and unrelenting damage. Ocular discomfort and corresponding motor responses, such as squinting and overgrooming, are reactions to respond to environmental insult. Expression of more noxious detecting receptors (i.e., TRPV1) across multiple corneal subclasses (i.e., non-peptidergic, cool sensing), act to improve detection of damaging stimuli and to initiate the release of neuromediators that can aid in epithelial healing and nerve fiber regeneration. Somal expression of RAG network transcription factors (i.e., SOX11, ATF3) proves critical to these neural protective processes, although undefined compensatory mechanisms have been revealed through the systematic downregulation of SOX11 in many corneal neurons. In the face of total disassembly, the cornea doesn't give up but instead implements a complex molecular cascade which fights to restore epithelial integrity, innervation density and sensory functioning.

These series of experiments support findings from prior studies and reports increases in both CGRP and ATF3 following corneal injury. CGRP contributes to multiple aspects of regeneration mechanisms (Mikulec et al., 1996; Chung et al., 2018) and likely acts in conjunction with ATF3 to support regenerative processes. Hindpaw injections of capsaicin induce ATF3 in sensory neurons through the activation of TRPV1. While in TRPV1 downregulated transgenic models, capsaicin does not induce ATF3 expression (Bráz et al., 2010). TRPV1 responds to noxious heat and capsaicin and the general acidic conditions created by inflammation which forms the injury phenotype (Bráz et al., 2010). Protons making up the acidic pathological corneal environment decrease the temperature threshold for TRPV1 activation, while ischemic or inflamed tissue causes greater activation of TRPV1 (Tominaga et al., 1998). Likely the lack of these TRPV1-mediated responses fails to signal ATF3-mediated

117

injury response cascades. During the acute period following injury, infiltration of inflammatory molecules decreases firing thresholds, increases activation of C-fibers and causes peripheral sensitization (Iyengar et al., 2017). ATF3 is part of a complex regeneration signaling network that promotes nerve healing and regeneration following injury. Sustained upregulation of ATF3 and other RAGs in response to chronic injury likely initiates a phenotypic shift of sensory processing in corneal neurons. In very recent studies, ATF3 has been identified in Mrgprd neurons and presents evidence to support a connection between ATF3 increases after injury and the precise regulation of TRPV1 and CGRP to aid in restoring some level of homeostatic functioning (Wang et al., 2021; Warwick et al., 2021). In accordance with these prior studies, our results indicate phenotypic shifts are occurring in corneal neurons after injury and are likely regulated by SOX11-ATF3 RAG network influences on CGRP and TRPV1 expression.

In addition to sensory receptor changes after injury, it likely the physical morphology of reinnervating nerves, inflamed corneal tissue and disrupted epithelial junctions are the cause of a portion of discomfort associated with dry eye and corneal injury (Bergmanson, 1990; Wenk et al., 2003; Azar et al., 2006; Beebe et al., 2007; Dartt, 2009; McDougal and Gamlin, 2015; Paunicka et al., 2015; Launay et al., 2016; Sharif and Sharif,2019). LGE corneas were observed to exhibit higher autofluorescence in whole-mount imaging, which may be attributed to increased inflammation (Shinomiya et al., 2018; Mecum et al., 2019) and corneal irregularity (Kim et al., 2016) which has been reported in earlier studies. Neovascularization and a clouded appearance of LGE and CA corneas was often noted after dissections. Our studies noted visually apparent disorganized terminal morphology during reinnervation periods and aberrant morphology in many naïve *Sox11fl/fl* animals. While different morphological analyses were attempted, generally these observations were subjective or based on the the absence of the typical subbasal whorl patterning (Shaheen et al., 2014; Cruzat et al., 2017; Marfurt et al., 2019;

Bouheraoua et al., 2019). While the whorl is not fully understood, it's likely that the precise organization and whorl pattern help to reduce physical interference with light waves passing through to the retina. With any substantial cornea pathology, clinical symptoms can include impairment to vision or discomfort due to increased refraction of light (Bettis et al., 2012). It seems likely that not only would abnormal disposition of epithelial cells cause visual impairment and discomfort due to light refraction, but with significantly altered nerve morphology, it is possible that the nerve themselves might create pathological backscatter of light waves on the retina.

It's likely without the intrinsic factors that normally present in tear film, axon organizational reinnervation guidance mechanisms could become impaired during the perpetual injury-regeneration process occurring in severe chronic dry eye conditions. Similarly, normally avascular corneal tissue, adapts to an aqueous-deficient environment with neovascularization and a robust inflammatory response. While these injury-response processes are likely important facilitators of axon terminal regeneration observed in this study, they may also account for visual acuity problems, decreased mobility and pain-like behaviors reported in prior studies. Healthy corneas have characteristic innervation organizational patterns that maximize space and create a uniform dispersion of axonal fibers throughout each epithelial layer (McKenna et al., 2011; Yang et al., 2018; He et al., 2016; Al-Aqaba et al., 2019; Labetoulle et al., 2019). Examining morphology with more advanced and object analysis techniques would likely reveal a morphological phenotype shift occurring during normal and transgenetically altered regeneration programs.

In treatment resistant clinical populations, the largest issue for patients and providers alike, are the sensations of irritation and pain that persist despite multifactored treatment (Bron et al., 2014; Craig et al., 2017; Li et al., 2019; Kojima et al., 2020; Goyal et al., 2016; Rosenthal

et al., 2016). It is at the expense of this discomfort which likely prevents this population from going blind due to corneal opacity or vascularization. Although increases of TRPV1 receptors in regenerating axon terminals likely creates a highly sensitized ocular surface, translating into constant irritation and pain, they are likely orchestrating changes seen in sensory function, epithelial healing and regeneration networks that allow the cornea to maintain functional ability despite severe injury.

Dry eye symptomatology is a worldwide problem that is only getting worse with reported in 5-21% of populations worldwide, with higher prevalence in females over 50 years old and in the elderly (Hikichi et al., 1995; Schein et al., 1997; Schaumberg et al., 2003; Schaumberg et al., 2009; Jie et al., 2009; Chao et al., 2014; Galor et al., 2016; Kovacs et al., 2016; Farrand et al., 2017; Kalangara et al., 2018). In recent years, with the increase of time spent viewing digital screens, even beginning in early childhood, has caused dry eye prevalence to spread throughout ages and genders and begin to significantly impact once unaffected populations (Miura et al., 2013; Sheppard et al., 2018; Coles-Brennan, 2019; Chawla et al., 2019). Behaviors creating the broadened impact of dry eye will likely persist in the future, with new wearable technology (i.e., google glass) and growing popularity of elective eye surgeries (i.e., LASIK, blepharoplasty) (Rosenfield, 2016; Zhang et al., 2020). Characterization of the entire network of molecular shifts occurring after corneal injury or during dry eye periods is essential to improving treatments for the ocular discomfort and neuropathic pain. Future experiments using high-throughput sequencing methods, combined with the insights gain from decades of characterizing corneal neurons after injury will be the only way forward to tailor precision treatments for chronic treatment-resistant patients.

BIBLIOGRAPHY

Adatia, F.A., Michaeli-Cohen, A., Naor, J., Caffery, B., Bookman, A. and Slomovic, A., 2004. Correlation between corneal sensitivity, subjective dry eye symptoms and corneal staining in Sjögren's syndrome. Canadian journal of ophthalmology, 39(7), pp.767-771.

Adil MT, Simons CM, Sonam S, Henry JJ. Understanding cornea homeostasis and wound healing using a novel model of stem cell deficiency in Xenopus. Exp Eye Res. 2019;187:107767. doi:10.1016/j.exer.2019.107767

Aicher, S.A., Hermes, S.M. and Hegarty, D.M., 2015. Denervation of the lacrimal gland leads to corneal hypoalgesia in a novel rat model of aqueous dry eye disease. Investigative ophthalmology & visual science, 56(11), pp.6981-6989.

Aigner, L., Arber, S., Kapfhammer, J. P., Laux, T., Schneider, C., Botteri, F., Brenner, H. R., and Caroni, P. (1995). Overexpression of the neural growth-associated protein GAP-43 induces nerve sprouting in the adult nervous system of transgenic mice. Cell 83, 269–278.

Al-Aqaba, M.A., Dhillon, V.K., Mohammed, I., Said, D.G. and Dua, H.S., 2019. Corneal nerves in health and disease. Progress in retinal and eye research, 73, p.100762.

Alamri, A., Bron, R., Brock, J.A. and Ivanusic, J.J., 2015. Transient receptor potential cation channel subfamily V member 1 expressing corneal sensory neurons can be subdivided into at least three subpopulations. Frontiers in neuroanatomy, 9, p.71.

Amitai-Lange, A., Berkowitz, E., Altshuler, A., Dbayat, N., Nasser, W., Suss-Toby, E., Tiosano, B., & Shalom-Feuerstein, R. (2015). A Method for Lineage Tracing of Corneal Cells Using Multi-color Fluorescent Reporter Mice. Journal of visualized experiments : JoVE, (106), e53370. https://doi.org/10.3791/53370

Arvidson, B., 1977. Retrograde axonal transport of horseradish peroxidase from cornea to trigeminal ganglion. Acta neuropathologica, 38(1), pp.49-52.

Averill, S., Michael, G.J., Shortland, P.J., Leavesley, R.C., King, V.R., Bradbury, E.J., McMahon, S.B. and Priestley, J.V., 2004. NGF and GDNF ameliorate the increase in ATF3 expression which occurs in dorsal root ganglion cells in response to peripheral nerve injury. European Journal of Neuroscience, 19(6), pp.1437-1445.

Azar DT. Corneal angiogenic privilege: angiogenic and antiangiogenic factors in corneal avascularity, vasculogenesis, and wound healing (an American Ophthalmological Society thesis). Trans Am Ophthalmol Soc. 2006;104:264-302.

Azuma T, Ao S, Saito Y, Yano K, Seki N, Wakao H, Masuho Y, Muramatsu M. Human SOX11, an upregulated gene during the neural differentiation, has a long 3' untranslated region. DNA Res. 1999 Oct 29;6(5):357-60. doi: 10.1093/dnares/6.5.357. PMID: 10574465.

Bannai, E., Yamashita, H., Takahashi, Y., Tsuchiya, H. and Mimori, A., 2015. Two cases of adult-onset Still's disease with orbital inflammatory lesions originating from the lacrimal gland. Internal Medicine, 54(20), pp.2671-2674.

Barabino, S., Chen, Y., Chauhan, S. and Dana, R., 2012. Ocular surface immunity: homeostatic mechanisms and their disruption in dry eye disease. Progress in retinal and eye research, 31(3), pp.271-285.

Batra, Y.K. and Bali, I.M., 1977. Corneal abrasions during general anesthesia. Anesthesia and analgesia, 56(3), pp.363-365.

Baudouin, C., 2001. The pathology of dry eye. Survey of ophthalmology, 45, pp.S211-S220.

Beebe DC. Maintaining transparency: a review of the developmental physiology and pathophysiology of two avascular tissues. Semin Cell Dev Biol. 2008;19(2):125-133. doi:10.1016/j.semcdb.2007.08.014

Beggs, S., Liu, X.J., Kwan, C. and Salter, M.W., 2010. Peripheral nerve injury and TRPV1-expressing primary afferent C-fibers cause opening of the blood-brain barrier. Molecular pain, 6(1), pp.1-12.

Belmonte C, Aracil A, Acosta MC, Luna C, Gallar J. Nerves and sensations from the eye surface. Ocul Surf. 2004 Oct;2(4):248-53. doi: 10.1016/s1542-0124(12)70112-x. PMID: 17216099.

Belmonte C, Giraldez F. Responses of cat corneal sensory receptors to mechanical and thermal stimulation. J Physiol. 1981;321:355-368. doi:10.1113/jphysiol.1981.sp013989

Belmonte, C., Acosta, M.C. and Gallar, J., 2004. Neural basis of sensation in intact and injured corneas. Experimental eye research, 78(3), pp.513-525.

Belmonte, C., Nichols, J. J., Cox, S. M., Brock, J. A., Begley, C. G., Bereiter, D. A., Dartt, D. A., Galor, A., Hamrah, P., Ivanusic, J. J., Jacobs, D. S., McNamara, N. A., Rosenblatt, M. I., Stapleton, F., & Wolffsohn, J. S. (2017). TFOS DEWS II pain and sensation report. The ocular surface, 15(3), 404–437. https://doi.org/10.1016/j.jtos.2017.05.002

Benítez-del-Castillo, J.M., Acosta, M.C., Wassfi, M.A., Díaz-Valle, D., Gegúndez, J.A., Fernandez, C. and García-Sánchez, J., 2007. Relation between corneal innervation with confocal microscopy and corneal sensitivity with noncontact esthesiometry in patients with dry eye. Investigative ophthalmology & visual science, 48(1), pp.173-181.

Bereiter, D.A., Rahman, M., Thompson, R., Stephenson, P. and Saito, H., 2018. TRPV1 and TRPM8 channels and nocifensive behavior in a rat model for dry eye. Investigative ophthalmology & visual science, 59(8), pp.3739-3746.

Bergmanson, J.P., 1990. Corneal damage in photokeratitis--why is it so painful?. Optometry and vision science: official publication of the American Academy of Optometry, 67(6), pp.407-413.

Bergsland, M., Werme, M., Malewicz, M., Perlmann, T., & Muhr, J. (2006). The establishment of neuronal properties is controlled by Sox4 and Sox11. Genes & development, 20(24), 3475–3486. https://doi.org/10.1101/gad.403406

Bettis DI, Hsu M, Moshirfar M. Corneal collagen cross-linking for nonectatic disorders: a systematic review. J Refract Surg. 2012 Nov;28(11):798-807. doi: 10.3928/1081597X-20121011-09. PMID: 23347375.

Beuerman, R.W. and Pedroza, L., 1996. Ultrastructure of the human cornea. Microscopy research and technique, 33(4), pp.320-335.

Bhattaram P, Penzo-Mendez A, Sock E, Colmenares C, Kaneko KJ, Vassilev A, Depamphilis ML, Wegner M, Lefebvre V 2010. Organogenesis relies on SoxC transcription factors for the survival of neural and mesenchymal progenitors. Nat Commun 1: 9 doi: 10.1038/ncomms1008

Bikbova, G., Oshitari, T., Baba, T. and Yamamoto, S., 2016. Neuronal changes in the diabetic cornea: perspectives for neuroprotection. BioMed research international, 2016.

Black, J. A., & Waxman, S. G. (2002). Molecular identities of two tetrodotoxin-resistant sodium channels in corneal axons. Experimental eye research, 75(2), 193-199.

Blanco-Mezquita T, Martinez-Garcia C, Proença R, Zieske JD, Bonini S, Lambiase A, Merayo-Lloves J. Nerve growth factor promotes corneal epithelial migration by enhancing expression of matrix metalloprotease-9. Invest Ophthalmol Vis Sci. 2013 Jun 4;54(6):3880-90. doi: 10.1167/iovs.12-10816. PMID: 23640040; PMCID: PMC5110072.

Boeshore, K. L., Schreiber, R. C., Vaccariello, S. A., Sachs, H. H., Salazar, R., Lee, J., Ratan, R. R., Leahy, P., and Zigmond, R. E. (2004). Novel changes in gene expression following axotomy of a sympathetic ganglion: a microarray analysis. J. Neurobiol. 59, 216–235.

Bonilla IE, Tanabe K, Strittmatter SM. Small proline-rich repeat protein 1A is expressed by axotomized neurons and promotes axonal outgrowth. J Neurosci. 2002; 22:1303–1315. (PubMed: 11850458)

Bonilla, I. E., Tanabe, K., & Strittmatter, S. M. (2002). Small proline-rich repeat protein 1A is expressed by axotomized neurons and promotes axonal outgrowth. Journal of Neuroscience, 22(4), 1303-1315.

Bonini S, Lambiase A, Rama P, Caprioglio G, Aloe L. Topical treatment with nerve growth factor for neurotrophic keratitis. Ophthalmology. 2000; 107(7):1347–51. discussion 1351–2. (PubMed: 10889110)

Bosse, F., Hasenpusch-Theil, K., Kury, P., and Muller, H. W. (2006). Gene expression profiling reveals that peripheral nerve regeneration is a consequence of both novel injury-dependent and reactivated developmental processes. J. Neurochem. 96, 1441–1457.

Bouheraoua, N., Fouquet, S., Marcos-Almaraz, M.T., Karagogeos, D., Laroche, L. and Chédotal, A., 2019. Genetic analysis of the organization, development, and plasticity of corneal innervation in mice. Journal of Neuroscience, 39(7), pp.1150-1168.

Bourcier, T., Acosta, M.C., Borderie, V., Borrás, F., Gallar, J., Bury, T., Laroche, L. and Belmonte, C., 2005. Decreased corneal sensitivity in patients with dry eye. Investigative ophthalmology & visual science, 46(7), pp.2341-2345.

Bráz JM, Basbaum AI. Differential ATF3 expression in dorsal root ganglion neurons reveals the profile of primary afferents engaged by diverse noxious chemical stimuli. Pain. 2010;150(2):290-301. doi:10.1016/j.pain.2010.05.005

Bron, R., Wood, R.J., Brock, J.A. and Ivanusic, J.J., 2014. Piezo2 expression in corneal afferent neurons. Journal of Comparative Neurology, 522(13), pp.2967-2979.

Bucelli, R.C., Gonsiorek, E.A., Kim, W.Y., Bruun, D., Rabin, R.A., Higgins, D. and Lein, P.J., 2008. Statins decrease expression of the proinflammatory neuropeptides calcitonin gene-related peptide and substance P in sensory neurons. Journal of Pharmacology and Experimental Therapeutics, 324(3), pp.1172-1180.

Bustin, M. and Reeves, R., 1996. High-mobility-group chromosomal proteins: architectural components that facilitate chromatin function. Progress in nucleic acid research and molecular biology, 54, pp.35-100b.

Caillaud, M., Richard, L., Vallat, J.M., Desmoulière, A. and Billet, F., 2019. Peripheral nerve regeneration and intraneural revascularization. Neural regeneration research, 14(1), p.24.

Cao, E., Liao, M., Cheng, Y. and Julius, D., 2013. TRPV1 structures in distinct conformations reveal activation mechanisms. Nature, 504(7478), pp.113-118.

Carpentras, D., Laforest, T., Künzi, M. and Moser, C., 2018. Effect of backscattering in phase contrast imaging of the retina. Optics express, 26(6), pp.6785-6795.

Cassagne, M., Laurent, C., Rodrigues, M., Galinier, A., Spoerl, E., Galiacy, S.D., Soler, V., Fournié, P. and Malecaze, F., 2016. Iontophoresis transcorneal delivery technique for transepithelial corneal collagen crosslinking with riboflavin in a rabbit model. Investigative ophthalmology & visual science, 57(2), pp.594-603.

Cattin, A.L., Burden, J.J., Van Emmenis, L., Mackenzie, F.E., Hoving, J.J., Calavia, N.G., Guo, Y., McLaughlin, M., Rosenberg, L.H., Quereda, V. and Jamecna, D., 2015. Macrophage-induced blood vessels guide Schwann cell-mediated regeneration of peripheral nerves. Cell, 162(5), pp.1127-1139.

Causey, G. and Palmer, E., 1953. The centrifugal spread of structural change at the nodes in degenerating mammalian nerves. Journal of Anatomy, 87(Pt 2), p.185.

Cavanaugh, D.J., Chesler, A.T., Bráz, J.M., Shah, N.M., Julius, D. and Basbaum, A.I., 2011. Restriction of transient receptor potential vanilloid-1 to the peptidergic subset of primary afferent neurons follows its developmental downregulation in nonpeptidergic neurons. Journal of Neuroscience, 31(28), pp.10119-10127.

Chang, J. H., Garg, N. K., Lunde, E., Han, K. Y., Jain, S., & Azar, D. T. (2012). Corneal neovascularization: an anti-VEGF therapy review. Survey of ophthalmology, 57(5), 415–429. https://doi.org/10.1016/j.survophthal.2012.01.007

Chang, K. C., Hertz, J., Zhang, X., Jin, X. L., Shaw, P., Derosa, B. A., Li, J. Y., Venugopalan, P., Valenzuela, D. A., Patel, R. D., Russano, K. R., Alshamekh, S. A., Sun, C., Tenerelli, K., Li, C., Velmeshev, D., Cheng, Y., Boyce, T. M., Dreyfuss, A., Uddin, M. S., … Goldberg, J. L. (2017). Novel Regulatory Mechanisms for the SoxC Transcriptional Network Required for Visual Pathway Development. The Journal of neuroscience : the official journal of the Society for Neuroscience, 37(19), 4967–4981. https://doi.org/10.1523/JNEUROSCI.3430-13.2017

Chang, Y.A., Wu, Y.Y., Lin, C.T., Kawasumi, M., Wu, C.H., Kao, S.Y., Yang, Y.P., Hsu, C.C., Hung, K.F. and Sun, Y.C., 2021. Animal models of dry eye: Their strengths and limitations for studying human dry eye disease. Journal of the Chinese Medical Association, 84(5), pp.459-464.

Chao, C., Golebiowski, B. and Stapleton, F., 2014. The role of corneal innervation in LASIK-induced neuropathic dry eye. The ocular surface, 12(1), pp.32-45.

Chao, C., Stapleton, F., Zhou, X., Chen, S., Zhou, S. and Golebiowski, B., 2015. Structural and functional changes in corneal innervation after laser in situ keratomileusis and their relationship with dry eye. Graefe's Archive for Clinical and Experimental Ophthalmology, 253(11), pp.2029-2039.

Chaudhary S, Namavari A, Yco L, Chang JH, Sonawane S, Khanolkar V, Sarkar J, Jain S. Neurotrophins and nerve regeneration-associated genes are expressed in the cornea after lamellar flap surgery. Cornea. 2012 Dec;31(12):1460-7. doi: 10.1097/ICO.0b013e318247b60e. PMID: 22673847; PMCID: PMC3612527.

Chawla, A., Lim, T.C., Shikhare, S.N., Munk, P.L. and Peh, W.C., 2019. Computer vision syndrome: Darkness under the shadow of light. Canadian Association of Radiologists Journal, 70(1), pp.5-9.

Chen, M.J., Liu, Y.T., Tsai, C.C., Chen, Y.C., Chou, C.K. and Lee, S.M., 2009. Relationship between central corneal thickness, refractive error, corneal curvature, anterior chamber depth and axial length. Journal of the Chinese Medical Association, 72(3), pp.133-137.

Chen, Sheng, and Hong-Sen Su. "Afferent connections of the thalamic paraventricular and parataenial nuclei in the rat—a retrograde tracing study with iontophoretic application of Fluoro-Gold." Brain research 522.1 (1990): 1-6.

Cho, Y.K., Archer, B. and Ambati, B.K., 2014. Dry eye predisposes to corneal neovascularization and lymphangiogenesis after corneal injury in a murine model. Cornea, 33(6), pp.621-627.

Choi, S. S., & Lahn, B. T. (2003). Adaptive evolution of MRG, a neuron-specific gene family implicated in nociception. Genome research, 13(10), 2252–2259. https://doi.org/10.1101/gr.1431603

Chung, A.M., 2018. Calcitonin gene-related peptide (CGRP): role in peripheral nerve regeneration. Reviews in the Neurosciences, 29(4), pp.369-376.

Coggeshall, R. E., Tate, S., & Carlton, S. M. (2004). Differential expression of tetrodotoxin-resistant sodium channels Nav1. 8 and Nav1. 9 in normal and inflamed rats. Neuroscience letters, 355(1-2), 45-48.

Coles-Brennan, C., Sulley, A. and Young, G., 2019. Management of digital eye strain. Clinical and experimental Optometry, 102(1), pp.18-29.

Coles, W.H. and Jaros, P.A., 1984. Dynamics of ocular surface pH. British journal of ophthalmology, 68(8), pp.549-552.

Cook, N., Mullins, A., Gautam, R., Medi, S., Prince, C., Tyagi, N. and Kommineni, J., 2019. Evaluating patient experiences in dry eye disease through social media listening research. Ophthalmology and therapy, 8(3), pp.407-420.

Cowie, A.M., Moehring, F., O'Hara, C. and Stucky, C.L., 2018. Optogenetic inhibition of CGRPα sensory neurons reveals their distinct roles in neuropathic and incisional pain. Journal of Neuroscience, 38(25), pp.5807-5825.

Craig, J.P., Nichols, K.K., Akpek, E.K., Caffery, B., Dua, H.S., Joo, C.K., Liu, Z., Nelson, J.D., Nichols, J.J., Tsubota, K. and Stapleton, F., 2017. TFOS DEWS II definition and classification report. The ocular surface, 15(3), pp.276-283.

Croom, J.E., Foreman, R.D., Chandler, M.J. and Barron, K.W., 1997. Cutaneous vasodilation during dorsal column stimulation is mediated by dorsal roots and CGRP. American Journal of Physiology-Heart and Circulatory Physiology, 272(2), pp.H950-H957.

Cruzat, A., Qazi, Y. and Hamrah, P., 2017. In vivo confocal microscopy of corneal nerves in health and disease. The ocular surface, 15(1), pp.15-47.

Dartt DA. Dysfunctional neural regulation of lacrimal gland secretion and its role in the pathogenesis of dry eye syndromes. Ocul Surf. 2004 Apr;2(2):76-91. doi: 10.1016/s1542-0124(12)70146-5. PMID: 17216081.

Dartt DA. Neural regulation of lacrimal gland secretory processes: relevance in dry eye diseases. Prog Retin Eye Res. 2009;28(3):155-177.

Dastjerdi MH, Dana R. Corneal nerve alterations in dry eye-associated ocular surface disease. Int Ophthalmol Clin. 2009 Winter;49(1):11-20. doi: 10.1097/IIO.0b013e31819242c9. PMID: 19125060.

David, S., and Aguayo, A. J. (1981). Axonal elongation into peripheral nervous system "bridges" after central nervous system injury in adult rats. Science 214, 931–933.

De Armentia, M.L., Cabanes, C. and Belmonte, C., 2000. Electrophysiological properties of identified trigeminal ganglion neurons innervating the cornea of the mouse. Neuroscience, 101(4), pp.1109-1115.

De Castro, F., Silos-Santiago, I., De Armentia, M.L., Barbacid, M. and Belmonte, C., 1998. Corneal innervation and sensitivity to noxious stimuli in trkA knockout mice. European Journal of Neuroscience, 10(1), pp.146-152.

De Felipe, J., González-Albo, M.C., Del Río, M.R. and Elston, G.N., 1999. Distribution and patterns of connectivity of interneurons containing calbindin, calretinin, and parvalbumin in visual areas of the occipital and temporal lobes of the macaque monkey. Journal of Comparative Neurology, 412(3), pp.515-526.

De Paiva, C.S. and Pflugfelder, S.C., 2004. Corneal epitheliopathy of dry eye induces hyperesthesia to mechanical air jet stimulation. American journal of ophthalmology, 137(1), pp.109-115.

DelMonte, D.W. and Kim, T., 2011. Anatomy and physiology of the cornea. Journal of Cataract & Refractive Surgery, 37(3), pp.588-598.

Dhillon VK, Elalfy MS, Messina M, Al-Aqaba M, Dua HS. Survival of corneal nerve/sheath structures in organ-cultured donor corneas. Acta Ophthalmol. 2018 May;96(3):e334-e340. doi: 10.1111/aos.13614. Epub 2017 Nov 29. PMID: 29193851.

Dhungel D, Shrestha GS. Visual symptoms associated with refractive errors among Thangka artists of Kathmandu valley. BMC Ophthalmol. 2017 Dec 21;17(1):258. doi: 10.1186/s12886-017-0659-0. PMID: 29268725; PMCID: PMC5740904.

Di G, Qi X, Zhao X, Zhang S, Danielson P, Zhou Q. Corneal Epithelium-Derived Neurotrophic Factors Promote Nerve Regeneration. Invest Ophthalmol Vis Sci. 2017 Sep 1;58(11):4695-4702. doi: 10.1167/iovs.16-21372. PMID: 28910445.

Dienes, L., Kiss, H.J., Perényi, K., Nagy, Z.Z., Acosta, M.C., Gallar, J. and Kovács, I., 2015. Corneal sensitivity and dry eye symptoms in patients with keratoconus. PLoS One, 10(10), p.e0141621.

Dietrich, J., Schlegel, C., Roth, M., Witt, J., Geerling, G., Mertsch, S. and Schrader, S., 2018. Comparative analysis on the dynamic of lacrimal gland damage and regeneration after Interleukin-1α or duct ligation induced dry eye disease in mice. Experimental eye research, 172, pp.66-77.

Donthineni, P.R., Shanbhag, S.S. and Basu, S., 2021, January. An Evidence-Based Strategic Approach to Prevention and Treatment of Dry Eye Disease, a Modern Global Epidemic. In Healthcare (Vol. 9, No. 1, p. 89). Multidisciplinary Digital Publishing Institute.

Dua, H.S., Said, D.G., Messmer, E.M., Rolando, M., Benitez-del-Castillo, J.M., Hossain, P.N., Shortt, A.J., Geerling, G., Nubile, M., Figueiredo, F.C. and Rauz, S., 2018. Neurotrophic keratopathy. Progress in retinal and eye research, 66, pp.107-131.

Dy P, Penzo-Méndez A, Wang H, Pedraza CE, Macklin WB, Lefebvre V. The three SoxC proteins--Sox4, Sox11 and Sox12--exhibit overlapping expression patterns and molecular properties. Nucleic Acids Res. 2008 May;36(9):3101-17. doi: 10.1093/nar/gkn162. Epub 2008 Apr 10. PMID: 18403418; PMCID: PMC2396431.

Elhusseiny, A.M., Khalil, A.A., El Sheikh, R.H., Bakr, M.A., Eissa, M.G. and El Sayed, Y.M., 2019. New approaches for diagnosis of dry eye disease. International journal of ophthalmology, 12(10), p.1618.

Erdélyi B, Kraak R, Zhivov A, Guthoff R, Németh J. In vivo confocal laser scanning microscopy of the cornea in dry eye. Graefes Arch Clin Exp Ophthalmol. 2007 Jan;245(1):39-44. doi: 10.1007/s00417-006-0375-6. Epub 2006 Jul 28. PMID: 16874525.

Esquenazi, S., Bazan, H.E., Bui, V., He, J., Kim, D.B. and Bazan, N.G., 2005. Topical combination of NGF and DHA increases rabbit corneal nerve regeneration after photorefractive keratectomy. Investigative ophthalmology & visual science, 46(9), pp.3121-3127.

Fagoe, N. D., Attwell, C. L., Kouwenhoven, D., Verhaagen, J., & Mason, M. R. (2015). Overexpression of ATF3 or the combination of ATF3, c-Jun, STAT3 and Smad1 promotes regeneration of the central axon branch of sensory neurons but without synergistic effects. Human molecular genetics, 24(23), 6788-6800.

Fakih, D., Guerrero-Moreno, A., Baudouin, C., Goazigo, A. R., & Parsadaniantz, S. M. (2021). Capsazepine decreases corneal pain syndrome in severe dry eye disease. Journal of neuroinflammation, 18(1), 111. https://doi.org/10.1186/s12974-021-02162-7

Fakih, D., Zhao, Z., Nicolle, P., Reboussin, E., Joubert, F., Luzu, J., Labbé, A., Rostène, W., Baudouin, C., Parsadaniantz, S.M. and Réaux-Le Goazigo, A., 2019. Chronic dry eye induced corneal hypersensitivity, neuroinflammatory responses, and synaptic plasticity in the mouse trigeminal brainstem. Journal of Neuroinflammation, 16(1), pp.1-20.

Fang M, Xu T, Fan S, Liu N, Li L, Gao J, Li W. SOX11 and FAK participate in the stretch-induced mechanical injury to alveolar type 2 epithelial cells. Int J Mol Med. 2021 Jan;47(1):361-373. doi: 10.3892/ijmm.2020.4795. Epub 2020 Nov 20. PMID: 33236128; PMCID: PMC7723679.

Farrand, K.F., Fridman, M., Stillman, I.Ö. and Schaumberg, D.A., 2017. Prevalence of diagnosed dry eye disease in the United States among adults aged 18 years and older. American journal of ophthalmology, 182, pp.90-98.

Feng Y, Simpson TL. Characteristics of human corneal psychophysical channels. Invest Ophthalmol Vis Sci. 2004 Sep;45(9):3005-10. doi: 10.1167/iovs.04-0102. PMID: 15326114.

Ferdousi, M., Petropoulos, I.N., Kalteniece, A., Azmi, S., Ponirakis, G., Efron, N., Soran, H. and Malik, R.A., 2018. No relation between the severity of corneal nerve, epithelial, and keratocyte cell morphology with measures of dry eye disease in type 1 diabetes. Investigative ophthalmology & visual science, 59(13), pp.5525-5530.

Fernyhough P, Mill JF, Roberts JL, Ishii DN. Stabilization of tubulin mRNAs by insulin and insulin-like growth factor I during neurite formation. Brain Res Mol Brain Res. 1989; 6(2–3):109– 20. (PubMed: 2693875)

Findlay, Q. and Reid, K., 2018. Dry eye disease: when to treat and when to refer. Australian prescriber, 41(5), p.160.

Gallar J, Pozo MA, Tuckett RP, Belmonte C. Response of sensory units with unmyelinated fibres to mechanical, thermal and chemical stimulation of the cat's cornea. J Physiol. 1993;468:609-622. doi:10.1113/jphysiol.1993.sp019791

Galor A, Covington D, Levitt AE, et al. Neuropathic Ocular Pain due to Dry Eye is Associated with Multiple Comorbid Chronic Pain Syndromes. J Pain. 2016;17(3):310-318. doi:10.1016/j.jpain.2015.10.019

Galor A, Levitt RC, Felix ER, Martin ER, Sarantopoulos CD. Neuropathic ocular pain: an important yet underevaluated feature of dry eye. Eye. 2015;29(3):301-312. doi:10.1038/eye.2014.263.

Gautron, L., Sakata, I., Udit, S., Zigman, J.M., Wood, J.N. and Elmquist, J.K., 2011. Genetic tracing of Nav1. 8-expressing vagal afferents in the mouse. Journal of Comparative Neurology, 519(15), pp.3085-3101.

Gayton JL. Etiology, prevalence, and treatment of dry eye disease. Clin Ophthalmol. 2009;3:405-412. doi:10.2147/opth.s

Geeven, G., Macgillavry, H. D., Eggers, R., Sassen, M. M., Verhaagen, J., Smit, A. B., De Gunst, M. C., and Van Kesteren, R. E. (2011). LLM3D: a log-linear modeling-based method to predict functional gene regulatory interactions from genome-wide expression data. Nucleic Acids Res. 39, 5313–5327.

Gey, M., Wanner, R., Schilling, C., Pedro, M. T., Sinske, D., & Knöll, B. (2016). Atf3 mutant mice show reduced axon regeneration and impaired regeneration-associated gene induction after peripheral nerve injury. Open biology, 6(8), 160091. https://doi.org/10.1098/rsob.160091

Gold ES, Ramsey SA, Sartain MJ, Selinummi J, Podolsky I, Rodriguez DJ, Moritz RL, Aderem A. ATF3 protects against atherosclerosis by suppressing 25-hydroxycholesterol-induced lipid body formation. J Exp Med. 2012;209:807–17.

Golebiowski, B., Long, J., Harrison, K., Lee, A., Chidi-Egboka, N., & Asper, L. (2020). Smartphone use and effects on tear film, blinking and binocular vision. Current Eye Research, 45(4), 428-434.

Gonzalez-Gonzalez, O., Bech, F., Gallar, J., Merayo-Lloves, J. and Belmonte, C., 2017. Functional properties of sensory nerve terminals of the mouse cornea. Investigative ophthalmology & visual science, 58(1), pp.404-415.

Goodwin GH, Sanders C, Johns EW. A new group of chromatin-associated proteins with a high content of acidic and basic amino acids. Eur J Biochem. 1973 Sep 21;38(1):14-9. doi: 10.1111/j.1432-1033.1973.tb03026.x. PMID: 4774120.

Goto E, Yagi Y, Matsumoto Y, Tsubota K. Impaired functional visual acuity of dry eye patients. Am J Ophthalmol. 2002 Feb;133(2):181-6. doi: 10.1016/s0002-9394(01)01365-4. PMID: 11812420.

Gowrisankaran, S., Sheedy, J.E. and Hayes, J.R., 2007. Eyelid squint response to asthenopia-inducing conditions. Optometry and vision science, 84(7), pp.611-619.

Goyal, P., Jain, A.K. and Malhotra, C., 2016. Oral Omega-3 Fatty Acid Supplementation for Laser In Situ Keratomileusis–Associated Dry Eye. Cornea, 36(2), pp.169-175.

Guerrero-Moreno A, Fakih D, Parsadaniantz SM, Réaux-Le Goazigo A. How does chronic dry eye shape peripheral and central nociceptive systems?. Neural Regen Res 2021;16:306-7

Guerrero-Moreno, A., Baudouin, C., Melik Parsadaniantz, S. and Goazigo, R.L., 2020. Morphological and functional changes of corneal nerves and their contribution to peripheral and central sensory abnormalities. Frontiers in Cellular Neuroscience, 14, p.436.

Guo Y, Liu S, Zhang X, Wang L, Zhang X, Hao A, Han A, Yang J. Sox11 promotes endogenous neurogenesis and locomotor recovery in mice spinal cord injury. Biochem Biophys Res Commun. 2014 Apr 18;446(4):830-5. doi: 10.1016/j.bbrc.2014.02.103. Epub 2014 Feb 28. PMID: 24589730.

Hai T, Wolfgang CD, Marsee DK, Allen AE, Sivaprasad U. ATF3 and stress responses. Gene Expression. 1999;7:321–5.

Hamrah, P., Qazi, Y., Shahatit, B., Dastjerdi, M.H., Pavan-Langston, D., Jacobs, D.S. and Rosenthal, P., 2017. Corneal nerve and epithelial cell alterations in corneal allodynia: an in vivo confocal microscopy case series. The ocular surface, 15(1), pp.139-151.

Hao, J., Li, S.K., Liu, C.Y. and Kao, W.W., 2009. Electrically assisted delivery of macromolecules into the corneal epithelium. Experimental eye research, 89(6), pp.934-941.

Hargrave M, Wright E, Kun J, Emery J, Cooper L, Koopman P. Expression of the Sox11 gene in mouse embryos suggests roles in neuronal maturation and epithelio-mesenchymal induction. Dev Dyn. 1997 Oct;210(2):79-86. doi: 10.1002/(SICI)1097-0177(199710)210:2<79::AID-AJA1>3.0.CO;2-6. PMID: 9337129.

Harley VR, Clarkson MJ, Argentaro A. The molecular action and regulation of the testis-determining factors, SRY (sex-determining region on the Y chromosome) and SOX9 (SRY-related high-mobility group (HMG) box 9). Endocr Rev. 2003 Aug;24(4):466-87. doi: 10.1210/er.2002-0025. PMID: 12920151.

Hatta, A., Kurose, M., Sullivan, C., Okamoto, K., Fujii, N., Yamamura, K. and Meng, I.D., 2019. Dry eye sensitizes cool cells to capsaicin-induced changes in activity via TRPV1. Journal of neurophysiology, 121(6), pp.2191-2201.

Hayman KJ, Kerse NM, La Grow SJ, Wouldes T, Robertson MC, Campbell AJ. Depression in older people: visual impairment and subjective ratings of health. Optom Vis Sci. 2007 Nov;84(11):1024-30. doi: 10.1097/OPX.0b013e318157a6b1. PMID: 18043421.

He, Jiucheng, Thang Luong Pham, Azucena H. Kakazu, and Haydee EP Bazan. "Remodeling of substance P sensory nerves and transient receptor potential melastatin 8 (TRPM8) cold receptors after corneal experimental surgery." Investigative ophthalmology & visual science 60, no. 7 (2019): 2449-2460.

Hegarty DM, Hermes SM, Morgan MM, Aicher SA. Acute hyperalgesia and delayed dry eye after corneal abrasion injury. Pain Rep. 2018 Jun 20;3(4):e664. doi: 10.1097/PR9.0000000000000664. PMID: 30123857; PMCID: PMC6085140.

Herdegen, T., Kummer, W., Fiallos, C. E., Leah, J., and Bravo, R. (1991). Expression of c-JUN, JUN B and JUN D proteins in rat nervous system following transection of vagus nerve and cervical sympathetic trunk. Neuroscience 45, 413–422.

Herrmann, W.A., Shah, C.P., von Mohrenfels, C.W., Gabler, B., Hufendiek, K. and Lohmann, C.P., 2005. Tear film function and corneal sensation in the early postoperative period after LASEK for the correction of myopia. Graefe's Archive for Clinical and Experimental Ophthalmology, 243(9), pp.911-916.

Hessen, M. and Akpek, E.K., 2014. Dry eye: an inflammatory ocular disease. Journal of ophthalmic & vision research, 9(2), p.240.

Hikichi, T., Yoshida, A., Fukui, Y., Hamano, T., Ri, M., Araki, K., Horimoto, K., Takamura, E., Kitagawa, K., Oyama, M. and Danjo, Y., 1995. Prevalence of dry eye in Japanese eye centers. Graefe's archive for clinical and experimental ophthalmology, 233(9), pp.555-558.

Hillenbrand, M., Holzbach, T., Matiasek, K., Schlegel, J. and Giunta, R.E., 2015. Vascular endothelial growth factor gene therapy improves nerve regeneration in a model of obstetric brachial plexus palsy. Neurological research, 37(3), pp.197-203.

Hirata A, Masaki T, Motoyoshi K, Kamakura K. Intrathecal administration of nerve growth factor delays GAP 43 expression and early phase regeneration of adult rat peripheral nerve. Brain Res. 2002; 19;944(1–2):146–56.

Hiura, A. and Nakagawa, H., 2012. Innervation of TRPV1-, PGP-, and CGRP-immunoreactive nerve fibers in the subepithelial layer of a whole mount preparation of the rat cornea. Okajimas folia anatomica Japonica, 89(2), pp.47-50.

Hodges RR, Dartt DA. Tear film mucins: front line defenders of the ocular surface; comparison with airway and gastrointestinal tract mucins. Exp Eye Res. 2013;117:62-78. doi:10.1016/j.exer.2013.07.027

Hoetzenecker W, Echtenacher B, Guenova E, Hoetzenecker K, Woelbing F, Bruck J, Teske A, Valtcheva N, Fuchs K, Kneilling M, Park J-H, Kim K-H, Kim K-W, Hoffmann P, Krenn C, Hai T, Ghoreschi K, Biedermann T, Rocken M. ROS-induced ATF3 causes susceptibility to secondary infections during sepsis-associated immunosuppression. Nat Med. 2012;18:128–34.

Honkanen, R.A., Huang, L. and Rigas, B., 2020. A Rabbit Model of Aqueous-Deficient Dry Eye Disease Induced by Concanavalin A Injection into the Lacrimal Glands: Application to Drug Efficacy Studies. Journal of visualized experiments: JoVE, (155).

Hos D, Bukowiecki A, Horstmann J, Bock F, Bucher F, Heindl LM, Siebelmann S, Steven P, Dana R, Eming SA, Cursiefen C. Transient Ingrowth of Lymphatic Vessels into the Physiologically Avascular Cornea Regulates Corneal Edema and Transparency. Sci Rep. 2017 Aug 3;7(1):7227. doi: 10.1038/s41598-017-07806-4. PMID: 28775329; PMCID: PMC5543160.

Hoshiba, Y., Toda, T., Ebisu, H., Wakimoto, M., Yanagi, S. and Kawasaki, H., 2016. Sox11 balances dendritic morphogenesis with neuronal migration in the developing cerebral cortex. Journal of Neuroscience, 36(21), pp.5775-5784.

Hsu Y. C. (2015). Theory and Practice of Lineage Tracing. Stem cells (Dayton, Ohio), 33(11), 3197–3204. https://doi.org/10.1002/stem.2123

Hu, G., Huang, K., Hu, Y., Du, G., Xue, Z., Zhu, X. and Fan, G., 2016. Single-cell RNA-seq reveals distinct injury responses in different types of DRG sensory neurons. Scientific reports, 6(1), pp.1-11.

Huang, Y.K., Lu, Y.G., Zhao, X., Zhang, J.B., Zhang, F.M., Chen, Y., Bi, L.B., Gu, J.H., Jiang, Z.J., Wu, X.M. and Li, Q.Y., 2020. Cytokine activin C ameliorates chronic neuropathic pain in peripheral nerve injury rodents by modulating the TRPV1 channel. British Journal of Pharmacology, 177(24), pp.5642-5657.

Hung, J.H., Leidreiter, K., White, J.S. and Bernays, M.E., 2020. Clinical characteristics and treatment of spontaneous chronic corneal epithelial defects (SCCEDs) with diamond burr debridement. Veterinary ophthalmology, 23(4), pp.764-769.

Ivanavicius, S.P., Ball, A.D., Heapy, C.G., Westwood, F.R., Murray, F. and Read, S.J., 2007. Structural pathology in a rodent model of osteoarthritis is associated with neuropathic pain: increased expression of ATF-3 and pharmacological characterisation. Pain, 128(3), pp.272-282.

Ivanusic, J.J., Wood, R.J. and Brock, J.A., 2013. Sensory and sympathetic innervation of the mouse and guinea pig corneal epithelium. Journal of Comparative Neurology, 521(4), pp.877-893.

Iyengar, S., Ossipov, M. H., & Johnson, K. W. (2017). The role of calcitonin gene-related peptide in peripheral and central pain mechanisms including migraine. Pain, 158(4), 543–559. https://doi.org/10.1097/j.pain.0000000000000831

Jabbur, N.S. and O'Brien, T.P., 2003. Incidence of intraoperative corneal abrasions and correlation with age using the Hansatome and Amadeus microkeratomes during laser in situ keratomileusis. Journal of Cataract & Refractive Surgery, 29(6), pp.1174-1178.

Jankowski, M. P., Cornuet, P. K., McIlwrath, S., Koerber, H. R., & Albers, K. M. (2006). SRY-box containing gene 11 (Sox11) transcription factor is required for neuron survival and neurite growth. Neuroscience, 143(2), 501–514. https://doi.org/10.1016/j.neuroscience.2006.09.010

Jankowski, M. P., McIlwrath, S. L., Jing, X., Cornuet, P. K., Salerno, K. M., Koerber, H. R., & Albers, K. M. (2009). Sox11 transcription factor modulates peripheral nerve regeneration in adult mice. Brain research, 1256, 43–54. https://doi.org/10.1016/j.brainres.2008.12.032

Jankowski, M. P., Miller, L., & Koerber, H. R. (2018). Increased expression of transcription factor SRY-box-containing gene 11 (Sox11) enhances neurite growth by regulating neurotrophic factor responsiveness. Neuroscience, 382, 93-104.

Jenkins, R., and Hunt, S. P. (1991). Long-term increase in the levels of c-jun mRNA and jun protein-like immunoreactivity in motor and sensory neurons following axon damage. Neurosci. Lett. 129, 107–110.

Jester, J.V., 2008, April. Corneal crystallins and the development of cellular transparency. In Seminars in cell & developmental biology (Vol. 19, No. 2, pp. 82-93). Academic Press.

Jester, J.V., Moller-Pedersen, T., Huang, J., Sax, C.M., Kays, W.T., Cavangh, H.D., Petroll, W.M. and Piatigorsky, J., 1999. The cellular basis of corneal transparency: evidence for 'corneal crystallins'. Journal of cell science, 112(5), pp.613-622.

Jie, Y., Xu, L., Wu, Y.Y. and Jonas, J.B., 2009. Prevalence of dry eye among adult Chinese in the Beijing Eye Study. Eye, 23(3), pp.688-693.

Jing, X., Wang, T., Huang, S., Glorioso, J. C., & Albers, K. M. (2012). The transcription factor Sox11 promotes nerve regeneration through activation of the regeneration-associated gene Sprr1a. Experimental neurology, 233(1), 221-232.

Jockusch, H. and Eberhard, D., 2007. Green fluorescent protein as a tracer in chimeric tissues: the power of vapor fixation. Methods in molecular biology (Clifton, NJ), 411, pp.145-154.

Jones, M.A. and Marfurt, C.F., 1998. Peptidergic innervation of the rat cornea. Experimental eye research, 66(4), pp.421-435.

Jones, R.F. and Maurice, D.M., 1966. New methods of measuring the rate of aqueous flow in man with fluorescein. Experimental eye research, 5(3), pp.208-220.

Kalangara, J.P., Galor, A., Levitt, R.C., Covington, D.B., McManus, K.T., Sarantopoulos, C.D. and Felix, E.R., 2017. Characteristics of ocular pain complaints in patients with idiopathic dry eye symptoms. Eye & contact lens, 43(3), p.192.

Kalha, S., Kuony, A. and Michon, F., 2018. Corneal epithelial abrasion with ocular burr as a model for cornea wound healing. JoVE (Journal of Visualized Experiments), (137), p.e58071.

Kalteniece A, Ferdousi M, Azmi S, Mubita WM, Marshall A, Lauria G, Faber CG, Soran H, Malik RA. Corneal confocal microscopy detects small nerve fibre damage in patients with painful diabetic neuropathy. Sci Rep. 2020 Feb 25;10(1):3371. doi: 10.1038/s41598-020-60422-7. PMID: 32099076; PMCID: PMC7042367.

Kaminer, J., Powers, A.S., Horn, K.G., Hui, C. and Evinger, C., 2011. Characterizing the spontaneous blink generator: an animal model. Journal of Neuroscience, 31(31), pp.11256-11267.

Katagiri A, Thompson R, Rahman M, Okamoto K, Bereiter DA. Evidence for TRPA1 involvement in central neural mechanisms in a rat model of dry eye. Neuroscience. 2015 Apr 2;290:204-13. doi: 10.1016/j.neuroscience.2015.01.046. Epub 2015 Jan 30. PMID: 25639234; PMCID: PMC4359622.

Kawarai, Y., Orita, S., Nakamura, J., Miyamoto, S., Suzuki, M., Inage, K., Hagiwara, S., Suzuki, T., Nakajima, T., Akazawa, T. and Ohtori, S., 2018. Changes in proinflammatory cytokines, neuropeptides, and microglia in an animal model of monosodium iodoacetate-induced hip osteoarthritis. Journal of Orthopaedic Research®, 36(11), pp.2978-2986.

Kee, Z., Kodji, X. and Brain, S.D., 2018. The role of calcitonin gene related peptide (CGRP) in neurogenic vasodilation and its cardioprotective effects. Frontiers in physiology, 9, p.1249.

Keller, A.S.A.F., 1999. The role of intrinsic circuitry in motor cortex plasticity. The Changing Nervous System: Neurobehavioral Consequences of Early Brain Disorders, p.428.

Khurana, A.K., Chaudhary, R., Ahluwalia, B.K. and Gupta, S., 1991. Tear film profile in dry eye. Acta ophthalmologica, 69(1), pp.79-86.

Kim, H.Y., Park, C.K., Cho, I.H., Jung, S.J., Kim, J.S. and Oh, S.B., 2008. Differential Changes in TRPV1 expression after trigeminal sensory nerve injury. The Journal of Pain, 9(3), pp.280-288.

Kim, Y.L., Walsh Jr, J.T., Goldstick, T.K. and Glucksberg, M.R., 2004. Variation of corneal refractive index with hydration. Physics in Medicine & Biology, 49(5), p.859.

King CY, Weiss MA. The SRY high-mobility-group box recognizes DNA by partial intercalation in the minor groove: a topological mechanism of sequence specificity. Proc Natl Acad Sci U S A. 1993 Dec 15;90(24):11990-4. doi: 10.1073/pnas.90.24.11990. PMID: 8265659; PMCID: PMC48111.

Klenkler, B., Sheardown, H. and Jones, L., 2007. Growth factors in the tear film: role in tissue maintenance, wound healing, and ocular pathology. The ocular surface, 5(3), pp.228-239.

Kobayashi NR, Fan DP, Giehl KM, Bedard AM, Wiegand SJ, Tetzlaff W. BDNF and NT-4/5 prevent atrophy of rat rubrospinal neurons after cervical axotomy, stimulate GAP-43 and Tα1- tubulin mRNA expression, and promote axonal regeneration. J Neurosci. 1997; 17(24):9583–95. (PubMed: 9391013)

Köbbert, C., Apps, R., Bechmann, I., Lanciego, J. L., Mey, J., & Thanos, S. (2000). Current concepts in neuroanatomical tracing. Progress in neurobiology, 62(4), 327-351.

Koehn, Demelza, et al. "Ketamine/xylazine-induced corneal damage in mice." PLoS One 10.7 (2015): e0132804.

Kojima, T., Dogru, M., Kawashima, M., Nakamura, S. and Tsubota, K., 2020. Advances in the diagnosis and treatment of dry eye. Progress in retinal and eye research, 78, p.100842.

Kovács, I., Luna, C., Quirce, S., Mizerska, K., Callejo, G., Riestra, A., Fernández-Sánchez, L., Meseguer, V.M., Cuenca, N., Merayo-Lloves, J. and Acosta, M.C., 2016. Abnormal activity of corneal cold thermoreceptors underlies the unpleasant sensations in dry eye disease. Pain, 157(2), p.399.

Kowtharapu, B.S. and Stachs, O., 2020. Corneal cells: fine-tuning nerve regeneration. Current eye research, 45(3), pp.291-302.

Kramer, D.J., Risso, D., Kosillo, P., Ngai, J. and Bateup, H.S., 2018. Combinatorial Expression of Grp and Neurod6 Defines Dopamine Neuron Populations with Distinct Projection Patterns and Disease Vulnerability. eNeuro, 5(3).

Kumar, S., Singh, U., Goswami, C. and Singru, P.S., 2017. Transient receptor potential vanilloid 5 (TRPV5), a highly Ca2+-selective TRP channel in the rat brain: relevance to neuroendocrine regulation. Journal of neuroendocrinology, 29(4).

Kurose, M. and Meng, I.D., 2013. Dry eye modifies the thermal and menthol responses in rat corneal primary afferent cool cells. Journal of neurophysiology, 110(2), pp.495-504.

Kuwajima T, Soares CA, Sitko AA, Lefebvre V, Mason C. SoxC Transcription Factors Promote Contralateral Retinal Ganglion Cell Differentiation and Axon Guidance in the Mouse Visual System. Neuron. 2017;93(5):1110-1125.e5. doi:10.1016/j.neuron.2017.01.029

Labbé, A., Terry, O., Brasnu, E., Van Went, C. and Baudouin, C., 2012. Tear film osmolarity in patients treated for glaucoma or ocular hypertension. Cornea, 31(9), pp.994-999.

Labetoulle M, Baudouin C, Calonge M, Merayo-Lloves J, Boboridis KG, Akova YA, Aragona P, Geerling G, Messmer EM, Benítez-Del-Castillo J. Role of corneal nerves in ocular surface homeostasis and disease. Acta Ophthalmol. 2019 Mar;97(2):137-145. doi: 10.1111/aos.13844. Epub 2018 Sep 17. PMID: 30225941.

Lagali N, Poletti E, Patel DV, McGhee CN, Hamrah P, Kheirkhah A, Tavakoli M, Petropoulos IN, Malik RA, Utheim TP, Zhivov A, Stachs O, Falke K, Peschel S, Guthoff R, Chao C, Golebiowski B, Stapleton F, Ruggeri A. Focused Tortuosity Definitions Based on Expert Clinical Assessment of Corneal Subbasal Nerves. Invest Ophthalmol Vis Sci. 2015 Aug;56(9):5102-9. doi: 10.1167/iovs.15-17284. PMID: 26241397.

Lamb, T.D., Collin, S.P. and Pugh, E.N., 2007. Evolution of the vertebrate eye: opsins, photoreceptors, retina and eye cup. Nature Reviews Neuroscience, 8(12), pp.960-976.

LANGLEY D, MACDONALD RK. Clinical method of observing changes in the rate of flow of aqueous humour in the human eye. II. In glaucoma. Br J Ophthalmol. 1952;36(9):499-505. doi:10.1136/bjo.36.9.499

Launay, P.S., Reboussin, E., Liang, H., Kessal, K., Godefroy, D., Rostene, W., Sahel, J.A., Baudouin, C., Parsadaniantz, S.M. and Le Goazigo, A.R., 2016. Ocular inflammation induces trigeminal pain, peripheral and central neuroinflammatory mechanisms. Neurobiology of disease, 88, pp.16-28.

Le Pichon, C.E. and Chesler, A.T., 2014. The functional and anatomical dissection of somatosensory subpopulations using mouse genetics. Frontiers in neuroanatomy, 8, p.21.

Lee HK, Kim KW, Ryu JS, Jeong HJ, Lee SM, Kim MK. Bilateral Effect of the Unilateral Corneal Nerve Cut on Both Ocular Surface and Lacrimal Gland. Invest Ophthalmol Vis Sci. 2019 Jan 2;60(1):430-441. doi: 10.1167/iovs.18-26051. PMID: 30703211.

Lee HK, Lee KS, Kim HC, Lee SH, Kim EK. Nerve growth factor concentration and implications in photorefractive keratectomy vs laser in situ keratomileusis. Am J Ophthalmol. 2005 Jun;139(6):965-71. doi: 10.1016/j.ajo.2004.12.051. PMID: 15953424.

Lele, P.P. and Weddell, G., 1959. Sensory nerves of the cornea and cutaneous sensibility. Experimental neurology, 1(4), pp.334-359.

Lemp, M.A., Bron, A.J., Baudouin, C., Del Castillo, J.M.B., Geffen, D., Tauber, J., Foulks, G.N., Pepose, J.S. and Sullivan, B.D., 2011. Tear osmolarity in the diagnosis and management of dry eye disease. American journal of ophthalmology, 151(5), pp.792-798.

Li Y, Struebing FL, Wang J, King R, Geisert EE. Different Effect of Sox11 in Retinal Ganglion Cells Survival and Axon Regeneration. Front Genet. 2018;9:633. Published 2018 Dec 18. doi:10.3389/fgene.2018.00633

Li Z, Burns AR, Han L, Rumbaut RE, Smith CW. IL-17 and VEGF are necessary for efficient corneal nerve regeneration. Am J Pathol. 2011; 178(3):1106–16. (PubMed: 21356362)

Li, D.Q. and Tseng, S.C., 1995. Three patterns of cytokine expression potentially involved in epithelial-fibroblast interactions of human ocular surface. Journal of cellular physiology, 163(1), pp.61-79.

Li, Y., Zhu, J., Chen, J.J., Yu, J., Jin, Z., Miao, Y., Browne, A.W., Zhou, Q. and Chen, Z., 2019. Simultaneously imaging and quantifying in vivo mechanical properties of crystalline lens and cornea using optical coherence elastography with acoustic radiation force excitation. APL photonics, 4(10), p.106104.

Li, Z., Burns, A.R., Han, L., Rumbaut, R.E. and Smith, C.W., 2011. IL-17 and VEGF are necessary for efficient corneal nerve regeneration. The American journal of pathology, 178(3), pp.1106-1116.

Liang G, Wolfgang CD, Chen BP, Chen TH, Hai T. ATF3 gene. Genomic organization, promoter, and regulation. J Biol Chem. 1996 Jan 19;271(3):1695-701. doi: 10.1074/jbc.271.3.1695. PMID: 8576171.

Lin, H. and Yiu, S.C., 2014. Dry eye disease: a review of diagnostic approaches and treatments. Saudi Journal of Ophthalmology, 28(3), pp.173-181.

Lin, Z., Santos, S., Padilla, K., Printzenhoff, D. and Castle, N.A., 2016. Biophysical and pharmacological characterization of Nav1. 9 voltage dependent sodium channels stably expressed in HEK-293 cells. PloS one, 11(8), p.e0161450.

Lindå, H., Sköld, M. K., & Ochsmann, T. (2011). Activating transcription factor 3, a useful marker for regenerative response after nerve root injury. Frontiers in neurology, 2, 30.

Lindwall, C., Dahlin, L., Lundborg, G. and Kanje, M., 2004. Inhibition of c-Jun phosphorylation reduces axonal outgrowth of adult rat nodose ganglia and dorsal root ganglia sensory neurons. Molecular and Cellular Neuroscience, 27(3), pp.267-279.

Liu, C., Li, C., Deng, Z., Du, E. and Xu, C., 2018. Long non-coding RNA BC168687 is involved in TRPV1-mediated diabetic neuropathic pain in rats. Neuroscience, 374, pp.214-222.

Ljubimov, A.V. and Saghizadeh, M., 2015. Progress in corneal wound healing. Progress in retinal and eye research, 49, pp.17-45.

López de Armentia M, Cabanes C, Belmonte C. Electrophysiological properties of identified trigeminal ganglion neurons innervating the cornea of the mouse. Neuroscience. 2000;101(4):1109-15. doi: 10.1016/s0306-4522(00)00440-1. PMID: 11113359.

Luiz, A. P., MacDonald, D. I., Santana-Varela, S., Millet, Q., Sikandar, S., Wood, J. N., & Emery, E. C. (2019). Cold sensing by NaV1.8-positive and NaV1.8-negative sensory neurons. Proceedings of the National Academy of Sciences of the United States of America, 116(9), 3811–3816. https://doi.org/10.1073/pnas.1814545116

Luo, L., Li, D.Q., Doshi, A., Farley, W., Corrales, R.M. and Pflugfelder, S.C., 2004. Experimental dry eye stimulates production of inflammatory cytokines and MMP-9 and activates MAPK signaling pathways on the ocular surface. Investigative ophthalmology & visual science, 45(12), pp.4293-4301.

Lyu, Y., Zeng, X., Li, F. and Zhao, S., 2019. The effect of the duration of diabetes on dry eye and corneal nerves. Contact Lens and Anterior Eye, 42(4), pp.380-385.

Ma, S., Yu, Z., Feng, S., Chen, H., Chen, H. and Lu, X., 2019. Corneal autophagy and ocular surface inflammation: a new perspective in dry eye. Experimental eye research, 184, pp.126-134.

MacGillavry HD, Stam FJ, Sassen MM, Kegel L, Hendriks WT, Verhaagen J, Smit AB, van Kesteren RE. NFIL3 and cAMP response element-binding protein form a transcriptional feedforward loop that controls neuronal regeneration-associated gene expression. Journal of Neuroscience. 2009 Dec 9;29(49):15542-50.

MacIver MB, Tanelian DL. Structural and functional specialization of A delta and C fiber free nerve endings innervating rabbit corneal epithelium. J Neurosci. 1993 Oct;13(10):4511-24. doi: 10.1523/JNEUROSCI.13-10-04511.1993. PMID: 8410200; PMCID: PMC6576377.

Madduri, S., Papaloïzos, M. and Gander, B., 2009. Synergistic effect of GDNF and NGF on axonal branching and elongation in vitro. Neuroscience research, 65(1), pp.88-97.

Madrid, R., Donovan-Rodríguez, T., Meseguer, V., Acosta, M.C., Belmonte, C. and Viana, F., 2006. Contribution of TRPM8 channels to cold transduction in primary sensory neurons and peripheral nerve terminals. Journal of Neuroscience, 26(48), pp.12512-12525.

Maier, D. L., Mani, S., Donovan, S. L., Soppet, D., Tessarollo, L., Mccasland, J. S., and Meiri, K. F. (1999). Disrupted cortical map and absence of cortical barrels in growth-associated protein (GAP)-43 knockout mice. Proc. Natl. Acad. Sci. U.S.A. 96, 9397–9402.

Mallik, R., Kundu, A., & Chaudhuri, S. (2018). High mobility group proteins: the multifaceted regulators of chromatin dynamics. The Nucleus, 61(3), 213-226.

Mapp, P.I. and Walsh, D.A., 2012. Mechanisms and targets of angiogenesis and nerve growth in osteoarthritis. Nature Reviews Rheumatology, 8(7), pp.390-398.

Marfurt C, Anokwute MC, Fetcko K, Mahony-Perez E, Farooq H, Ross E, Baumanis MM, Weinberg RL, McCarron ME, Mankowski JL. Comparative Anatomy of the Mammalian Corneal Subbasal Nerve Plexus. Invest Ophthalmol Vis Sci. 2019 Dec 2;60(15):4972-4984. doi: 10.1167/iovs.19-28519. PMID: 31790560; PMCID: PMC6886725.

Marfurt CF, Ellis LC, Jones MA. Sensory and sympathetic nerve sprouting in the rat cornea following neonatal administration of capsaicin. Somatosens Mot Res. 1993;10(4):377-98. doi: 10.3109/08990229309028845. PMID: 7508667.

Marfurt CF. The central projections of trigeminal primary afferent neurons in the cat as determined by the tranganglionic transport of horseradish peroxidase. J Comp Neurol. 1981;203:785–798.

Marfurt, C.F. and Dvorscak, L., 2006. Peptidergic and Non–Peptidergic Innervation of the Rat Cornea. Investigative Ophthalmology & Visual Science, 47(13), pp.2724-2724.

Marfurt, C.F. and Ellis, L.C., 1993. Immunohistochemical localization of tyrosine hydroxylase in corneal nerves. Journal of Comparative Neurology, 336(4), pp.517-531.

Marfurt, C.F., Cox, J., Deek, S. and Dvorscak, L., 2010. Anatomy of the human corneal innervation. Experimental eye research, 90(4), pp.478-492.

Marfurt, C.F., Kingsley, R.E. and Echtenkamp, S.E., 1989. Sensory and sympathetic innervation of the mammalian cornea. A retrograde tracing study. Investigative ophthalmology & visual science, 30(3), pp.461-472.

Marrazzo, G., Bellner, L., Halilovic, A., Li Volti, G., Drago, F., Dunn, M.W. and Schwartzman, M.L., 2011. The role of neutrophils in corneal wound healing in HO-2 null mice. PloS one, 6(6), p.e21180.

Masoudi Alavi, N., Sharifitabar, Z., Shaeri, M. and Adib Hajbaghery, M., 2014. An audit of eye dryness and corneal abrasion in ICU patients in Iran. Nursing in critical care, 19(2), pp.73-77.

Mastropasqua, L., Massaro-Giordano, G., Nubile, M. and Sacchetti, M., 2017. Understanding the pathogenesis of neurotrophic keratitis: the role of corneal nerves. Journal of cellular physiology, 232(4), pp.717-724.

Matsuura, Y., Ohtori, S., Iwakura, N., Suzuki, T., Kuniyoshi, K. and Takahashi, K., 2013. Expression of activating transcription factor 3 (ATF3) in uninjured dorsal root ganglion neurons in a lower trunk avulsion pain model in rats. European Spine Journal, 22(8), pp.1794-1799.

McDougal DH, Gamlin PD. Autonomic control of the eye. Compr Physiol. 2015;5(1):439-473. doi:10.1002/cphy.c140014

McKay, T.B., Seyed-Razavi, Y., Ghezzi, C.E., Dieckmann, G., Nieland, T.J., Cairns, D.M., Pollard, R.E., Hamrah, P. and Kaplan, D.L., 2019. Corneal pain and experimental model development. Progress in retinal and eye research, 71, pp.88-113.

McKenna, C.C. and Lwigale, P.Y., 2011. Innervation of the mouse cornea during development. Investigative ophthalmology & visual science, 52(1), pp.30-35.

Mcmonnies CW. The potential role of neuropathic mechanisms in dry eye syndromes. Journal of Optometry. 2017;10(1):5-13. doi:10.1016/j.optom.2016.06.002.

McPhail, L. T., Fernandes, K. J., Chan, C. C., Vanderluit, J. L., & Tetzlaff, W. (2004). Axonal reinjury reveals the survival and re-expression of regeneration-associated genes in chronically axotomized adult mouse motoneurons. Experimental neurology, 188(2), 331-340.

Mecum NE, Cyr D, Malon J, Demers D, Cao L, Meng ID. Evaluation of Corneal Damage After Lacrimal Gland Excision in Male and Female Mice. Invest Ophthalmol Vis Sci. 2019;60(10):3264–3274. doi:10.1167/iovs.18-2645

Mecum NE, Demers D, Sullivan CE, Denis TE, Kalliel JR, Meng ID. Lacrimal gland excision in male and female mice causes ocular pain and anxiety-like behaviors. Sci Rep. 2020;10(1):17225. Published 2020 Oct 14. doi:10.1038/s41598-020-73945-w

Medeiros, C.S. and Santhiago, M.R., 2020. Corneal nerves anatomy, function, injury and regeneration. Experimental Eye Research, 200, p.108243.

Meek, K. M., & Knupp, C. (2015). Corneal structure and transparency. Progress in retinal and eye research, 49, 1–16. https://doi.org/10.1016/j.preteyeres.2015.07.001

Meng ID, Barton ST, Mecum NE, Kurose M. Corneal sensitivity following lacrimal gland excision in the rat. Invest Ophthalmol Vis Sci. 2015;56(5):3347–3354. doi:10.1167/iovs.15-16717

Meng J, Ovsepian SV, Wang J, Pickering M, Sasse A, Aoki KR, Lawrence GW, Dolly JO. Activation of TRPV1 mediates calcitonin gene-related peptide release, which excites trigeminal sensory neurons and is attenuated by a retargeted botulinum toxin with anti-nociceptive potential. J Neurosci. 2009 Apr 15;29(15):4981-92. doi: 10.1523/JNEUROSCI.5490-08.2009. PMID: 19369567; PMCID: PMC6665337.

Meng, I.D. and Kurose, M., 2013. The role of corneal afferent neurons in regulating tears under normal and dry eye conditions. Experimental eye research, 117, pp.79-87.

Meng, I.D., Barton, S.T., Goodney, I., Russell, R. and Mecum, N.E., 2019. Progesterone application to the rat forehead produces corneal antinociception. Investigative ophthalmology & visual science, 60(5), pp.1706-1713.

Mikami, Norihisa, et al. "Calcitonin gene-related peptide regulates type IV hypersensitivity through dendritic cell functions." PLoS One 9.1 (2014): e86367.

Mikulec AA, Tanelian DL. CGRP increases the rate of corneal re-epithelialization in an in vitro whole mount preparation. Journal of ocular pharmacology and therapeutics. 1996;12(4):417-23.

Mishima, S. and Hedbys, B.O., 1968. Physiology of the cornea. International ophthalmology clinics, 8(3), pp.527-560.

Mitchison T, Kirschner M. Cytoskeletal dynamics and nerve growth. Neuron. 1988; 1(9):761–72. (PubMed: 3078414)

Miura, D.L., Hazarbassanov, R.M., Yamasato, C.K.N., e Silva, F.B., Godinho, C.J. and Gomes, J.Á.P., 2013. Effect of a light-emitting timer device on the blink rate of non-dry eye individuals and dry eye patients. British Journal of Ophthalmology, 97(8), pp.965-967.

Moore, D.L. and Goldberg, J.L., 2011. Multiple transcription factor families regulate axon growth and regeneration. Developmental neurobiology, 71(12), pp.1186-1211.

Moos, D.D. and Lind, D.M., 2006. Detection and treatment of perioperative corneal abrasions. Journal of PeriAnesthesia Nursing, 21(5), pp.332-338.

Moreira, T.V., Gover, T.D. and Weinreich, D., 2007. Electrophysiological properties and chemosensitivity of acutely dissociated trigeminal somata innervating the cornea. Neuroscience, 148(3), pp.766-774.

Moulton EA, Borsook D. C-Fiber Assays in the Cornea vs. Skin. Brain Sci. 2019;9(11):320. Published 2019 Nov 12. doi:10.3390/brainsci9110320

Mu, Z., Zhang, S., He, C., Hou, H., Liu, D., Hu, N., & Xu, H. (2017). Expression of SoxC Transcription Factors during Zebrafish Retinal and Optic Nerve Regeneration. Neuroscience bulletin, 33(1), 53–61. https://doi.org/10.1007/s12264-016-0073-2

Müller LJ, Vrensen GF, Pels L, Cardozo BN, Willekens B. Architecture of human corneal nerves. Invest Ophthalmol Vis Sci. 1997 Apr;38(5):985-94. PMID: 9112994.

Müller, L.J., Marfurt, C.F., Kruse, F. and Tervo, T.M., 2003. Corneal nerves: structure, contents and function. Experimental eye research, 76(5), pp.521-542.

Murata, Y. and Masuko, S., 2006. Peripheral and central distribution of TRPV1, substance P and CGRP of rat corneal neurons. Brain research, 1085(1), pp.87-94.

Nakamori, K., Odawara, M., Nakajima, T., Mizutani, T. and Tsubota, K., 1997. Blinking is controlled primarily by ocular surface conditions. American journal of ophthalmology, 124(1), pp.24-30.

Nakamura, A., Hayakawa, T., Kuwahara, S., Maeda, S., Tanaka, K., Seki, M. and Mimura, O., 2007. Morphological and immunohistochemical characterization of the trigeminal ganglion neurons innervating the cornea and upper eyelid of the rat. Journal of chemical neuroanatomy, 34(3-4), pp.95-101.

Nascimento, D., Pozza, D.H., Castro-Lopes, J.M. and Neto, F.L., 2011. Neuronal injury marker ATF-3 is induced in primary afferent neurons of monoarthritic rats. Neurosignals, 19(4), pp.210-221.

Netter, F.H., 2010. Atlas of neuroanatomy and neurophysiology.

Neumann, S., & Woolf, C. J. (1999). Regeneration of dorsal column fibers into and beyond the lesion site following adult spinal cord injury. Neuron, 23(1), 83-91.

Nichols KK, Redfern RL, Jacob JT, Nelson JD, Fonn D, Forstot SL, Huang JF, Holden BA, Nichols JJ; members of the TFOS International Workshop on Contact Lens Discomfort. The TFOS International Workshop on Contact Lens Discomfort: report of the definition and classification subcommittee. Invest Ophthalmol Vis Sci. 2013 Oct 18;54(11):TFOS14-9. doi: 10.1167/iovs.13-13074. PMID: 24058134.

Nichols, K.K., Bacharach, J., Holland, E., Kislan, T., Shettle, L., Lunacsek, O., Lennert, B., Burk, C. and Patel, V., 2016. Impact of dry eye disease on work productivity, and patients' satisfaction with over-the-counter dry eye treatments. Investigative ophthalmology & visual science, 57(7), pp.2975-2982.

Nicolle, P., Labbe, A., Reboussin, E., Kessal, K., Melik-Parsadaniantz, S., Baudouin, C., & Réaux-Le-Goazigo, A. (2016). Extraorbital lacrimal and Harderian glands excision in mice: a new pre-clinical animal model of dry eye. Investigative Ophthalmology & Visual Science, 57(12), 5708-5708.

Nishida, T., Chikama, T.I., Morishige, N., Yanai, R., Yamada, N. and Saito, J., 2007. Persistent epithelial defects due to neurotrophic keratopathy treated with a substance p-derived peptide and insulin-like growth factor 1. Japanese journal of ophthalmology, 51(6), pp.442-447.

Norsworthy, M.W., Bei, F., Kawaguchi, R., Wang, Q., Tran, N.M., Li, Y., Brommer, B., Zhang, Y., Wang, C., Sanes, J.R. and Coppola, G., 2017. Sox11 expression promotes regeneration of some retinal ganglion cell types but kills others. Neuron, 94(6), pp.1112-1120.

Nunomura, S., Nanri, Y., Lefebvre, V. and Izuhara, K., 2021. Epithelial SOX11 regulates eyelid closure during embryonic eye development. Biochemical and Biophysical Research Communications, 549, pp.27-33.

Pan, Y., Liu, F., Qi, X., Hu, Y., Xu, F., & Jia, H. (2018). Nerve Growth Factor Changes and Corneal Nerve Repair after Keratoplasty. Optometry and vision science : official publication of the American Academy of Optometry, 95(1), 27–31. https://doi.org/10.1097/OPX.0000000000001158

Park, C.Y., Zhuang, W., Lekhanont, K., Zhang, C., Cano, M., Lee, W.S., Gehlbach, P.L. and Chuck, R.S., 2007. Lacrimal gland inflammatory cytokine gene expression in the botulinum toxin B-induced murine dry eye model. Mol Vis, 13(252-255), pp.2222-2232.

Parra, A., Madrid, R., Echevarria, D., Del Olmo, S., Morenilla-Palao, C., Acosta, M.C., Gallar, J., Dhaka, A., Viana, F. and Belmonte, C., 2010. Ocular surface wetness is regulated by TRPM8-dependent cold thermoreceptors of the cornea. Nature medicine, 16(12), pp.1396-1399.

Patel, S. and Tutchenko, L., 2019. The refractive index of the human cornea: A review. Contact Lens and Anterior Eye, 42(5), pp.575-580.

Patel, S., Alió, J.L. and Pérez-Santonja, J.J., 2004. Refractive index change in bovine and human corneal stroma before and after LASIK: a study of untreated and re-treated corneas implicating stromal hydration. Investigative ophthalmology & visual science, 45(10), pp.3523-3530.

Patodia, S., & Raivich, G. (2012). Role of transcription factors in peripheral nerve regeneration. Frontiers in molecular neuroscience, 5, 8.

Paunicka KJ, Mellon J, Robertson D, Petroll M, Brown JR, Niederkorn JY. Severing corneal nerves in one eye induces sympathetic loss of immune privilege and promotes rejection of future corneal allografts placed in either eye. Am J Transplant. 2015;15(6):1490-1501. doi:10.1111/ajt.13240

Pellegrini JJ, Horn AK, Evinger C. The trigeminally evoked blink reflex. I. Neuronal circuits. Exp Brain Res. 1995;107(2):166-80. doi: 10.1007/BF00230039. PMID: 8773237.

Pflugfelder, S.C., Geerling, G., Kinoshita, S., Lemp, M.A., McCulley, J.P., Nelson, D., Novack, G.N., Shimazaki, J. and Wilson, C., 2007. Management and therapy of dry eye disease: report of the Management and Therapy Subcommittee of the International Dry Eye WorkShop (2007). Ocular Surface, 5(2), pp.163-178.

Pham, T.L. and Bazan, H.E., 2021. Docosanoid signaling modulates corneal nerve regeneration: effect on tear secretion, wound healing, and neuropathic pain. Journal of lipid research, 62.

Pham, T.L., Kakazu, A., He, J. and Bazan, H.E., 2019. Mouse strains and sexual divergence in corneal innervation and nerve regeneration. The FASEB Journal, 33(3), pp.4598-4609.

Philipp, W., Speicher, L. and Humpel, C., 2000. Expression of vascular endothelial growth factor and its receptors in inflamed and vascularized human corneas. Investigative ophthalmology & visual science, 41(9), pp.2514-2522.

Piña, R., Ugarte, G., Campos, M., Íñigo-Portugués, A., Olivares, E., Orio, P., Belmonte, C., Bacigalupo, J. and Madrid, R., 2019. Role of TRPM8 channels in altered cold sensitivity of corneal primary sensory neurons induced by axonal damage. Journal of Neuroscience, 39(41), pp.8177-8192.

Piper AS, Yeats JC, Bevan S, Docherty RJ. A study of the voltage dependence of capsaicin-activated membrane currents in rat sensory neurones before and after acute desensitization. J Physiol. 1999;518 (Pt 3)(Pt 3):721-733. doi:10.1111/j.1469-7793.1999.0721p.

Price, M.O. and Price Jr, F.W., 2007. Descemet stripping with endothelial keratoplasty for treatment of iridocorneal endothelial syndrome. Cornea, 26(4), pp.493-497.

Qi, H., Li, D. Q., Shine, H. D., Chen, Z., Yoon, K. C., Jones, D. B., & Pflugfelder, S. C. (2008). Nerve growth factor and its receptor TrkA serve as potential markers for human corneal epithelial progenitor cells. Experimental eye research, 86(1), 34–40. https://doi.org/10.1016/j.exer.2007.09.003

Raivich, G., Bohatschek, M., Da Costa, C., Iwata, O., Galiano, M., Hristova, M., Nateri, A. S., Makwana, M., Riera-Sans, L., Wolfer, D. P., Lipp, H. P., Aguzzi, A., Wagner, E. F., and Behrens, A. (2004). The AP-1 transcription factor c-Jun is required for efficient axonal regeneration. Neuron 43, 57–67.

Reeves R. (2010). Nuclear functions of the HMG proteins. Biochimica et biophysica acta, 1799(1-2), 3–14. https://doi.org/10.1016/j.bbagrm.2009.09.001

Richardson, P. M., Mcguinness, U. M., and Aguayo, A. J. (1982). Peripheral nerve autografts to the rat spinal cord: studies with axonal tracing methods. Brain Res. 237, 147–162.

Robbins, A., Kurose, M., Winterson, B.J. and Meng, I.D., 2012. Menthol activation of corneal cool cells induces TRPM8-mediated lacrimation but not nociceptive responses in rodents. Investigative ophthalmology & visual science, 53(11), pp.7034-7042.

Rosenbaum T, Simon SA. TRPV1 Receptors and Signal Transduction. In: Liedtke WB, Heller S, editors. TRP Ion Channel Function in Sensory Transduction and Cellular Signaling Cascades. Boca Raton (FL): CRC Press/Taylor & Francis; 2007. Chapter 5. Available from: https://www.ncbi.nlm.nih.gov/books/NBK5260/

Rosenfield, M., 2016. Computer vision syndrome (aka digital eye strain). Optometry, 17(1), pp.1-10.

Rosenthal P, Borsook D. Ocular neuropathic pain. Br J Ophthalmol. 2016 Jan;100(1):128-34. doi: 10.1136/bjophthalmol-2014-306280. Epub 2015 May 5. PMID: 25943558; PMCID: PMC4717373.

Rowsey TG, Karamichos D. The role of lipids in corneal diseases and dystrophies: a systematic review. Clin Transl Med. 2017 Dec;6(1):30. doi: 10.1186/s40169-017-0158-1. Epub 2017 Aug 11. PMID: 28782089; PMCID: PMC5552625.

Rózsa AJ, Beuerman RW. Density and organization of free nerve endings in the corneal epithelium of the rabbit. Pain. 1982 Oct;14(2):105-120. doi: 10.1016/0304-3959(82)90092-6. PMID: 7177676.

Russell FA, King R, Smillie SJ, Kodji X, Brain SD. Calcitonin gene-related peptide: physiology and pathophysiology. Physiol Rev. 2014;94(4):1099-1142. doi:10.1152/physrev.00034.2013

Sacchetti, M. and Lambiase, A., 2017. Neurotrophic factors and corneal nerve regeneration. Neural regeneration research, 12(8), p.1220.

Saito, K., Hitomi, S., Suzuki, I., Masuda, Y., Kitagawa, J., Tsuboi, Y., Kondo, M., Sessle, B.J. and Iwata, K., 2008. Modulation of trigeminal spinal subnucleus caudalis neuronal activity following regeneration of transected inferior alveolar nerve in rats. Journal of neurophysiology, 99(5), pp.2251-2263.

Salerno, K. M., Jing, X., Diges, C. M., Cornuet, P. K., Glorioso, J. C., & Albers, K. M. (2012). Sox11 modulates brain-derived neurotrophic factor expression in an exon promoter-specific manner. Journal of neuroscience research, 90(5), 1011–1019. https://doi.org/10.1002/jnr.23010

Salerno, K.M., Jing, X., Diges, C.M., Davis, B.M. and Albers, K.M., 2013. TRAF family member-associated NF-kappa B activator (TANK) expression increases in injured sensory neurons and is transcriptionally regulated by Sox11. Neuroscience, 231, pp.28-37.

Sangwan, P., Singh, P., Yadav, V. and Kumar, S., 2018. A Review about various Nanomaterials in Drug Delivery Systems and their Applications. International Journal of Research and Development in Pharmacy & Life Sciences, 7(3), pp.2969-2981.

Schaumberg, D.A., Dana, R., Buring, J.E. and Sullivan, D.A., 2009. Prevalence of dry eye disease among US men: estimates from the Physicians' Health Studies. Archives of ophthalmology, 127(6), pp.763-768.

Schaumberg, D.A., Sullivan, D.A., Buring, J.E. and Dana, M.R., 2003. Prevalence of dry eye syndrome among US women. American journal of ophthalmology, 136(2), pp.318-326.

Schein, O.D., MUÑO, B., Tielsch, J.M., Bandeen-Roche, K. and West, S., 1997. Prevalence of dry eye among the elderly. American journal of ophthalmology, 124(6), pp.723-728.

Schmitt, A.B., Breuer, S., Liman, J., Buss, A., Schlangen, C., Pech, K., Hol, E.M., Brook, G.A., Noth, J. and Schwaiger, F.W., 2003. Identification of regeneration-associated genes after central and peripheral nerve injury in the adult rat. BMC neuroscience, 4(1), pp.1-13.

Schofield, B.R., 2008. Retrograde axonal tracing with fluorescent markers. Current protocols in neuroscience, 43(1), pp.1-17.

Schou WS, Ashina S, Amin FM, Goadsby PJ, Ashina M. Calcitonin gene-related peptide and pain: a systematic review. J Headache Pain. 2017;18(1):34. doi:10.1186/s10194-017-0741-2

Schreyer, D.J. and Skene, J.H., 1991. Fate of GAP-43 in ascending spinal axons of DRG neurons after peripheral nerve injury: delayed accumulation and correlation with regenerative potential. Journal of Neuroscience, 11(12), pp.3738-3751.

Schwab, I.R., 2018. The evolution of eyes: major steps. The Keeler lecture 2017: centenary of Keeler Ltd. Eye, 32(2), pp.302-313.

Seijffers R, Allchorne AJ, Woolf CJ. The transcription factor ATF-3 promotes neurite outgrowth. Mol Cell Neurosci. 2006 May-Jun;32(1-2):143-54. doi: 10.1016/j.mcn.2006.03.005. Epub 2006 May 19. PMID: 16713293.

Seijffers, R., Mills, C. D., & Woolf, C. J. (2007). ATF3 increases the intrinsic growth state of DRG neurons to enhance peripheral nerve regeneration. The Journal of neuroscience : the official journal of the Society for Neuroscience, 27(30), 7911–7920. https://doi.org/10.1523/JNEUROSCI.5313-06.2007

Shah S, Jani H. Prevalence and associated factors of dry eye: Our experience in patients above 40 years of age at a Tertiary Care Center. Oman J Ophthalmol. 2015;8(3):151-156. doi:10.4103/0974-620X.169910

Shaheen BS, Bakir M, Jain S. Corneal nerves in health and disease. Surv Ophthalmol. 2014;59(3):263–285. doi:10.1016/j.survophthal.2013.09.002

Sharif Z, Sharif W. Corneal neovascularization: updates on pathophysiology, investigations & management. Rom J Ophthalmol. 2019;63(1):15-22.

Sheppard, J.D., Torkildsen, G.L., Geffin, J.A., Dao, J., Evans, D.G., Ousler, G.W., Wilson, J., Baba, S.N., Senchyna, M. and Holland, E.J., 2019. Characterization of tear production in subjects with dry eye disease during intranasal tear neurostimulation: results from two pivotal clinical trials. The ocular surface, 17(1), pp.142-150.

Sheridan, M. and Douthwaite, W.A., 1989. Corneal asphericity and refractive error. Ophthalmic and Physiological Optics, 9(3), pp.235-238.

Shin, H.Y., Kwon, M.J., Lee, E.M., Kim, K., Oh, Y.J., Kim, H.S., Hwang, D.H. and Kim, B.G., 2021. Role of Myc proto-oncogene as a transcriptional hub to regulate the expression of regeneration-associated genes following preconditioning peripheral nerve injury. Journal of Neuroscience, 41(3), pp.446-460.

Shin, J.E., Ha, H., Kim, Y.K., Cho, Y. and DiAntonio, A., 2019. DLK regulates a distinctive transcriptional regeneration program after peripheral nerve injury. Neurobiology of disease, 127, pp.178-192.

Shinomiya, K., Ueta, M. and Kinoshita, S., 2018. A new dry eye mouse model produced by exorbital and intraorbital lacrimal gland excision. Scientific reports, 8(1), pp.1-10.

Singh, S., Mishra, D.K., Shanbhag, S., Vemuganti, G., Singh, V., Ali, M.J. and Basu, S., 2021. Lacrimal gland involvement in severe dry eyes after Stevens-Johnson syndrome. Ophthalmology, 128(4), pp.621-624.

Situ, P., Simpson, T.L., Fonn, D. and Jones, L.W., 2008. Conjunctival and corneal pneumatic sensitivity is associated with signs and symptoms of ocular dryness. Investigative ophthalmology & visual science, 49(7), pp.2971-2976.

Skene JH, Willard M. Axonally transported proteins associated with axon growth in rabbit central and peripheral nervous systems. J Cell Biol. 1981; 89:96–103. (PubMed: 6164683)

Skene, J. H. (1989). Axonal growth-associated proteins. Annu. Rev. Neurosci. 12, 127–156.

Skene, J. H., and Willard, M. (1981). Axonally transported proteins associated with axon growth in rabbit central and peripheral nervous systems. J. Cell Biol. 89, 96–103.

Skrzypecki J, Tomasz H, Karolina C. Variability of Dry Eye Disease Following Removal of Lacrimal Glands in Rats. Adv Exp Med Biol. 2019;1153:109-115. doi: 10.1007/5584_2019_348. PMID: 30806916.

Song, B., Zhao, M., Forrester, J. and McCaig, C., 2004. Nerve regeneration and wound healing are stimulated and directed by an endogenous electrical field in vivo. Journal of cell science, 117(20), pp.4681-4690.

Song, J., Yu, D., Song, A., Palmares, T., Song, H.S. and Song, M., 2014. Corneal thinning and opacity following selective laser trabeculoplasty: a case report. Journal of Advances in Medicine and Medical Research, pp.279-287.

Soong, H.K., Farjo, Q., Meyer, R.F. and Sugar, A., 2002. Diamond burr superficial keratectomy for recurrent corneal erosions. British journal of ophthalmology, 86(3), pp.296-298.

Sorge, R.E., LaCroix-Fralish, M.L., Tuttle, A.H., Sotocinal, S.G., Austin, J.S., Ritchie, J., Chanda, M.L., Graham, A.C., Topham, L., Beggs, S. and Salter, M.W., 2011. Spinal cord Toll-like receptor 4 mediates inflammatory and neuropathic hypersensitivity in male but not female mice. Journal of Neuroscience, 31(43), pp.15450-15454.

Sorge, R.E., Mapplebeck, J.C., Rosen, S., Beggs, S., Taves, S., Alexander, J.K., Martin, L.J., Austin, J.S., Sotocinal, S.G., Chen, D. and Yang, M., 2015. Different immune cells mediate mechanical pain hypersensitivity in male and female mice. Nature neuroscience, 18(8), pp.1081-1083.

Soullier, S., Jay, P., Poulat, F., Vanacker, J.M., Berta, P. and Laudet, V., 1999. Diversification pattern of the HMG and SOX family members during evolution. Journal of molecular evolution, 48(5), pp.517-527.

Spierer, O., Felix, E.R., McClellan, A.L., Parel, J.M., Gonzalez, A., Feuer, W.J., Sarantopoulos, C.D., Levitt, R.C., Ehrmann, K. and Galor, A., 2016. Corneal mechanical thresholds negatively associate with dry eye and ocular pain symptoms. Investigative ophthalmology & visual science, 57(2), pp.617-625.

Sretavan, D. W., and Kruger, K. (1998). Randomized retinal ganglion cell axon routing at the optic chiasm of GAP-43-deficient mice: association with midline recrossing and lack of normal ipsilateral axon turning. J. Neurosci. 18, 10502–10513.

Sridhar MS. Anatomy of cornea and ocular surface. Indian J Ophthalmol. 2018;66(2):190-194. doi:10.4103/ijo.IJO_646_17

Stam, F. J., Mason, M. R., Smit, A. B., and Verhaagen, J. (2008). "A meta-analysis of large-scale gene expression studies of the injured PNS: toward the genetic networks that govern successful regeneration," in Neural Degeneration and Repair: Gene Expression Profiling, Proteomics, Glycomics, and Systems Biology, ed. H. W. Muller (Hoboken, NJ: Wiley), 35–60.

Starkey ML, Davies M, Yip PK, Carter LM, Wong DJN, McMahon SB, Bradbury EJ. Expression of the regeneration-associated protein SPRR1A in primary sensory neurons and spinal cord of the adult mouse following peripheral and central injury. J Comp Neurol. 2009; 513(1):51–68. (PubMed: 19107756)

Stelmack J. Quality of life of low-vision patients and outcomes of low-vision rehabilitation. Optom Vis Sci. 2001 May;78(5):335-42. doi: 10.1097/00006324-200105000-00017. PMID: 11384011.

Stenberg, L. and Dahlin, L.B., 2014. Gender differences in nerve regeneration after sciatic nerve injury and repair in healthy and in type 2 diabetic Goto-Kakizaki rats. BMC neuroscience, 15(1), pp.1-10.

Stephens, D.N. and McNamara, N.A., 2015. Altered mucin and glycoprotein expression in dry eye disease. Optometry and Vision Science, 92(9), pp.931-938.

Stepp MA, Pal-Ghosh S, Tadvalkar G, Li L, Brooks SR, Morasso MI. Molecular basis of Mitomycin C enhanced corneal sensory nerve repair after debridement wounding. Sci Rep. 2018;8(1):16960. Published 2018 Nov 16. doi:10.1038/s41598-018-35090-3

Stepp, M.A., Zieske, J.D., Trinkaus-Randall, V., Kyne, B.M., Pal-Ghosh, S., Tadvalkar, G. and Pajoohesh-Ganji, A., 2014. Wounding the cornea to learn how it heals. Experimental eye research, 121, pp.178-193.

Stevenson W, Chen Y, Lee SM, Lee HS, Hua J, Dohlman T, Shiang T, Dana R. Extraorbital lacrimal gland excision: a reproducible model of severe aqueous tear-deficient dry eye disease. Cornea. 2014 Dec;33(12):1336-41. doi: 10.1097/ICO.0000000000000264. PMID: 25255136.

Streilein JW. New thoughts on the immunology of corneal transplantation. Eye (Lond). 2003 Nov;17(8):943-8. doi: 10.1038/sj.eye.6700615. PMID: 14631401.

Strickland, I.T., Martindale, J.C., Woodhams, P.L., Reeve, A.J., Chessell, I.P. and McQueen, D.S., 2008. Changes in the expression of NaV1. 7, NaV1. 8 and NaV1. 9 in a distinct population of dorsal root ganglia innervating the rat knee joint in a model of chronic inflammatory joint pain. European journal of pain, 12(5), pp.564-572.

Strittmatter, S. M., Fankhauser, C., Huang, P. L., Mashimo, H., and Fishman, M. C. (1995). Neuronal pathfinding is abnormal in mice lacking the neuronal growth cone protein GAP-43. Cell 80, 445–452.

Sullivan, D.A., Rocha, E.M., Aragona, P., Clayton, J.A., Ding, J., Golebiowski, B., Hampel, U., McDermott, A.M., Schaumberg, D.A., Srinivasan, S. and Versura, P., 2017. TFOS DEWS II sex, gender, and hormones report. The ocular surface, 15(3), pp.284-333.

Suwan-apichon O, Rizen M, Rangsin R, Herretes S, Reyes JM, Lekhanont K, Chuck RS. Botulinum toxin B-induced mouse model of keratoconjunctivitis sicca. Invest Ophthalmol Vis Sci. 2006 Jan;47(1):133-9. doi: 10.1167/iovs.05-0380. PMID: 16384954.

Szpara, M. L., Vranizan, K., Tai, Y. C., Goodman, C. S., Speed, T. P., and Ngai, J. (2007). Analysis of gene expression during neurite outgrowth and regeneration. BMC Neurosci. 8, 100. doi: 10.1186/1471-2202-8-100

Takeda, M., Kato, H., Takamiya, A., Yoshida, A. and Kiyama, H., 2000. Injury-specific expression of activating transcription factor-3 in retinal ganglion cells and its colocalized expression with phosphorylated c-Jun. Investigative ophthalmology & visual science, 41(9), pp.2412-2421.

Tan MH, Bryars J, Moore J. Use of nerve growth factor to treat congenital neurotrophic corneal ulceration. Cornea. 2006; 25(3):352–5. (PubMed: 16633039)

Tanabe K, Bonilla I, Winkles JA, Strittmatter SM. Fibroblast growth factor-inducible-14 is induced in axotomized neurons and promotes neurite outgrowth. J Neurosci. 2003 Oct 22;23(29):9675-86. doi: 10.1523/JNEUROSCI.23-29-09675.2003. PMID: 14573547; PMCID: PMC6740475.

Tanelian DL, Beuerman RW. Responses of rabbit corneal nociceptors to mechanical and thermal stimulation. Exp Neurol. 1984 Apr;84(1):165-78. doi: 10.1016/0014-4886(84)90013-x. PMID: 6705882.

Tepelus TC, Chiu GB, Huang J, Huang P, Sadda SR, Irvine J, Lee OL. Correlation between corneal innervation and inflammation evaluated with confocal microscopy and symptomatology in patients with dry eye syndromes: a preliminary study. Graefes Arch Clin Exp Ophthalmol. 2017 Sep;255(9):1771-1778. doi: 10.1007/s00417-017-3680-3. Epub 2017 May 20. PMID: 28528377.

Tetzlaff, W., Alexander, S. W., Miller, F. D., and Bisby, M. A. (1991). Response of facial and rubrospinal neurons to axotomy: changes in mRNA expression for cytoskeletal proteins and GAP-43. J. Neurosci. 11, 2528–2544.

Thein DC, Thalhammer JM, Hartwig AC, Crenshaw EB 3rd, Lefebvre V, Wegner M, Sock E 2010. The closely related transcription factors Sox4 and Sox11 function as survival factors during spinal cord development. J Neurochem 115: 131–141

Toda M, Suzuki T, Hosono K, Kurihara Y, Kurihara H, Hayashi I, Kitasato H, Hoka S, Majima M. Roles of calcitonin gene-related peptide in facilitation of wound healing and angiogenesis. Biomed Pharmacother. 2008 Jul-Aug;62(6):352-9. doi: 10.1016/j.biopha.2008.02.003. Epub 2008 Mar 6. PMID: 18430544.

Tominaga M, Caterina MJ, Malmberg AB, Rosen TA, Gilbert H, Skinner K, Raumann BE, Basbaum AI, Julius D. The cloned capsaicin receptor integrates multiple pain-producing stimuli. Neuron. 1998 Sep;21(3):531-43. doi: 10.1016/s0896-6273(00)80564-4. PMID: 9768840.

Tomlinson, A., Khanal, S., Ramaesh, K., Diaper, C. and McFadyen, A., 2006. Tear film osmolarity: determination of a referent for dry eye diagnosis. Investigative ophthalmology & visual science, 47(10), pp.4309-4315.

Tsubota, K., 1998. Tear dynamics and dry eye. Progress in retinal and eye research, 17(4), pp.565-596.

Tsujino H, Kondo E, Fukuoka T, Dai Y, Tokunaga A, Miki K, Yonenobu K, Ochi T, Noguchi K. Activating transcription factor 3 (ATF3) induction by axotomy in sensory and motoneurons: A novel neuronal marker of nerve injury. Mol Cell Neurosci. 2000 Feb;15(2):170-82. doi: 10.1006/mcne.1999.0814. PMID: 10673325.

Tuisku, I.S., Konttinen, Y.T., Konttinen, L.M. and Tervo, T.M., 2008. Alterations in corneal sensitivity and nerve morphology in patients with primary Sjögren's syndrome. Experimental eye research, 86(6), pp.879-885.

Turner, Patricia V., and Mudher A. Albassam. "Susceptibility of rats to corneal lesions after injectable anesthesia." Comparative medicine 55.2 (2005): 175-182.

Uchino M, Schaumberg DA. Dry Eye Disease: Impact on Quality of Life and Vision. Curr Ophthalmol Rep. 2013 Jun;1(2):51-57. doi: 10.1007/s40135-013-0009-1. PMID: 23710423; PMCID: PMC3660735.

Ueda, S., del Cerro, M., LoCascio, J.A. and Aquavella, J.V., 1989. Peptidergic and catecholaminergic fibers in the human corneal epithelium: an immunohistochemical and electron microscopic study. Acta Ophthalmologica, 67(S192), pp.80-90.

Ugolini, G., 2011. Rabies virus as a transneuronal tracer of neuronal connections. In Advances in virus research (Vol. 79, pp. 165-202). Academic Press.

Upadhyay, M.P., Karmacharya, P.C., Koirala, S., Shah, D.N., Shakya, S., Shrestha, J.K., Bajracharya, H., Gurung, C.K. and Whitcher, J.P., 2001. The Bhaktapur eye study: ocular trauma and antibiotic prophylaxis for the prevention of corneal ulceration in Nepal. British Journal of Ophthalmology, 85(4), pp.388-392.

Uwanogho D, Rex M, Cartwright EJ, Pearl G, Healy C, Scotting PJ, Sharpe PT. Embryonic expression of the chicken Sox2, Sox3 and Sox11 genes suggests an interactive role in neuronal development. Mech Dev. 1995 Jan;49(1-2):23-36. doi: 10.1016/0925-4773(94)00299-3. PMID: 7748786.

Van Kesteren, R. E., Mason, M. R., MacGillavry, H. D., Smit, A. B., & Verhaagen, J. (2011). A gene network perspective on axonal regeneration. Frontiers in molecular neuroscience, 4, 46.

Vehof, J., Kozareva, D., Hysi, P.G., Harris, J., Nessa, A., Williams, F.K., Bennett, D.L., McMahon, S.B., Fahy, S.J., Direk, K. and Spector, T.D., 2013. Relationship between dry eye symptoms and pain sensitivity. JAMA ophthalmology, 131(10), pp.1304-1308.

Villani E, Baudouin C, Efron N, et al. In vivo confocal microscopy of the ocular surface: from bench to bedside. Curr Eye Res. 2014;39(3):213-231. doi:10.3109/02713683.2013.842592

Vo, R.C., Chen, J.L., Sanchez, P.J., Yu, F. and Aldave, A.J., 2015. Long-term outcomes of epithelial debridement and diamond burr polishing for corneal epithelial irregularity and recurrent corneal erosion. Cornea, 34(10), pp.1259-1265.

Vu HT, Keeffe JE, McCarty CA, Taylor HR. Impact of unilateral and bilateral vision loss on quality of life. Br J Ophthalmol. 2005 Mar;89(3):360-3. doi: 10.1136/bjo.2004.047498. PMID: 15722319; PMCID: PMC1772562.

Wang Z, Xu D, Ding H-F, Kim J, Zhang J, Hai T, Yan C. Loss of ATF3 promotes Akt activation and prostate cancer development in a Pten knockout mouse model. Oncogene. 2015;34:4975–84.

Wang, H., Xiao, C., Dong, D., Lin, C., Xue, Y., Liu, J., Wu, M., He, J., Fu, T., Pan, H. and Jiao, X., 2018. Epothilone B speeds corneal nerve regrowth and functional recovery through microtubule stabilization and increased nerve beading. Scientific reports, 8(1), pp.1-14.

Wang, K., Wang, S., Chen, Y. et al. Single-cell transcriptomic analysis of somatosensory neurons uncovers temporal development of neuropathic pain.Cell Res 31, 904–918 (2021). https://doi.org/10.1038/s41422-021-00479-9

Wang, Z., Reynolds, A., Kirry, A., Nienhaus, C., & Blackmore, M. G. (2015). Overexpression of Sox11 promotes corticospinal tract regeneration after spinal injury while interfering with functional recovery. The Journal of neuroscience : the official journal of the Society for Neuroscience, 35(7), 3139–3145. https://doi.org/10.1523/JNEUROSCI.2832-14.2015

Warwick, C., Cassidy, C., Hachisuka, J., Wright, M. C., Baumbauer, K. M., Adelman, P. C., Lee, K. H., Smith, K. M., Sheahan, T. D., Ross, S. E., & Koerber, H. R. (2021). MrgprdCre lineage neurons mediate optogenetic allodynia through an emergent polysynaptic circuit. Pain, 162(7), 2120–2131. https://doi.org/10.1097/j.pain.0000000000002227

Wenk, H.N., Nannenga, M.N. and Honda, C.N., 2003. Effect of morphine sulphate eye drops on hyperalgesia in the rat cornea. Pain, 105(3), pp.455-465.

Weissman, B., Chun, M.W. and Barnhart, L.A., 1994. Corneal abrasion associated with contact lens correction of keratoconus--a retrospective study. Optometry and vision science: official publication of the American Academy of Optometry, 71(11), pp.677-681.

Wilson, S.E. and Perry, H.D., 2007. Long-term resolution of chronic dry eye symptoms and signs after topical cyclosporine treatment. Ophthalmology, 114(1), pp.76-79.

Wilson, S.E., 2020. Corneal wound healing. Experimental eye research, 197, p.108089.

Wilson, S.E., Mohan, R.R., Mohan, R.R., Ambrósio Jr, R., Hong, J. and Lee, J., 2001. The corneal wound healing response:: cytokine-mediated interaction of the epithelium, stroma, and inflammatory cells. Progress in retinal and eye research, 20(5), pp.625-637.

Wolford CC, McConoughey SJ, Jalgaonkar SP, Leon M, Merchant AS, Dominick JL, Yin X, Chang Y, Zmuda EJ, O'Toole SA, Millar EKA, Roller SL, Shapiro CL, Ostrowski MC, Sutherland RL, Hai T. Transcription factor ATF3 links host adaptive response to breast cancer metastasis. J Clin Invest. 2013;123:2893–906.

Wong, A. W., Osborne, P. B., & Keast, J. R. (2018). Axonal Injury Induces ATF3 in Specific Populations of Sacral Preganglionic Neurons in Male Rats. Frontiers in neuroscience, 12, 766. https://doi.org/10.3389/fnins.2018.00766

Wooten M, Weng HJ, Hartke TV, et al. Three functionally distinct classes of C-fibre nociceptors in primates. Nat Commun. 2014;5:4122. Published 2014 Jun 20. doi:10.1038/ncomms5122

Wright EM, Snopek B, Koopman P. Seven new members of the Sox gene family expressed during mouse development. Nucleic Acids Res. 1993 Feb 11;21(3):744. doi: 10.1093/nar/21.3.744. PMID: 8441686; PMCID: PMC309180.

Wu X, Nguyen B, Dziunycz P, Chang S, Brooks Y, Lefort K, Hofbauer G, Dotto G. Opposing roles for calcineurin and ATF3 in squamous skin cancer. Nature. 2010;465:368–72.

Xiao, Y., Barbosa, C., Pei, Z., Xie, W., Strong, J.A., Zhang, J.M. and Cummins, T.R., 2019. Increased resurgent sodium currents in Nav1. 8 contribute to nociceptive sensory neuron hyperexcitability associated with peripheral neuropathies. Journal of Neuroscience, 39(8), pp.1539-1550.

Xu G, Pierson CR, Murakawa Y, Sima AA. Altered tubulin and neurofilament expression and impaired axonal growth in diabetic nerve regeneration. J Neuropathol Exp Neurol. 2002; 61(2): 164–75. (PubMed: 11855383)

Xue, Y., He, J., Xiao, C., Guo, Y., Fu, T., Liu, J., Lin, C., Wu, M., Yang, Y., Dong, D. and Pan, H., 2018. The mouse autonomic nervous system modulates inflammation and epithelial renewal after corneal abrasion through the activation of distinct local macrophages. Mucosal immunology, 11(5), pp.1496-1511.

Yamazaki, R., Yamazoe, K., Yoshida, S., Hatou, S., Inagaki, E., Okano, H., Tsubota, K. and Shimmura, S., 2017. The Semaphorin 3A inhibitor SM-345431 preserves corneal nerve and epithelial integrity in a murine dry eye model. Scientific reports, 7(1), pp.1-9.

Yang, D., Tewary, P., de la Rosa, G., Wei, F. and Oppenheim, J.J., 2010. The alarmin functions of high-mobility group proteins. Biochimica et Biophysica Acta (BBA)-Gene Regulatory Mechanisms, 1799(1-2), pp.157-163.

Yazdanpanah G, Jabbehdari S, Djalilian AR. Limbal and corneal epithelial homeostasis. Curr Opin Ophthalmol. 2017;28(4):348-354. doi:10.1097/ICU.0000000000000378

You L, Ebner S, Kruse FE. Glial cell-derived neurotrophic factor (GDNF)-induced migration and signal transduction in corneal epithelial cells. Invest Ophthalmol Vis Sci. 2001; 4:2496–2504. (PubMed: 11581189)

You L, Kruse FE, Völcker HE. Neurotrophic factors in the human cornea. Invest Ophthalmol Vis Sci. 2000 Mar;41(3):692-702. PMID: 10711683.

Yu CQ, Zhang M, Matis KI, Kim C, Rosenblatt MI. Vascular endothelial growth factor mediates corneal nerve repair. Invest Ophthalmol Vis Sci. 2008; 49(9):3870–8. (PubMed: 18487369)

Yu, C.Q. and Rosenblatt, M.I., 2007. Transgenic corneal neurofluorescence in mice: a new model for in vivo investigation of nerve structure and regeneration. Investigative ophthalmology & visual science, 48(4), pp.1535-1542.

Yuan X, Yu L, Li J, Xie G, Rong T, Zhang L, Chen J, Meng Q, Irving AT, Wang D, Williams ED, Liu JP, Sadler AJ, Williams BR, Shen L, Xu D. ATF3 suppresses metastasis of bladder cancer by regulating gelsolin-mediated remodeling of the actin cytoskeleton. Cancer Res. 2013;73:3625–37.

Zagon, Ian S., et al. "Use of topical insulin to normalize corneal epithelial healing in diabetes mellitus." Archives of Ophthalmology 125.8 (2007): 1082-1088.

Zakir, H.M., Mostafeezur, R.M., Suzuki, A., Hitomi, S., Suzuki, I., Maeda, T., Seo, K., Yamada, Y., Yamamura, K., Lev, S. and Binshtok, A.M., 2012. Expression of TRPV1 channels after nerve injury provides an essential delivery tool for neuropathic pain attenuation.

Zeev MS-B, Miller DD, Latkany R. Diagnosis of dry eye disease and emerging technologies. Clinical Ophthalmology (Auckland, NZ). 2014;8:581-590. doi:10.2147/OPTH.S45444.

Zhang X, Huang J, McNaughton PA. NGF rapidly increases membrane expression of TRPV1 heat-gated ion channels. EMBO J. 2005;24(24):4211-4223. doi:10.1038/sj.emboj.7600893

Zhang, Yangyang, et al. "Role of VIP and sonic hedgehog signaling pathways in mediating epithelial wound healing, sensory nerve regeneration, and their defects in diabetic corneas." Diabetes 69.7 (2020): 1549-1561.

Zhang, S. Y., Yan, Y., & Fu, Y. (2020). Cosmetic blepharoplasty and dry eye disease: a review of the incidence, clinical manifestations, mechanisms and prevention. International journal of ophthalmology, 13(3), 488–492. https://doi.org/10.18240/ijo.2020.03.18

Zhao, J., Li, X., Guo, M. et al. The common stress responsive transcription factor ATF3 binds genomic sites enriched with p300 and H3K27ac for transcriptional regulation. BMC Genomics 17, 335 (2016). https://doi.org/10.1186/s12864-016-2664-8

Zhu, Q., and Julien, J. P. (1999). A key role for GAP-43 in the retinotectal topographic organization. Exp. Neurol. 155, 228–242.

Zujovic, V., Luo, D., Baker, H.V., Lopez, M.C., Miller, K.R., Streit, W.J. and Harrison, J.K., 2005. The facial motor nucleus transcriptional program in response to peripheral nerve injury identifies Hn1 as a regeneration-associated gene. Journal of neuroscience research, 82(5), pp.581-591.

BIOGRAPHY OF THE AUTHOR

Cara Sullivan was born and raised in Connecticut. She graduated Pomfret School in 2003 and graduated from the College of the Holy Cross in 2007, with a dual Bachelor of Arts degree in Psychology and East Asian Studies. Her dedication to service and education that began in childhood continued into her career. She spent her early career working for non-profits and engaging in direct care and service activities for special needs and at-risk populations. She transitioned to an administrative role where she gained experience in computer programming, database administration, and process change management for similar social programs. To satiate her interests in medicine and neuroscience, she became a certified Emergency Medical Technician during the same period. She earned her Master of Science degree in Neuroscience from the University of Hartford in August 2015. While she loved her career, her passion for delving into the field of Neuroscience was even more robust. So she moved to Maine and began her journey in the Graduate School for Biomedical Science and Engineering Ph.D. program at the University of Maine in September 2015. During this period, she has had the fortune to take many different classrooms based and immersive seminars in various disciplines and research techniques. Her goal for this period of her life has been to learn about a broad range of subjects and gain concrete skills in diverse fields. The University of Maine unlocked innumerable resources and learning opportunities to which Cara would never have had access. Cara is a candidate for the Doctor of Philosophy degree in Biomedical Science from the University of Maine in August 2021.